HISTORICAL MINING CONTAMINATION AND FLOODPLAIN EVOLUTION ALONG LOWER PEARSON CREEK, SW MISSOURI

A Masters Thesis
Presented to
The Graduate College of
Missouri State University

In Partial Fulfillment
Of the Requirements for the Degree
Master of Science, Geospatial Sciences in Geography and Geology

By
Patrick J. Womble
December 2009

HISTORICAL MINING CONTAMINATION AND FLOODPLAIN EVOLUTION ALONG LOWER PEARSON CREEK, SW MISSOURI

Geography, Geology, and Planning

Missouri State University, December 2009

Master of Science

Patrick J. Womble

ABSTRACT

Contaminated historical mining sediment has been used in the past as a stratigraphic tracer to study the effects of settlement on floodplain deposition. Lead and zinc mining near Pearson Creek watershed (58 km^2), Springfield, Missouri began around 1885, peaked around 1912, and ended by 1920. The purpose of this study is to use the historical stratigraphic record in floodplain deposits to determine channel response to land use changes. The objectives are to (1) determine the magnitude and distribution of mining-contaminated sediment within active and historical alluvial deposits; (2) identify geo-stratigraphic assemblages using floodplain sedimentology and trace-metal dating; and (3) use geo-stratigraphic assemblages to develop a geomorphic model of historical floodplain evolution. Geochemical and textural data from soil samples collected along cross-sections were used to identify geo-stratigraphic assemblages and calculate sedimentation rates. Three assemblages were identified based on down-core stratigraphic patterns of Zn and soil color: Terrace Veneer, Floodplain Drape, and Channel Fill. Mean Zn concentration increased from Terrace Veneer (85 ppm) to Floodplain Drape (396 ppm) to Channel Fill (1,441 ppm). Sedimentation rates were highest during the mining period (mean=2.20 cm/yr) and decreased during the post-mining period (mean=0.64 cm/yr). Terrace abandonment and vertical accretion of uncontaminated sediment were dominant during the pre-mining period. Lateral migration upstream and vertical accretion downstream dominated during the mining-period. Vertical accretion has dominated the post-mining period. Alluvial deposits along lower Pearson Creek are contaminated with mining-related Zn and post-settlement land use changes have influenced floodplain sedimentation patterns.

KEYWORDS: floodplains, geomorphology, Pearson Creek, mining pollution, land use

This abstract is approved as to form and content

Robert T. Pavlowsky
Chairperson, Advisory Committee
Missouri State University

HISTORICAL MINING CONTAMINATION AND FLOODPLAIN EVOLUTION ALONG LOWER PEARSON CREEK, SW MISSOURI

By

Patrick J. Womble

A Masters Thesis
Submitted to the Graduate College
Of Missouri State University
In Partial Fulfillment of the Requirements
For the Degree of Master of Science, Geospatial Sciences in Geography and Geology

December 2009

Approved:

Robert T. Pavlowsky, PhD

Douglas Gouzie, PhD

Melida Gutiérrez, PhD

Frank Einhellig, Graduate College Dean

ACKNOWLEDGEMENTS

Many people contributed their time in helping me complete this thesis research. I would first like to thank my committee members Drs. Robert Pavlowsky, Douglas Gouzie, and Melida Gutiérrez for their guidance and technical advice. Special thanks go to Dr. Robert Pavlowsky for advising and mentoring me throughout this process. I would also like to thank Marc Owen, Heather Hoggard, and Derek Martin of the Ozarks Environmental and Water Resources Institute (OEWRI) for their unfailing GIS, field, and laboratory support; my colleagues Pat Dryer, David Speer, Jess Whitson, Lucas Rengstorf, and Elijah Robison also deserve many thanks for their willingness to assist me in the field and Sarah Morris for her help in the laboratory; and the Faculty and Staff of the Department of Geography, Geology, and Planning for their support and Missouri State University for allowing me this opportunity to further my education.

The primary source of my GA funding was EPA Grant No. X7-98772501 awarded to Dr. Pavlowsky. Funding for this thesis project was also provided by a $500 Thesis Funding Award from the Graduate College at Missouri State University. Funding for travel to professional conferences to present my thesis topic was provided by the Graduate College, the College of Natural and Applied Sciences, the Department of Geography, Geology, and Planning, and OEWRI.

Special thanks go to Mr. John Hopkins, who allowed me access to his Pearson Creek property and my study area. Thanks must also go to Atalie Albin for her unfailing support and for graciously spending time editing and proofing this document. Finally, without encouragement and support from my family and friends, this would not have been possible.

TABLE OF CONTENTS

LIST OF TABLES

LIST OF FIGURES

CHAPTER 1

INTRODUCTION

Concerns exist worldwide over the long-term effects of mining pollution on water quality and sediment contamination in rivers. Historical mining for base metals such as lead and zinc released large amounts of metalliferous waste into nearby streams, potentially contaminating food and drinking water sources and altering the natural balance of ecosystems. Pearson Creek (Figure 1) is an outlying sub-district of the Tri-State Mining District located near the junction between Missouri, Oklahoma, and Kansas. Lead and zinc mining near Pearson Creek began in the early 1840s, intensified during the late 1880s, and ended around 1920 (Thomson, 1986). During those times, mining waste disposal was not regulated and mining operations would dispose of waste in unstable tailings piles or discharge mill waste directly into Pearson Creek (Fairbanks and Tuck, 1915). A previous screening-level study indicated that a significant volume of mining sediment is stored within the alluvial deposits of nearby floodplains and active stream channel deposits (Owen and Pavlowsky, 2000). Mining-related metal contamination has also been released from Pearson Creek into the James River (Owen and Pavlowsky, 2000; Frederick, 2001) and more recently Lake Springfield (Tannehill, 2002). However, the spatial distribution of mining sediment within floodplain deposits along lower Pearson Creek remains largely unknown.

Watershed-scale contamination of river systems by metals released from mining operations is dependent on the sediment transport and storage capacity of the stream. Concentrations of contaminated sediment tend to be high close to abandoned mine sites and decrease with distance downstream (Bradley and Cox, 1986; Graf, 1996; Carlson,

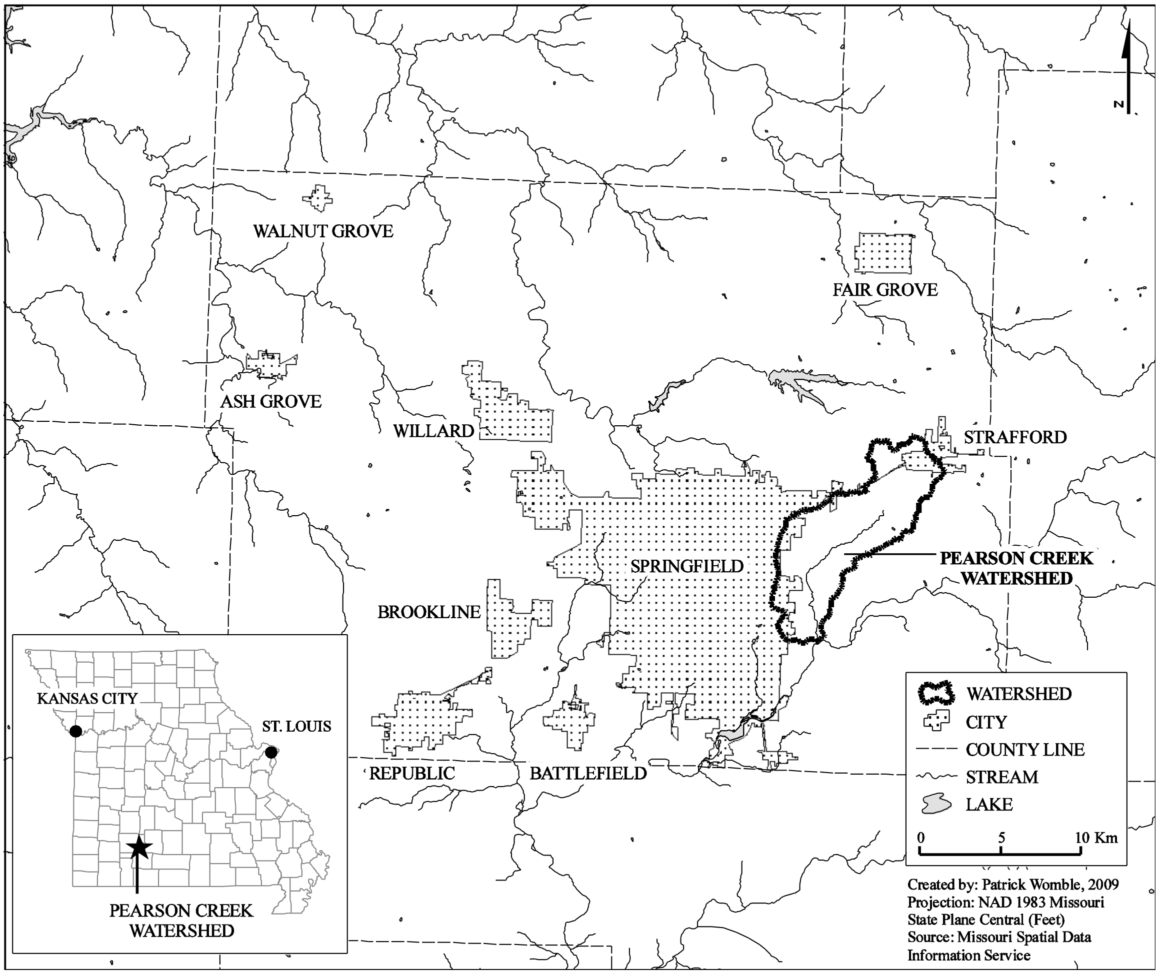

Created by: Patrick Womble, 2009
Projection: NAD 1983 Missouri
State Plane Central (Feet)
Source: Missouri Spatial Data
Information Service

Figure 1. Pearson Creek watershed.

1999; Lecce and Pavlowsky, 2001; Trimble, 2001). At the local scale, the magnitude and distribution of contaminated sediment can vary considerably depending on the types of fluvial forms present, how and when they were formed, and how effectively they store sediment. Mining sediment can be sorted by fluvial processes in a reach where fines are deposited on floodplains or flushed downstream and/or where sand and gravel are deposited on the bed or in temporary bar forms (Graf, 1996, Hudson-Edwards, 2003).

Sediment stored in fluvial systems is often remobilized or recycled back into the stream. This process can be physical and/or chemical in nature and may result in continuing pollution long after mining has ended as contamination is re-introduced back into the channel for transport (Lewin et al., 1977). Physical processes, such as erosion caused by channel migration, can reincorporate metalliferous material back into the flow while chemical processes, such as dissolution and pedogenesis, can alter the geochemistry of the metals into forms readily transported in solution or more bioavailable to plants (Horowitz, 1991). The long-term risk of pollution is more of a geomorphic problem in areas where physical processes (erosion and channel migration) occur at much faster rates than chemical releases. In such areas, physical processes occur relatively fast so there is not sufficient time for chemical weathering or pedogenesis to take effect. Therefore, factors that cause channel instability such as increased sediment and/or water supply increase the chances that contaminated sediment stored in floodplains will be remobilized.

Stream channels have a natural tendency to migrate, but when the process is accelerated by anthropogenic activities such as urbanization or agriculture, sediment remobilization occurs at a greater rate. It is well known that land use changes in a watershed influence geomorphic processes such as floodplain sedimentation rates, erosion, and channel form (Knox, 1977; Trimble and Lund, 1982; Magiligan, 1985; Beach, 1994; Jacobson and Primm, 1994; Faulkner, 1998; Walling, 1999). To explore the effects of anthropogenic influence on a watershed, geomorphologists study the stratigraphy and geomorphic history of the streams within it. To do this, the stratigraphy of physical, chemical, biological, or anthropogenic materials within alluvial sediments are used to serve as temporal markers to date sediment. Types of indicators, or tracers, include, but are not limited to, buried soils, pollen, archaeological artifacts, geochemical changes in substrate, radioisotopes, and trace elements. Mining-contaminated sediment has been used by many workers in the United States and abroad to investigate timing and rates of sedimentation, sediment provenance, floodplain evolution, anthropogenic impacts on the watershed, and patterns of floodplain sediment storage (Lewin et al., 1977; Bradley and Cox, 1986; Knox, 1987; Bradley 1989; Marron, 1992; Graf, 1996; Brewer and Taylor, 1997; Hudson-Edwards et al., 1998; Smith et al., 1998; 1999; Lecce and Pavlowsky, 2001; Ciszewski and Malik, 2004; Lecce et al., 2008).

Studies by Knox (1987) and Lecce and Pavlowsky (2001) demonstrate the feasibility of using Zn-contaminated sediment as a reliable method for dating alluvial deposits. Knox (1987) used Zn concentrations and buried soils in floodplain sediment to date sediment layers and determine overbank sedimentation rates in the Galena River watershed in Wisconsin and Illinois. He found that sedimentation rates were higher during periods of intense agriculture prior to the use of conservation practices and that channel enlargement decreased sedimentation rates over time by containing larger floods. Similarly, in the same region, Lecce and Pavlowsky (2001) also used buried soils and mining-related Zn concentrations to date channel and floodplain deposits to investigate how floodplain sedimentation changed over time within the Blue River Watershed in

Wisconsin. They found that sedimentation rates were high early on in the headwaters, metal peaks were buried deeper downstream, and lateral migration terraced historical floodplains. Both studies found high sedimentation rates in the headwaters and low sedimentation in the lower valleys during the pre-mining period. Following this, channel widening in the headwaters enabled those streams to contain and convey sediment and floods downstream, decreasing sedimentation in the headwaters and increasing sedimentation in the lower valleys.

Previous Studies near Pearson Creek

There have been previous studies of mining-affected stream sediment in the Tri-State Aurora sub-district in Lawrence County, Missouri by Carlson (1999) and Trimble (2001). Carlson (1999) explored floodplain sedimentation rates using mining tracers in Honey Creek while Trimble (2001) calculated in-channel and overbank sediment budgets to estimate contamination release and risk in Chat Creek. Carlson found that Zn concentrations were as much as 575 times background concentrations and overbank floodplain sedimentation rates immediately following land clearing and during mining averaged 0.82 cm/yr and decreased to 0.60 cm/yr after mining. Trimble found that bank erosion releases 929 Mg of sediment and that 321 kg of Zn are released into to Chat Creek each year. Both of these studies used bank exposures to estimate contamination and did not explore the spatial distribution of contaminants in floodplain deposits across the valley floor.

Nearer to Pearson Creek, Frederick (2001) examined phosphorous concentrations in active channel sediments along the James River and included Zn concentration data. Three of Frederick's sites were located near Pearson Creek: one upstream of Pearson

Creek on the James River, one on Pearson Creek, and one downstream of the confluence. For Zn, Frederick reported 54 ppm upstream, 1,100 ppm in Pearson Creek, and 264 ppm just downstream. The five-fold concentration increase from the upstream site to the downstream site indicates that Pearson Creek is presently discharging mining-related Zn into the James River. Tannehill (2002) supported this conclusion while studying metal concentrations in the bottom sediment of Lake Springfield, approximately 7.5 kilometers downstream of where Pearson Creek enters the James River. The mean value for Zn in all lake bottom sediment was 113 ppm, over double the concentration found by Frederick (2001) upstream of Pearson Creek. These two studies show that Zn from historical mining along Pearson Creek is probably entering the James River and being transported downstream and deposited in Lake Springfield.

A Brownfield Targeted Assessment (BTA) conducted in 2007 by the Missouri Department of Natural Resources near Pearson Creek and Ash Grove focused on near-surface topsoil contamination of lead, zinc, and asbestos in neighborhoods in the lower and middle portion of the watershed (MoDNR, 2008). The report concluded that mining operations in the area did not significantly contaminate topsoil and would not pose a large threat to the surrounding community. However, sample sites in the MoDNR study were located on the surrounding uplands, not in the valley bottoms.

An initial undergraduate study by Owen and Pavlowsky (2000) focused on the distribution of historical mining pollution within the floodplain deposits in the current study area. The study examined sixteen in-channel sediment samples and six cutbank exposures along lower Pearson Creek and the James River. Three bank sites were located on historical floodplains and three on older, pre-mining terraces. Two main findings were: (1) in-channel sediment samples from Pearson Creek and the James River, upstream and downstream of the confluence, revealed high zinc concentrations along lower Pearson Creek that decreased in the downstream direction; and (2) terrace surfaces were capped by only 30-60 cm of contaminated sediment, while historical, lower elevation floodplain surfaces were contaminated throughout. They concluded that the stream experienced a significant amount of sedimentation since the mining period and considerable amounts of contaminated sediment are actively moving and stored within the system.

The previously highlighted studies in southwest Missouri show that (1) a question of the degree and extent of contamination along lower Pearson Creek remains and (2) metal contamination trends across the valley floor of Pearson Creek have not been determined. Furthermore, excluding the Owen and Pavlowsky (2000) study, no research has addressed the dissemination of mining-related Zn in historical and recent floodplain sediment near Pearson Creek. This study expands on the findings of Owen and Pavlowsky to characterize the vertical and lateral trends of mining-related contamination in lower Pearson Creek. In addition, this study attempts to develop a timeline of geomorphic change using contaminated historical mining sediment as a tracer.

Purpose and Objectives

Ozark streams as a whole have not been widely studied from the environmental and geomorphic perspective which has resulted in a severe gap in the literature as to how they have responded to historic land use changes induced by settlement. Exceptions include work by Jacobson and Primm (1994) on the effects of land use changes on streams in eastern Missouri, several Missouri State University Master's Theses regarding historical channel changes and channel geometry in streams in southwest Missouri

(Legleiter, 1999; Horton, 2003; Wyllie, 2002), and the previously mentioned mining-related studies by Carlson (1999), Trimble (2001), MoDNR (2008), and Owen and Pavlowsky (2000). However, none of these studies specifically examined Pearson Creek pollution or the sedimentology and distribution of mining sediment at the Pearson Creek-James River confluence zone. The purpose of this study is to better document the distribution of Zn in floodplain deposits and to use the historical mining record in floodplain deposits to determine channel response to land use changes since European settlement. The objectives are to:

(1) Determine the magnitude and distribution of mining-contaminated sediment within active and historical floodplain and terrace alluvial deposits;

(2) Identify geo-stratigraphic assemblages using floodplain sedimentology and trace-metal dating; and

(3) Develop a geomorphic-based model to describe contamination patterns in floodplain deposits and interpret stratigraphic relationships among contaminated floodplain deposits.

Benefits

First, this research will help us understand how streams in the Ozarks have responded to historical land use change by exploring spatial-stratigraphic relationships of mining-contaminated floodplain deposits. Second, this study examines stratigraphic sedimentation patterns and relates them to land use changes in a tributary-main stem confluence zone. The literature surrounding confluence zones has largely ignored confluence stratigraphy due to its complex nature and instead mainly focused on hydrologic flow modeling (Rhoads and Kenworthy, 1994; De Serres et al., 1999), textural and morphological characteristics of channel beds (Biron et al., 1993; Rhoads et al., 2009; Unde and Dhakal, 2009), and spatial patterns of channel change (Roy and Woldenberg, 1986). Finally, this study will document the environmental contamination in Pearson Creek, which managers can use to assess the risks associated with the remobilization of contaminated sediment and respond appropriately. Information presented here can lead to a better understanding of long-term metal contamination of river systems in the Tri-State District in general, including the more heavily mined areas in the Spring River Basin to the west and the Big River Basin to the east.

CHAPTER 2

GEOMORPHIC CONTROLS ON THE DISTRIBUTION OF MINING CONTAMINATION IN RIVERS

This chapter reviews the processes controlling sediment transport and distribution in fluvial systems, how those processes control the fate of contaminated sediment, and how geomorphologists use contaminated sediment profiles to interpret past geomorphic change. Geomorphic approaches have been used to understand how the dispersal patterns of metals in fluvial sediment are linked to anthropogenic alteration in watersheds (Lewin et al., 1977; Bradley and Cox, 1986; Knox, 1987; Lecce and Pavlowsky, 2001). These studies used metals as tracers to determine the timing and magnitude of changes in channel configuration and sedimentation rates in response to human impacts. In this study, mining sediment is composed of a range of relatively mobile tailings and mill waste material introduced to land areas and streams by mining operations.

Watershed Systems

Geology, climate, physiography, and land use of a watershed control the behavior of streams within it (Knighton, 1998). Changes in these variables alter the hydrologic regime of the system and bring about changes in the supply and nature of sediment transported through the watershed. Once in the fluvial system, fluvial processes govern the transport, storage, and distribution of sediment. Sediment introduced into the system has three broad origins: anthropogenic, accelerated, and natural. Anthropogenic inputs are those introduced or created directly by human activities such as direct dumping of mine tailings into the stream. Accelerated inputs include soil erosion due to agricultural land clearing, construction, and clear-cutting. Natural inputs are dependent on the geology of the system and originate from natural erosion processes along channel boundaries, inputs from tributaries upstream, or slope wash (Knighton, 1998). After being introduced, sediment is transported downstream and can get trapped, often multiple times, in storage areas such as floodplains or lakes. Storage can be short- or long-term depending on whether it is closer to (proximal) or farther from (distal) the active channel. In general, proximal sediment is more temporary than distal sediment. Over time, sediment will continue to migrate downstream and out of the watershed to successively larger rivers (Knighton, 1998).

Human Impacts on Overbank Sedimentation

It is well documented that land use change affects sedimentation in fluvial systems (Lewin et al., 1977; Knox, 1977, 1987, 1989; Trimble and Lund, 1982; Magilligan, 1985; Jacobson and Primm, 1994). Vegetation on hillslopes dissipates energy and reduces the erosivity of runoff by interrupting its flow path. When vegetation is removed or soil is exposed, the resistance of hillslopes decreases, allowing the erosivity of runoff to increase. The lack of vegetation also decreases the infiltration rate and capacity of soils in the watershed, generating more runoff. Excess runoff enables the stream to carry more material and accelerates erosion, causing the formation of rills and gullies on hillslopes. Introduction of material removed during hillslope erosion can have negative impacts on aquatic habitats, destroy crops growing on floodplains, and damage infrastructure downstream. Higher rates of overland flow also increase the magnitude and frequency of floods. Channels respond to increased discharge by deepening, widening, and altering bed forms and can get big enough to effectively cut off overbank events altogether, conveying more sediment downstream (Brakenridge, 1988; Lecce, 1997). Human-induced changes can also include introducing pollutants into alluvial sediments.

Metal pollutants are introduced into streams via industrial, municipal, agricultural, and mining operations. Industrial and municipal metal pollutants are widespread and can include sewage, water treatment effluent, airborne particulates from power plants, landfills, and surface pollutants removed by storm water runoff. Agricultural pollutants are mainly limited to metals derived from fertilization. Base-metal mining pollutants typically include metals mobilized by tailings dam failure, eroded from tailings piles, or chemically leached from waste piles. In addition, other metal pollutants may be released by acid mine drainage, dust particulates, and waste water effluent. Pollutants derived from base-metal mining operations are the primary focus of this study.

Mining Contaminants in Fluvial Systems

Sediment Characteristics. The main sources of contamination in watersheds with a history of mining are abandoned mines, mine waste piles, and reworked colluvial and alluvial deposits (Hudson-Edwards, 2003). In early Pb/Zn mining operations, ore was sorted by hand, broken up with hammers, and separated from gangue (host rock) with small hand jigs, a process known as concentration. As mining operations became more mechanical, ore concentration was done with large jigs operated by steam, air, or electricity (Taggart, 1945). Water was used to increase the buoyancy of the grains and allow grains with higher specific gravity than the gangue to migrate down through the vat and settle to the bottom more easily (Taggart, 1945). Screens at the bottom of the jig would catch larger gangue particles and allow passage of the concentrate. Jets of water were commonly used to speed up the process and convey the resulting gangue slurry into nearby streams or to tailings piles. Although convenient, jigging is blind to what it sorts. For example, if grains of ore and gangue had comparable specific gravities, they would be treated equally by the system, flushed through it, and discarded. The inefficiency of this method was acceptable in areas where ore was coarsely disseminated through the host rock or at small operations because it was not economically viable to reprocess the tailings. In large operations that reprocessed sediment, the sand-sized fraction would be further ground into silt-sized sediment (fines), concentrated via flotation, and transported to holding ponds. However, slimes, the smallest size fraction (<50 μm), could not be concentrated and went out with the wash water during jigging. In addition, relatively small fragments of metalliferous minerals are attached to the gangue and also ended up in tailings piles.

Many physical (grain size, surface area, specific gravity, surface charge) and chemical (adsorption, precipitation and coprecipitation, organometallic bonding, incorporation in crystalline minerals) factors control metal concentrations in sediment (Horowitz, 1991). Horowitz (1991) explained that physical and chemical controls are highly interrelated and grain size plays a role in all of these processes. Fine-grained particles have large unit surface areas and net negative surface charges, which attract positively charged metal ions (Horowitz, 1991). Therefore, since surface area increases as grain size decreases, the concentration of metals in fine-grained sediment will be higher than in coarse-grained sediment. Similarly, organic matter can concentrate metal ions due to large surface areas, high cation exchange capacity, high negative surface charge, and physical trapping. Metal ions can also be incorporated, via replacement, into Fe and Mn oxide coatings as they form on sediment grains or in soils.

Transport and Dispersal Trends. The suspended sediment load in a stream contains much higher concentrations of trace elements than the dissolved load and is the dominant means by which most metal contaminants are transported downstream (Horowitz, 1991). The fate of bed and suspended sediment, and thus contaminated sediment, is determined by sorting processes inherent to stream systems which preferentially transport sediment based on size and density. Fine-grained sediment is transported farther downstream or across floodplains than coarse-grained sediment due to the relative ease with which it is entrained. Local-scale distribution can vary considerably and obscure large-scale trends (Axtmann and Luoma, 1991). However, metal concentrations in both channel and floodplain deposits tend to be highest closer to abandoned mine sites and decrease with distance downstream (Lewin and Wolfenden, 1978; Bradley and Cox, 1986; Graf, 1996; Carlson, 1999; Lecce and Pavlowsky, 2001; Trimble, 2001). Downstream reductions in concentration are often attributed to physical dilution and mixing between contaminated and uncontaminated sediment (Leenaers, 1989). Sources of "clean" sediment include tributary inputs from unmined watersheds and bank erosion (Graf, 1996). Another factor controlling the decrease in concentration downstream is storage or removal of contaminants from the stream. Graf (1996) observed that local-scale variations in metal concentrations downstream are based on trap efficiency and storage capacity, and that areas capable of effectively trapping more sediment, such as wide channels or valleys, will have more contamination present than narrow zones.

Alluvial Storage. As sediment is transported downstream, it is stored over different timescales in channel and overbank floodplain areas (Bradley, 1989). Floodplains can form through point bar construction, vertical accretion, or a combination of the two. Point bars are formed on the inside of meander bends as channels migrate across the valley bottom. Increased flow separation and/or bed resistance on the inside of the bend decreases the velocity of the water and causes sediment to fall out of suspension, which then becomes a nucleus for additional deposition laterally and vertically (Brakenridge, 1988). As it builds upward, flows of greater magnitude are required to inundate the surface and eventually result in the construction of a floodplain through vertical accretion. Vertical accretion is the process where, during flood events, successive deposition of fine-grained sediment slowly increases the height of the banks (Brakenridge, 1988). As the bank height increases, the rate of deposition decreases due to the greater volume of water needed to breach the banks (Brakenridge, 1988; Knighton, 1998). This type of floodplain formation is more common in low energy streams where coarse-grained sediment transport is lacking (Lecce and Pavlowsky, 2001). Floodplain deposits typically contain higher concentrations of mining-related contaminated sediment than their in-channel counterparts (Lecce and Pavlowsky, 1997; Carlson, 1999; Trimble, 2001). In fact, Lecce and Pavlowsky (1997) found that Zn levels in floodplains were as much as five times higher than those in adjacent point bar sediments.

Metal pollutants in floodplains can behave as non-point sources if remobilized and released back into the stream (Lewin et al., 1977; Knox, 1987; Bradley, 1989; Pavlowsky, 1995; Lecce and Pavlowsky, 1997; Smith et al., 1998). Remobilization is the process whereby previously stored sediment is recycled back into the streamflow due to bank erosion and stream course changes. The duration of storage between periods of remobilization is known as residence time, the length of which increases with distance from the active channel: beds (event), bars (annually), short-term floodplains (decades to centuries), and long-term floodplains or terraces (centuries to millennia). If these landforms are contaminated, residence time estimates can help managers determine the threat and timing of contaminated sediment remobilization and thus prepare accordingly.

Floodplain Distribution. Floodplain contamination trends differ depending on the process controlling floodplain formation. Brewer and Taylor (1997) describe three styles of contaminant distribution controlled by vertical accretion or lateral migration in the Severn Basin, UK: flood frequency, channel incision, and lateral reworking (Figure 2). Flood frequency-controlled floodplains (Figure 2A) are located in systems with stable terrace surfaces and are controlled by how often a surface is inundated by flood waters. Smaller and more frequent floods inundate low surfaces and deposit sediment more often than higher surfaces, which require larger and less frequent floods to submerge them. Similarly, as channels incise (Figure 2B), higher terrace surfaces are progressively flooded less often over time, decreasing the amount of contaminated sediment deposited on higher surfaces as time advances. The difference between flood frequency and channel incision styles of floodplain formation is that the elevation of the channel bed in the flood frequency style is constant whereas the elevation of the bed in the channel incision style decreases. Lateral reworking (Figure 2C) is controlled by lateral bank instability of the channel and surfaces are built successively across the valley floor. Laterally reworked deposits can contain appreciable amounts of mining pollutants as well as reworked floodplain sediment.

Tracer Studies

Tracer studies are based on the assumption that there is a temporal connection between the date mining sediment was released and the timing of deposition downstream. Metal tracers are a popular and reliable tool to identify geomorphic change in fluvial

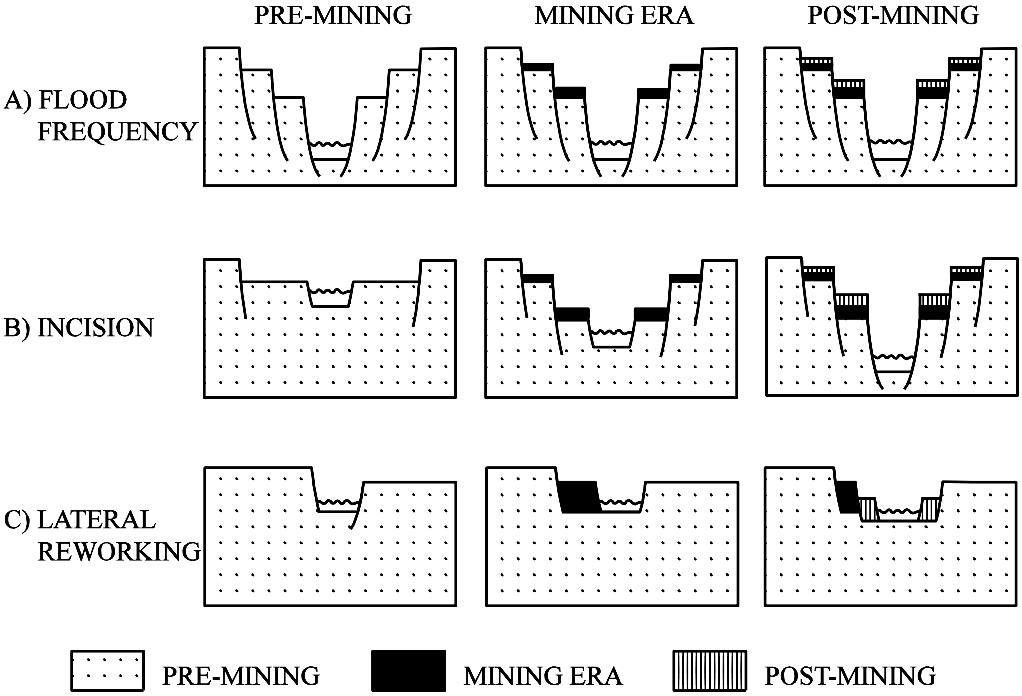

Figure 2. Styles of floodplain formation. Three floodplain styles (A) flood frequency, (B) channel incision, and (C) lateral reworking show the distribution of sediment during the pre-mining, mining era, and post-mining period. Modified from Brewer and Taylor (1997).

environments (Macklin, 1985; Knox, 1987; Bradley, 1989; Lecce and Pavlowsky, 2001). Zinc profiles in historical mining sediments can be used as stratigraphic markers to date recent sediments and calculate historical and recent sedimentation rates (Lecce and Pavlowsky, 2001). Assuming that the present surface material has not been significantly scoured or removed, two stratigraphic intervals can usually be identified: mining initiation to peak mining, and peak mining to present day. In the Zn profile, the first occurrence depth coincides with the year mining began, the peak concentration is associated with peak mining production, and everything above the peak Zn depth is representative of post-mining deposition (Lecce and Pavlowsky, 2001). Sedimentation rates can be determined by dividing each thickness by the corresponding time span related to mining production records. The presence of other stratigraphic markers such as buried soils, artifacts, or radioisotopes can help to more precisely determine timing of sedimentation.

However, one concern associated with sediment tracer studies is the mobility of the metal being investigated. The average solubility of Zn in soils ranges between 4 ppb and 270 ppb depending on soil chemistry and the method used to analyze the soil (Kiekens, 1995). Organic matter content, pH, and grain size control the solubility of Zn in soils (Kabata-Pendias and Pendias, 2000). Mobility of the Zn^{2+} ion is reduced as organic matter and pH increase or as grain size decreases. Organic matter and clay-sized particles are capable of strongly arresting Zn^{2+} ions in basic environments (Kabata-Pendias and Pendias, 2000) while acidic environments promote solubilization and desorption (Horowitz, 1991; Marron, 1992, Merrington and Alloway, 1994; Pavlowsky, 1995; Hudson-Edwards et al., 1998). Pavlowsky (1995) suggested that carbonate environments neutralize water and sediment pH, reducing the production of acid and making Zn a reliable and stable indicator of mining sediment presence. In the Ozarks, Shepard and Gutiérrez (1999) performed sequential extraction on a soil contaminated by sewage sludge to assess the availability and mobility of heavy metals. The results showed that heavy metals only leach downward about 20 cm at most, but are bioavailable to fescue grass. Because the mineralization at Pearson Creek is hosted by limestone (typically >90% calcite), chemical mobility over periods of a century of so should not be a large factor influencing the distribution of Zn concentrations in floodplain profiles.

CHAPTER 3

STUDY AREA

Regional Setting

Pearson Creek watershed (58 km^2) is located in Greene County, Missouri (Figure 1). The creek is a major tributary of the James River that drains the southeastern portion of the county. The watershed relief spans more than 100 m; from 353 masl in the north to 455 masl where Pearson Creek enters the James River. In July 2007, Springfield, the largest city in Greene County, had the third largest population in the state at an estimated 154,777 persons; the next largest city in the County, Republic, had an estimated population of 13,021 (U.S. Census Bureau, 2008a). Other cities in Greene County include Battlefield, Brookline, Willard, Strafford, Ash Grove, Walnut Grove, and Fair Grove (Figure 1). Pearson Creek drains the eastern portion of Springfield and the southern half of Strafford, Missouri.

Geologic Setting

The Ozarks in Missouri are part of a large asymmetric dome, the high point of which is formed by the St. Francois Mountains (Sauer, 1920). Pearson Creek is situated in the Ozark Plateau Region atop the Springfield Plateau (Thomson, 1986). The Springfield Plateau is a topographic feature dominated by Mississippian-age carbonate rocks (Thomson, 1986). The Mississippian-age rocks in the area are the Osagean (Burlington-Keokuk Limestone, Elsey, and Pierson Formations) and Kinderhookian (Northview, Compton, and Bachelor Formations) Series (Table 1; Figure 3). Chert nodules are abundant in the Lower Burlington-Keokuk, Elsey, and Pierson Formations

Table 1. General geologic stratigraphy of Greene County, Missouri from Thomson (1986) and Fairbanks and Tuck (1915).

System	Series	Group or Formation	Lithology	Thickness (ft)	Mineralization
Quaternary		Alluvium (Qal)	Sand and Gravel	Variable	
		Terrace Deposits (Qt)		Variable	
Pennsylvanian		Channel Sand Deposits (Pcs)	Sandstone	Variable	
Mississippian	Meramecian	Warsaw Formation (Mw)	Limestone	>50	
	Osagean	Burlington-Keokuk (Mbk)	Limestone	120-340	
		Elsey Formation (Me)	Cherty Limestone	50-80	
		Pierson Formation	Dolomitic Limestone	30-40	
	Kinderhookian	Northview Formation (Mnv)	Shale	5-80	Pb/Zn deposits along faults
		Compton Formation (Mc)	Limestone	7-25	
		Bachelor Formation	Sandstone	≤2	
Ordovician	Canadian	Cotter Dolomite (Oc)	Dolomite	50-175	
		Jefferson City Formation	Dolomite	190-220	
		Roubidoux Formation	Dolomite/Sandstone	140-180	

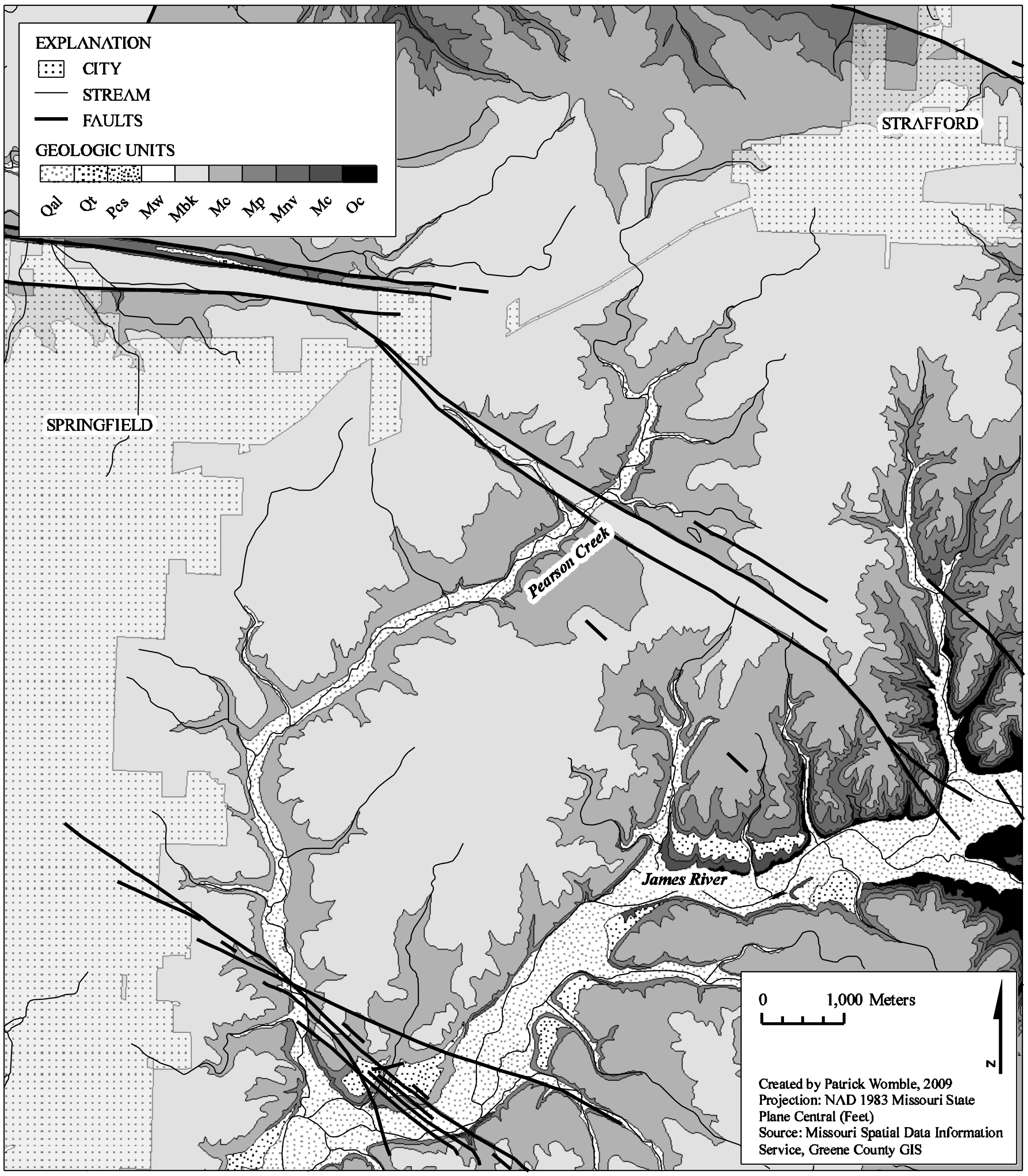

Figure 3. Stratigraphic and structural geology map of Pearson Creek watershed.

and they are found as gravel fragments in bed and bar deposits in streams. Surficial deposits include residuum, alluvium, colluvium, and Pleistocene loess (Hughes, 1982). Red cherty residuum formed from the weathering of the limestone lies on top of the surrounding ridges while alluvium and colluvium reside in the valleys and form terraces, floodplains, alluvial fans, and other features.

Faults are present in the northern and southern parts of the watershed (Figure 3) that formed as a result of the Ozark Uplift. Mineralization is concentrated along these fault zones in the Northview shale just above the Bachelor Sandstone (Thomson, 1986). Mineral deposits consisting of galena and sphalerite, and minor amounts pyrite and chalcopyrite, are typically disseminated in tallow or gumbo clay accumulations in these faults (Fairbanks and Tuck, 1915; Thomson, 1986).

A karst landscape is found in the study area and all across the Ozarks where horizontally-bedded limestone is at the surface. Karst features are formed when dissolution processes expand bedding planes and fractures in carbonate rock to form caves and conduits. Some karst features present in Greene County include cutters, pinnacles, sinkholes, springs, caves, and losing streams (Thomson, 1986). In and around the Pearson Creek watershed are numerous springs, losing streams, caves, and sinkholes.

Soils

The parent material of upland soils in the watershed is generally composed of loess over residuum. Goss, Wilderness, and Peridge soil series are present on the uplands around Pearson Creek (Figure 4, Table 2; Hughes, 1982). Goss soils are deep, well-drained, and located on hillsides and formed in residuum weathered from cherty limestone or dolomite. Wilderness soils, also formed from weathered cherty limestone,

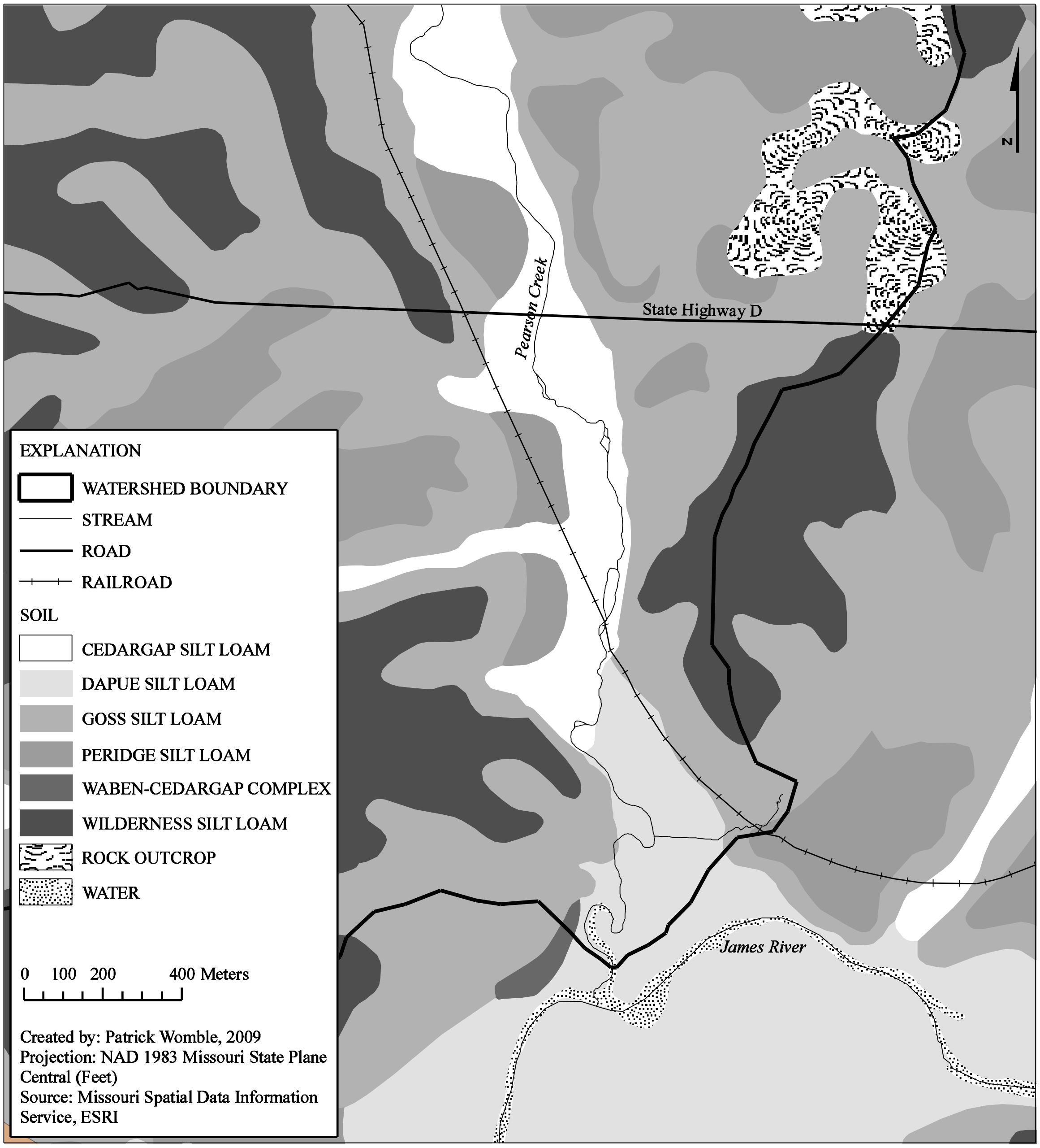

Figure 4. Soils along lower Pearson Creek.

Table 2. General description of soil series found along Pearson Creek (Hughes, 1982; NRCS, 2008).

	Soil Series	Parent Material	Landform Position	Slope (percent)	Taxonomic Class
UPLAND SOILS	Goss	Colluvium and residuum weathered from cherty limestone	Upland slopes	2 to 20	Clayey-skeletal, mixed, active, mesic Typic Paleudalfs
	Wilderness	Colluvium and residuum weathered from cherty limestone	Upland flats/ broad areas	2 to 9	Loamy-skeletal, siliceous, active, mesic Oxyaquic Fragiudalfs
	Peridge	Older alluvium to colluvium and residuum weathered from cherty limestone or loess	Upland/ Terrace	0 to 8	Fine-silty, mixed, active, mesic Typic Paleudalfs
ALLUVIAL SOILS	Dapue	Silty alluvium	Low Terrace Floodplain	0 to 3	Fine-silty, mixed, active, mesic Fluventic Hapludolls
	Cedargap	Alluvium	Floodplain	0 to 5	Loamy-skeletal, mixed, superactive, mesic Cumulic Hapludolls
	Waben-Cedargap Complex	Cherty alluvium or colluvium	Alluvial-colluvial fan, foot slope	0 to 5	Loamy-skeletal, siliceous, active, mesic Ultic Hapludalfs/Loamy-skeletal, mixed, superactive, mesic Cumulic Hapludolls

are located on the tops and sides of upland ridges, and are moderately well-drained. Peridge soils, found on the tops and sides of upland ridges, in upland depressions, and as Pleistocene (or older) alluvial terraces and upland benches, can be formed from cherty limestone residuum or weathered Pleistocene loess.

The alluvial soils series found along Pearson Creek are Dapue, Cedargap, and the Waben-Cedargap complex (Figure 4, Table 2). Dapue soils are found in the southern portion of the study area, near the confluence of Pearson Creek and the James River. They are well-drained soils formed in silty alluvium and are found on floodplains and low stream terraces of rivers (NRCS, 2008). Cedargap soils are limited to the northwest corner of the study area. They are typically found on floodplains of small streams near active channels and are characterized by a high content of chert fragments (Hughes, 1982). The Waben-Cedargap complex, a combination of Cedargap (40%) and Waben (45%) soils, is found near the confluence between Pearson Creek and the James River. Waben soils are very deep, well-drained, and form in cherty alluvium or colluvium sometimes associated with alluvial fans (NRCS, 2008).

Climate

The climate in the region of Pearson Creek is characterized by warm, humid summers and mild, cool winters. Weather fronts generally move west to east with warm, moist air moving north from the Gulf of Mexico, and cool air moving south from Canada. The mean annual temperature between 1971 and 2000 recorded at the Springfield-Branson Airport was 56.2° Fahrenheit, the annual mean low was 45.0° Fahrenheit, and the annual mean high was 67.4° Fahrenheit. The mean annual precipitation between 1971 and 2000 was approximately 45 inches. The months with the lowest annual mean precipitation (December, January, and February) also have the coldest mean annual temperatures. The wettest months are typically April, May, June, September, and November and the two hottest months are July and August (Figure 5).

Hydrology

The limestone geology in the area has led to complex karst hydrology, demonstrating its influence through the presence of gaining and losing streams, sinkholes, and springs. All of the tributaries along Pearson Creek, with the exception of Jones Branch, are classified as losing streams (Figure 6). Also, the main stem of Pearson Creek has a losing segment just above the Jones Branch tributary input (Bullard et al., 2001). There are a few small sinkholes scattered throughout the watershed (Figure 6). Just outside the eastern and western boundaries of the watershed are large fields of documented sinkholes.

A gaging station operated by the USGS along Pearson Creek is located just upstream of the study area (Figure 7). Flow records for the gage were available from 1999-2008 and are summarized in Table 3. The mean annual discharge is 24.0 cfs. Backflooding from the James River is common during floods and can back water up past where the railroad bridge crosses Pearson Creek in a 10-year flood (USACE, 1970). The highest recorded flood during this time period was on June 13, 2008 and had a discharge of 2,980 cfs. Flood waters from the James River backed up Pearson Creek far enough to inundate the entire study area.

Land Use History

Population around Pearson Creek is influenced by the City of Springfield.

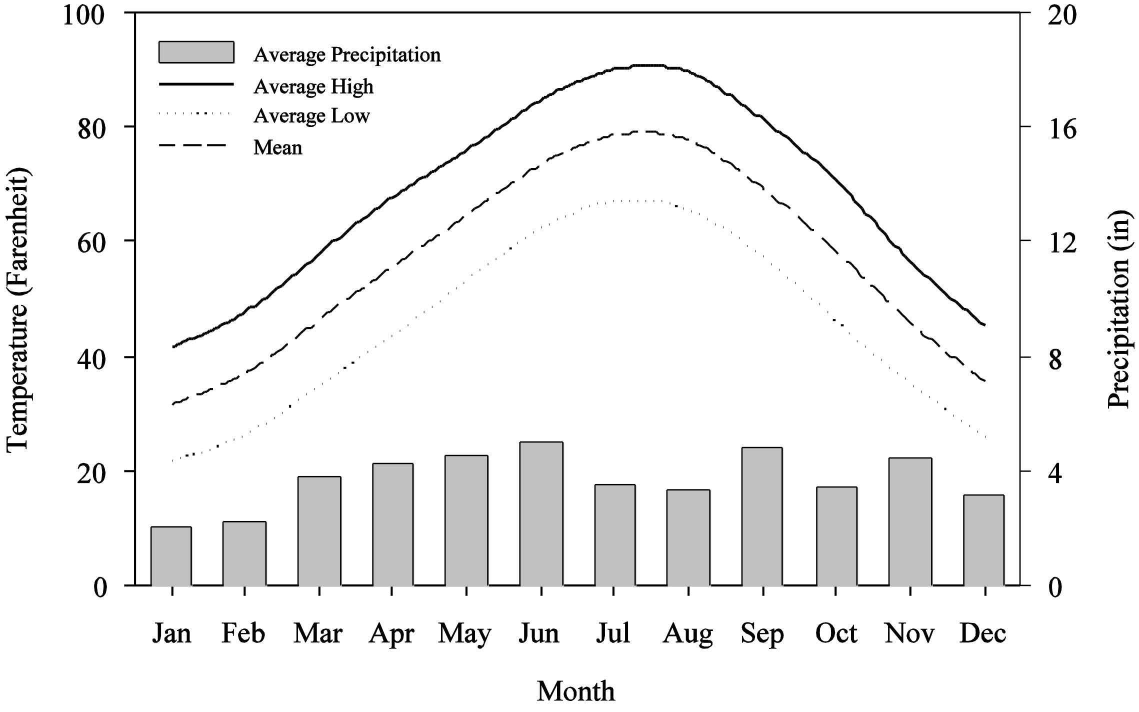

Figure 5. Monthly average temperatures and precipitation. Data recorded at the Springfield-Branson National Airport between 1971 and 2000 (Midwestern Regional Climate Center, 2009).

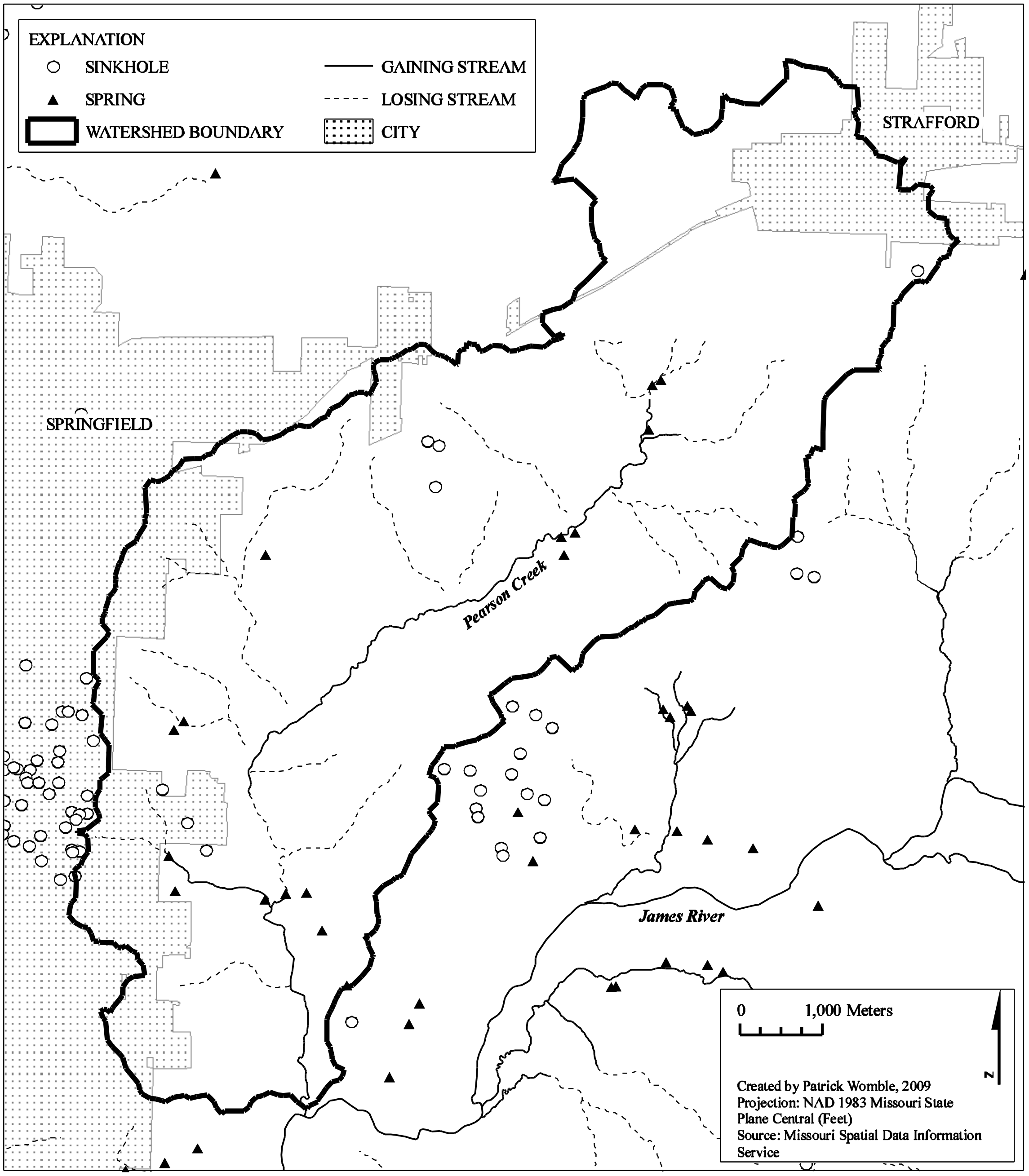

Figure 6. Karst features in Pearson Creek watershed.

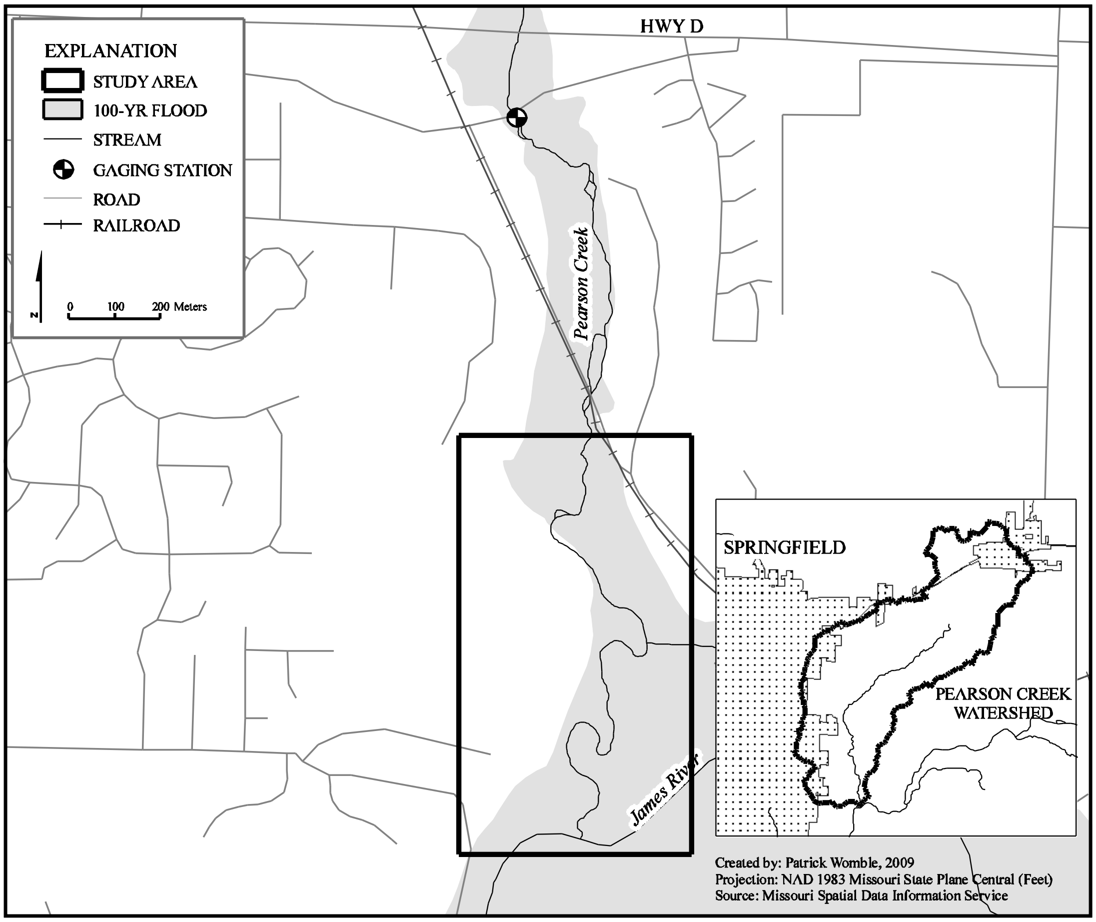

Created by: Patrick Womble, 2009
Projection: NAD 1983 Missouri State Plane Central (Feet)
Source: Missouri Spatial Data Information Service

Figure 7. Location of USGS gaging station and 100-year flood.

Table 3. Annual discharge statistics from USGS gage 07050690 located upstream of the study area (USGS, 2008).

Period of Record	Mean Q (cfs)	Max Q (cfs)	Percentile		
			10th (cfs)	50th (cfs)	90th (cfs)
1999-2008	24.0	2,980	52	9.4	2.4

Springfield grew rapidly during the late 1800s and early 1900s. Land clearing practices in the Ozarks began as early as the 1830s (Rafferty, 1980), significantly altering upland and lowland environments. Grazing is currently the dominant form of land use in the watershed and urbanization is occurring in the most southern portion.

Land Use Change. The presettlement vegetation in the Ozarks largely consisted of oak-hickory forests with scattered bluestem prairies (Rafferty, 1980; Rafferty, 1996). Land use and land clearing in the Ozarks began to change as settlers initiated subsistence and livestock farming. During the 1870s, subsistence farming transitioned to farming for profit (also referred to as general farming) with the invention of new technology that made farming more efficient (Rafferty, 1980). General farming continued to dominate until the 1940s when dairy farming became more profitable (Rafferty, 1980). Since the 1960s, livestock (cattle) farming has been more widespread in the Ozarks than any other form of agriculture (Rafferty, 1980). Figure 8 illustrates Rafferty's four periods of Ozarks land use related to agricultural production, number and type of livestock, and population in Greene County since settlement. One thing to note in the figure is that trends in farming production match fairly well with the four periods described by Rafferty. However, the dairy farming era in Greene County began sooner than Rafferty suggests, overlapping more with the general farming (i.e. corn and wheat). Furthermore, Rafferty does not take into account swine farming, which in Greene County was present throughout Rafferty's subsistence and general farming periods.

Each type of farming has a different amount of impact on the land surrounding it. In general, soil is more likely to be eroded during corn and wheat (row crop) farming due to the loose nature of the soil in the fields. In pastured areas, roots from grasses reduce

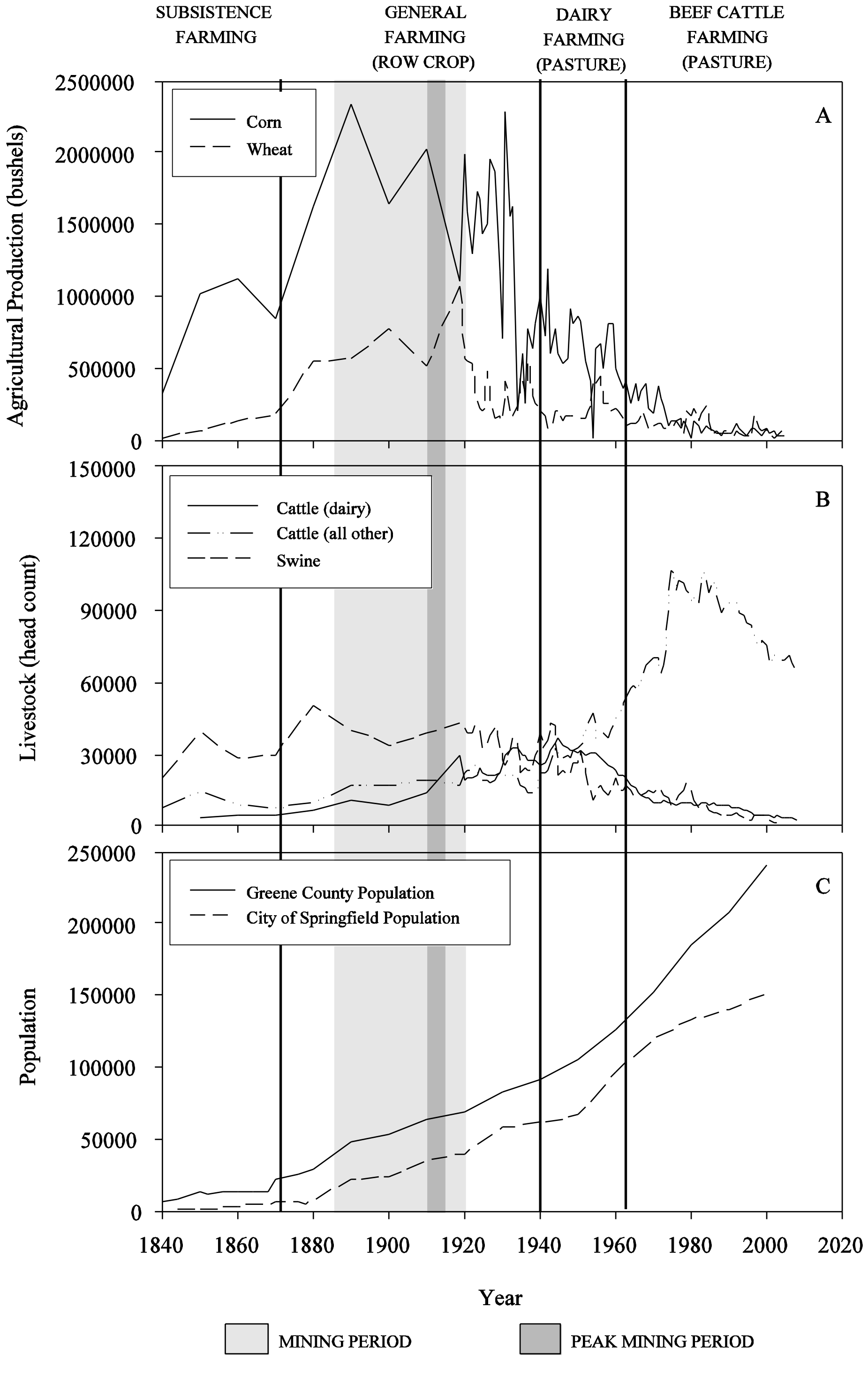

Figure 8. Land use time periods for the Ozarks and Greene County, Missouri. Four land use time periods are shown in relation to trends in agricultural production (A), livestock inventory (B), and population (C) for Greene County, Missouri (Rafferty, 1980; SGCL, 2007).

erosion by trapping and holding soil in place. Also, soil conservation practices put in place slow the erosional impact of various farming practices. Therefore, it makes sense that the amount of erosion occurring in the watershed would have decreased as land use changed from general farming (row crops) to pasture farming, and as soil conservation practices were implemented. However, the combination of swine, dairy farming, and general farming from the early 1800s to early 1900s would have likely caused accelerated hillslope erosion.

According to land use/land cover (LU/LC) data from 2003, the major LU/LC classes present in the Pearson Creek watershed are grassland (57.5%), low intensity urban (14.5%), and deciduous forest (11.4%). Less abundant LU/LC classes are impervious (5.9%), high intensity urban (0.3%), barren or sparsely vegetated (0.6%), cropland (5.1%), evergreen forest (0.3%), deciduous woody/herbaceous (4.0%), herbaceous-dominated wetland (0.1%), and open water (0.3%). The majority of the urban development is located in the southern part of the watershed near the Springfield city limits (Figure 9).

Population. Settlement in Greene County began in the 1820s with the arrival of frontier settlers from the east (Fairbanks and Tuck, 1915). The area became popular due to the abundance of springs and fertile soil, despite some early conflicts with the local Delaware Indians (Fairbanks and Tuck, 1915). The population of Greene County has increased at a nearly exponential rate since the mid 1800s (Figure 8C). The population of Greene County was first reported in the 1840 Census as 5,372, quadrupled by 1870 (21,549), then again doubled by 1890 (48,616), with nearly half the population (21,850) residing in the City of Springfield. The Springfield Metropolitan Statistical Area was ranked the 49th fastest growing metropolitan area in the nation after an increase in

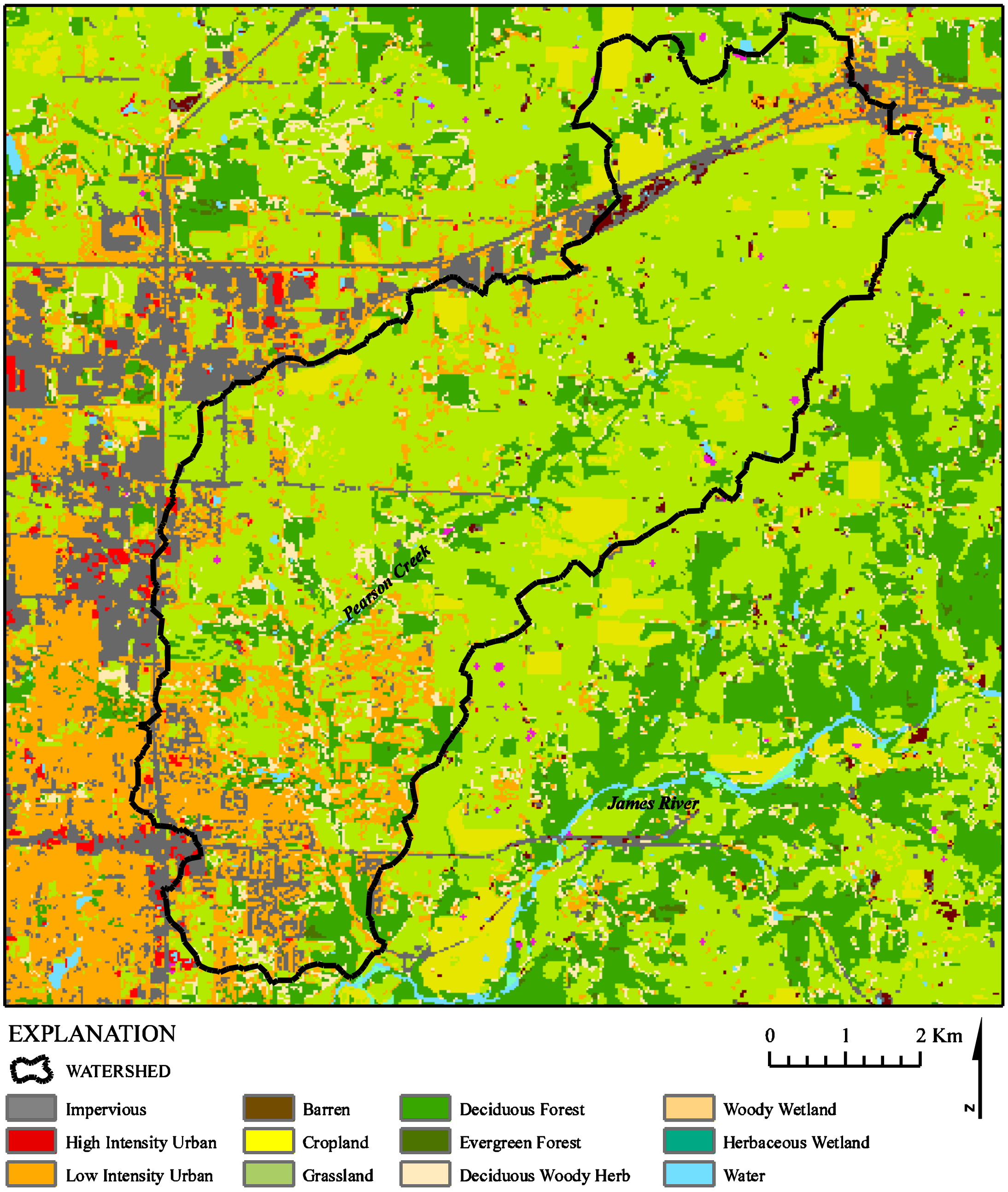

Figure 9. Land use/land cover of Pearson Creek watershed in 2005.

population from 410,619 to 420,020 between 2006 and 2007 (Census Bureau, 2008b).

Mining history

Henry R. Schoolcraft was the first European explorer to document the presence of lead and zinc ore in the Pearson Creek area on an expedition through Arkansas and southern Missouri in 1819 (Rafferty, 1996). Prior to Schoolcraft's expedition, Delaware Indians and trappers in the area mined and smelted lead on a small-scale to create bullets (Rafferty, 1996). Schoolcraft described the lead as "situated in the west bank, and in the bottom of the river, as lumps of ore can be seen through the water." He also noted that the ore was "imbedded in the bank of the river in red clay."

The mines at Pearson Creek are considered to be a sub-district of the Tri-State Mining District, which is located at the junction of Missouri, Kansas, and Oklahoma. Production in the Tri-State area began in the early 1840s as small operations first in Greene (Pearson Creek Mines) and Webster Counties near Springfield, MO and later near Joplin, MO in 1848 (Figure 10; Rafferty, 1980). Large deposits near Joplin were discovered in 1854. Mining in the Tri-State District ended in 1967 and produced over 23 million tons of zinc and 650,000 tons of lead (Rafferty, 1980; Brosius and Sawin, 2001).

The first documented mining prospects near Pearson Creek and the present study area began in 1844 at the Phelps Diggings, located 1.5 km southeast of the Pearson Creek-James River confluence, not in the watershed itself (Figure 10; Fairbanks and Tuck, 1915; Rafferty, 1996). Mining stopped shortly after it began due to transportation expenses and falling lead prices caused by increased production in the Tri-State District and Old Lead Belt mines. Mining south of the James River did not recommence until 1875 (Fairbanks and Tuck, 1915). Shortly after mining at the Phelps Diggings was

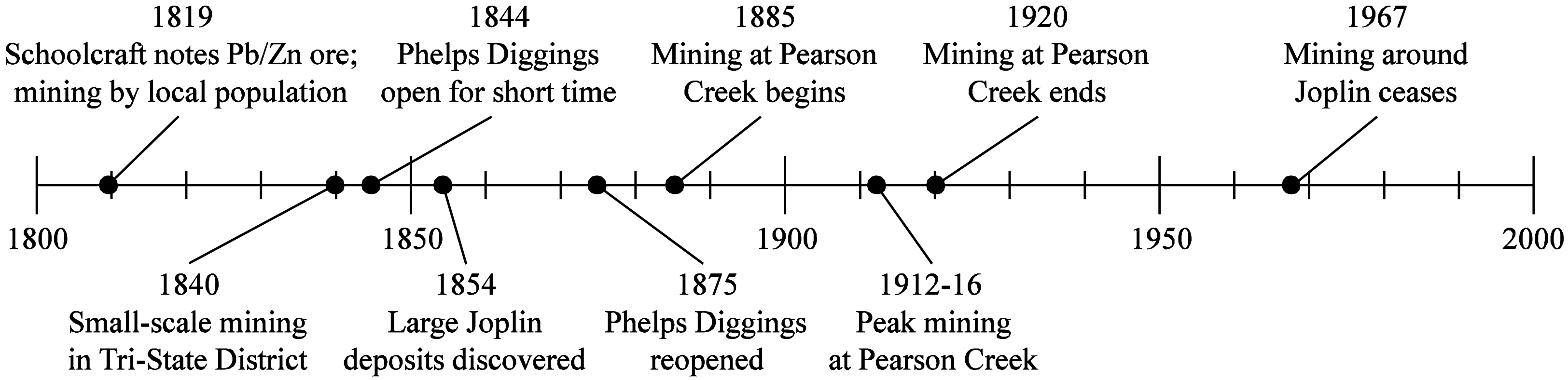

Figure 10. Timeline of mining in the Tri-State District (Fairbanks and Tuck, 1915; Rafferty, 1980; Thomson, 1986; Brosius and Sawin, 2001).

restarted, the Kershner mines (later known as the Suffolk Shafts) were opened to the northwest along the NW trending fault, still outside of the watershed (Figure 11).

Lead and zinc mining in the lower Pearson Creek valley began around 1885, reached its peak around 1912, and ended by 1920 (Figure 10; Thomson, 1986). Approximately 40 mines and prospects were situated in the area during the 35-year span (DGLS, 2008). Mining operations consisted of horizontal tunnels from the valley floor and vertical shafts sunk from the top of the ridge (Figure 12; Thomson, 1986). The mineralized zones probably originated from the injection of mineral-charged fluids along faults, during or just following the Ozark uplift (Thomson, 1986). The weathered Northview Shale, in which the ore was located, was sticky gray clay that made extraction difficult (Fairbanks and Tuck, 1915). Fairbanks and Tuck (1915) describe that due to extraction difficulties, the tailings piles contained a considerable amount of unextracted ore. Today's evidence of mine waste piles cover approximately 168 acres (0.68 km^2) and are mainly located on the east side of the valley (Figure 11).

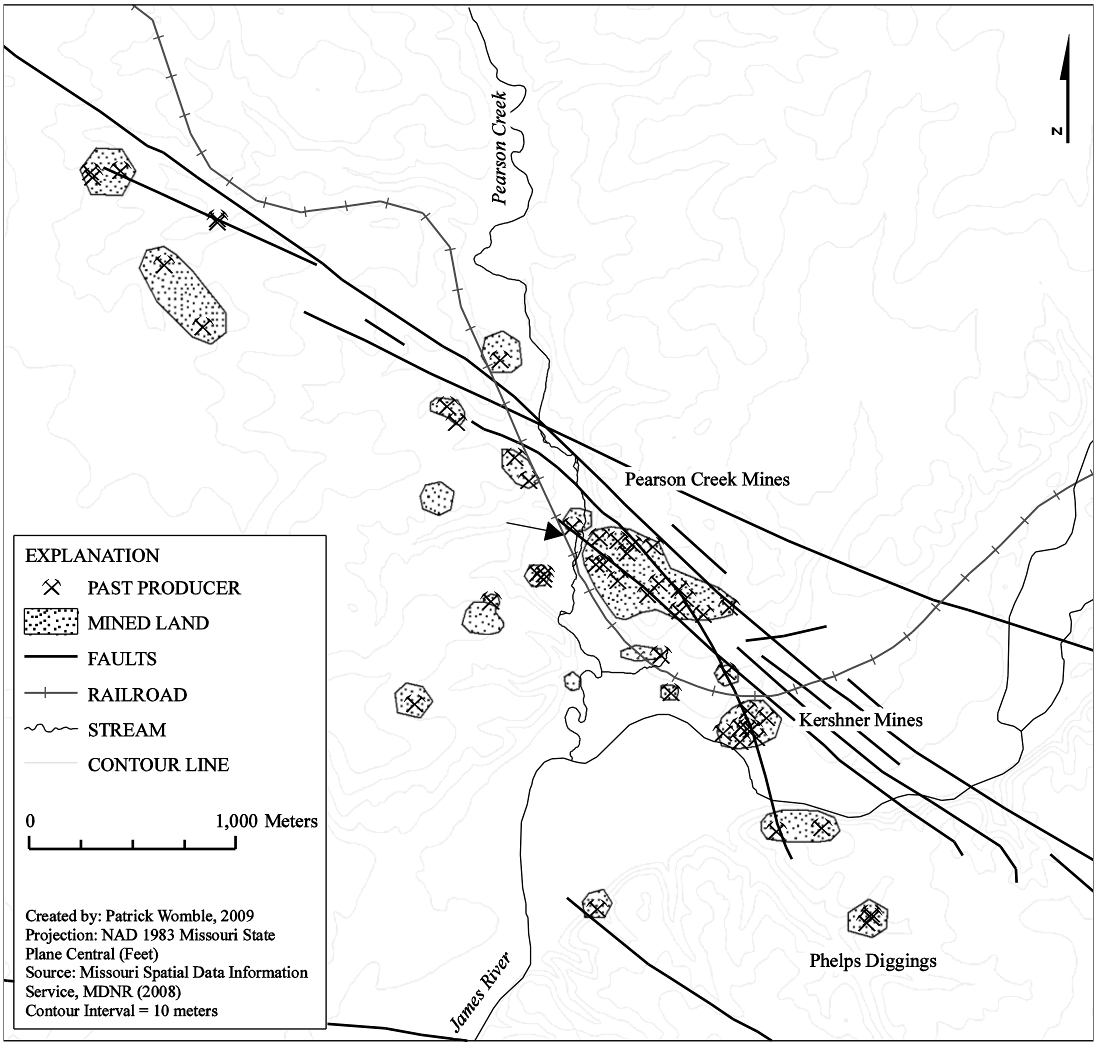

Figure 11. Mining locations in the vicinity of the study area. Note that the majority of the mines are located along the NW-trending faults. Arrow indicates the direction from which the photographs in Figure 12 were taken.

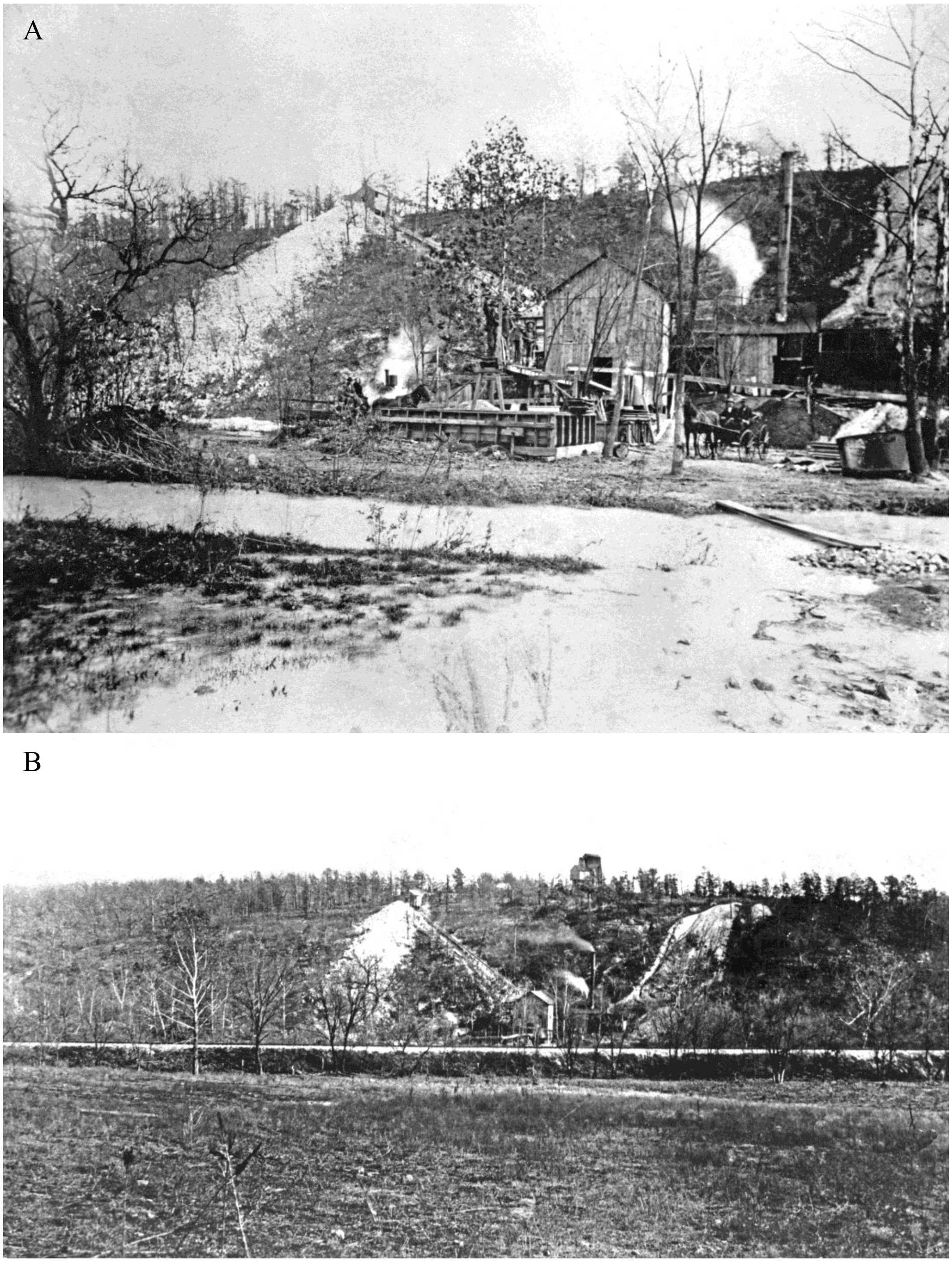

Figure 12. Historic photographs of a mining operation circa 1900. Historic photographs of a mining operation circa 1900. The top photograph (A) shows a close up view of a mine located just upstream of where the railroad bridge crosses Pearson Creek. Pearson Creek is in the foreground with a steam operation next to it and a mill up on the ridge in the distance. The bottom photograph (B) shows the same mining operation from a distance and highlights the extent of mining waste produced by the mine (white mound in the center of the photograph). Courtesy of the History Museum for Springfield-Greene County.

CHAPTER 4

METHODOLOGY

This chapter describes the field, laboratory, and data analysis methods used in this study. Field work and laboratory analysis were conducted between March of 2008 and August of 2009. In the field, cross-section locations were identified and surveyed in order to select the best sites for soil cores. Soil cores were then sampled and transported to the laboratory for geochemical analysis. Geochemical analyses included quantifying zinc concentrations; total carbon, nitrogen, and sulfur content; and grain-size. All laboratory work was completed in the Ozarks Environmental and Water Resources Institute's Geomorphology Laboratory at Missouri State University. Data was analyzed using Excel spreadsheets, SigmaPlot, Logplot, and the geographic information system ArcMap.

Site Selection

Eleven cross-valley transects along Pearson Creek were selected to sample stratigraphic and geochemical attributes of historical overbank and recent near-channel deposits (Figure 13). Transects included areas of the flood valley that would typically be inundated by flows of the 10-year flood. Sites were chosen based on the degree of disturbance at the location and the abundance of geomorphic surfaces present adjacent to the stream. Sites containing more surfaces provide a better representation of recent and historical changes in the locality of the channel. Background samples were collected from 3 different locations near the middle of the watershed and from one site outside of the Pearson Creek watershed along the James River at Turners Station (approximately

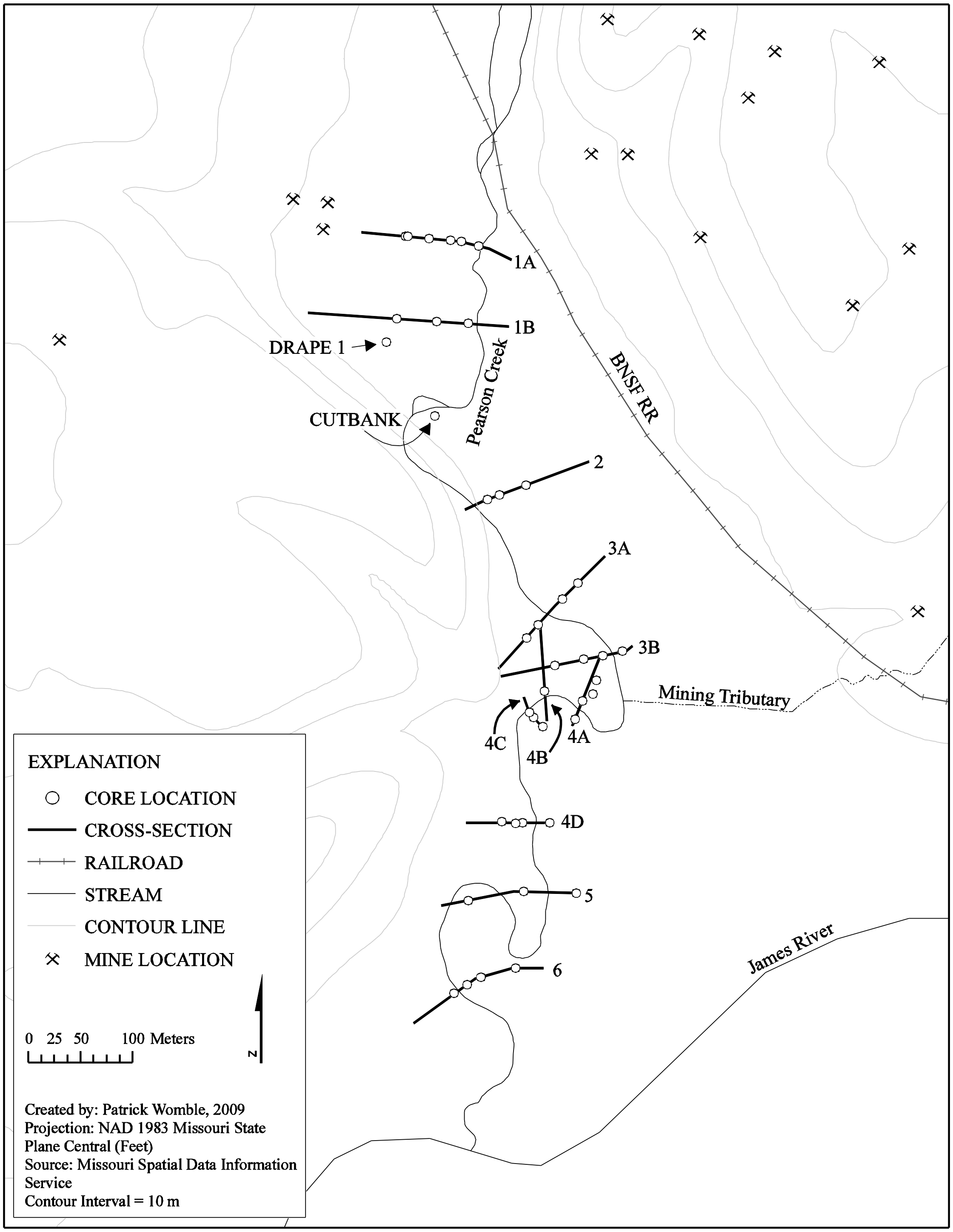

Figure 13. Cross-section and soil core locations.

6 km upstream of the confluence) to determine the natural concentrations of Zn present in alluvial sediment (Figure 14). Two tailings piles, located along a small tributary immediately downstream of Site 3B, were sampled to determine Zn concentration of one source of Zn. Active channel bed sediment in the mining tributary was also sampled to investigate the extent to which this source could be releasing contaminated sediment into Pearson Creek. Sediment collected from Pearson Creek with concentrations above the mean background level plus three times the standard deviation were considered contaminated.

Field Methods

Fieldwork was mainly conducted between winter of 2008 and fall of 2009 on the property of Mr. John Hopkins, who graciously allowed unlimited access to the Pearson Creek study area. Surveying and soil sample collection were the primary field objectives. Soil samples were then prepared back in the laboratory for geochemical and grain-size analysis.

Eleven valley bottom cross-sections were surveyed using an auto-level to determine geomorphic surface elevations relative to the active channel bed. A measuring tape was stretched across the channel at each site and a stadia rod was placed along the tape on the ground surface at 2-3 meter intervals or breaks in slope. Each reading was recorded in a field book and compiled upon returning from the field. Wooden survey stakes were placed at the beginning, middle, or near the banks of the cross-sections and then surveyed with the total station during the longitudinal profile survey. This allowed lines to be drawn between the stakes in a GIS, depicting the actual location and extent of the cross-sections.

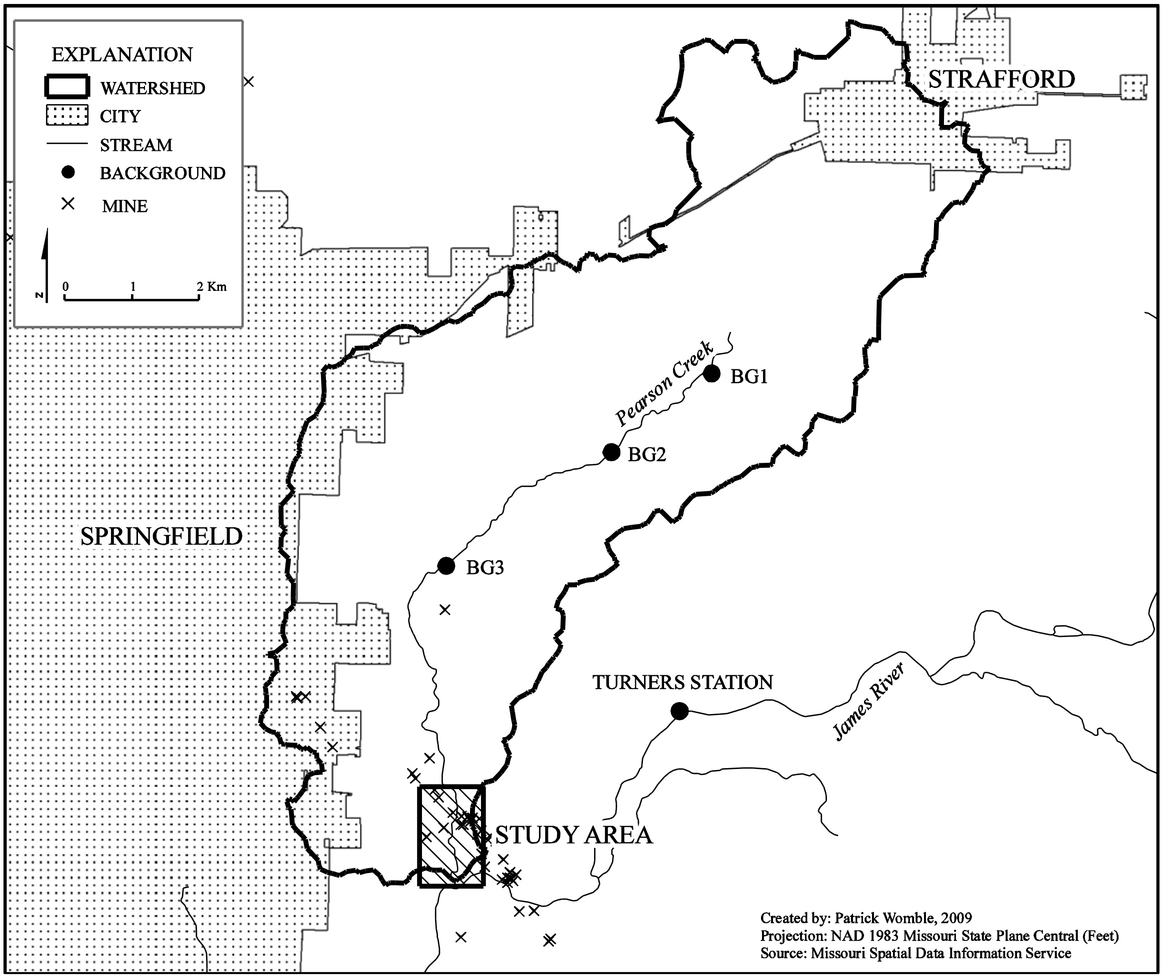

Created by: Patrick Womble, 2009
Projection: NAD 1983 Missouri State Plane Central (Feet)
Source: Missouri Spatial Data Information Service

Figure 14. Background sampling locations. Nine samples were retrieved along Pearson Creek and 28 from the Turners Station site.

An Oakfield soil corer (¾" dia.) was used along cross-sections to sample at 38 soil core locations to ascertain floodplain stratigraphy and geochemical makeup (Figure 13). Two different types of cores, short and long, were collected on landforms. Short cores were sampled ~1 m below the surface while long cores were sampled to refusal or where gleying began. Cores were sampled in increments based on the length of the soil tube on the Oakfield, typically 20-30 cm. After each increment was retrieved from the core hole it was placed in a soil tray and aligned with the previous increment. Once refusal was reached, or it was decided that no further sampling was necessary, soil properties such as color, texture, horizon, and horizon thickness were recorded in a field book. Core length and hole depth were measured to determine if the core was compressed during sampling and recorded in the field book as well. Soil cores were subdivided and sampled based on horizon or observable stratigraphic units such as mining sediment. Sample sizes exceeding 30 cm yielded results that were too general and were thus avoided. Samples of less than 10 cm lacked sufficient volume to be analyzed reliably with the XRF analyzer and were also avoided. Samples were then placed in labeled plastic freezer bags for transport back to the laboratory. The total number of soil samples collected for this study was 391: 9 from background sites, 377 from cross-sections, and 5 from the mining tributary and tailings piles.

Along each cross-section, depth to refusal was measured using an AMS steel tile probe. Depth to refusal was measured across different surfaces as well as in the channel bed. Depth was recorded in a field book and entered into a spreadsheet to be plotted with the cross-section.

A Trimble GeoXH handheld GPS unit was used to plot cross-sections and sample locations in a Geographic Information System (GIS). It was also used to map boundaries of geomorphic surfaces to create the final geomorphic landform map. The GeoXH GPS was connected to a Zephyr antenna and placed next to or on top of the feature being recorded. Each of the points were allowed to collect at least 1,400 positions at one-second intervals during the longitudinal survey and at least 20 positions at one-second intervals during surface mapping. Differential correction of GPS points was done with Trimble's GPS Pathfinder Office V3.10 software using nearby base stations. The corrected data points were used to plot core locations.

Laboratory Methods

All laboratory work was completed by the Ozarks Environmental and Water Resources Institute (OEWRI) Geomorphology Laboratory at Missouri State University. Samples were prepared and subject to geochemical, grain size, and organic matter analyses. These soil properties were used to identify stratigraphic sequences.

Immediately following collection, soil sample bags were opened and placed in an oven to dry at 60 C for several days. Once dried, each sample was labeled with a unique identification number, disaggregated with a mortar and pestle, and passed through a 2 mm sieve to remove any large rock fragments or organic detritus. Between each sample, the mortar, pestle, 2 mm sieve, and sieve tray were cleaned with a solution of 1% hydrochloric acid to remove any residual metals that could cross contaminate subsequent samples. Samples were then transferred into metal-free bags for analysis with the XRF.

An X-MET 3000TXS+ was used to conduct XRF analysis per instructions from the standard operating procedures (OEWRI, 2007b) on all 398 samples. Zinc, Fe, and Ca were detected in 100% of the samples, Pb in 90% of the samples, and Mn in 97% of the samples. Samples in metal-free bags were loaded into the sample holder on the XRF.

The X-MET 3000TXS+ uses a miniature X-ray tube to bombard samples with X-ray radiation for 90 seconds. The instrument reads the intensity and magnitude of fluorescence that is induced by the X-ray bombardment and then calculates element concentrations based on the number of spectral hits in the sample. Results are saved to a porAppendix Digital assistant (PDA) for later download to a computer. For every twenty samples, two laboratory duplicates (LDs), one standard, and one bag blank were analyzed.

Grain-size analysis was performed with an LS 13-320 Laser Diffraction Particle Size Analyzer per the standard operating procedures (OEWRI, 2008) on all 398 samples. After sample preparation, a 200 mg portion of each sample was transferred into separate sample tubes. To remove organic matter, 3 ml of de-ionized water, 600 µl of 30% H_2O_2, and 1 drop of 1% acetic acid were added. Each sample was stirred using a Daigger Vortex Genie for approximately 5 seconds, left to digest for 24 hours, and centrifuged for 3 more minutes. The liquid supernatant was removed and 3 ml of 3% sodium-hexametaphosphate was added to each sample and stirred with a Daigger Vortex Genie for approximately 5 seconds. The purpose of sodium-hexametaphosphate is to aid the disaggregation of sediment particles during sonification. Each sample was stirred again, allowed to settle for approximately 5 minutes, and loaded into the auto-prep station on the instrument where an additional sonification prepared them to be pumped into the aqueous liquid module (ALM). The ALM suspends the samples and re-circulates it through the optical system where particle size is measured. The optical system employs 126 photodetectors that record scattered light intensity patterns as it passes through the sample. The instrument is capable of detecting sediment between 0.04 µm and 2000 µm.

Data Processing and Analysis

After returning from the field, cross-section, depth of refusal, and core profile data were transferred from the field book into a Microsoft Excel spreadsheet, which was used to compile and store all data received from each of the laboratory instruments and plot cross-sections, CNS, Zn, and grain size trends, and calculate various values such as mean depth to peak Zn, local and average sedimentation rates, and background values for Zn.

ArcMap from ESRI was used to accomplish all GIS and cartographic tasks. A 10 m DEM was used to determine the extent of the watershed via tools in the Watershed Toolbox. Base map photography was a 2005 color aerial obtained by MSU through Greene County with a resolution of 0.5 feet. Relevant map layers were downloaded from the Missouri Spatial Data Information Service (MSDIS) and the Center for Applied Research and Environmental Systems (CARES), hosted by the University of Missouri. Additional data was obtained from the United States Geological Survey (USGS) and Missouri Department of Natural Resources. The projection used for all map layers was North American Datum 1983 Missouri State Plane (Central).

Sedimentation rates for the time intervals of 1885-1912 and 1912-2008 were calculated based on the total depth of contamination and the depth to peak contamination. The depth at which Zn concentrations exceed background coincides with the year mining began (1885 at Pearson Creek) while the peak is associated with peak mining production (1912 at Pearson Creek). Everything above the peak Zn depth is representative of how much sediment has been deposited since 1912. Sedimentation rates during the mining period can be determined by calculating the depth between the first occurrence and the peak Zn concentration and dividing it by the time span those values represent, which, at

Pearson Creek, is 27 years. In the same fashion, the sedimentation rates for 1912-2008 can be calculated. One problem when calculating sedimentation rates is establishing the date of the surface. Erosional processes acting upon the surface can remove the sedimentary record and expose sediment deposited at an earlier time. If it was assumed that the date of the surface was contemporary, then the sedimentation rates calculated would be underestimates. However, it is difficult to identify the age of surficial sediment lacks tracers, which is the case at Pearson Creek. Therefore, in this study, the age of the surface was assumed to be the year 2008.

The amount of a pollutant stored in soil is calculated by multiplying the total mass of contaminated soil by the concentration of the pollutant (in percent). The mass of contaminated sediment is determined by:

$$M_{soil} = (A * Dc) * \rho_s \qquad \text{Equation 1}$$

where A is the area of the contaminated soil (in square meters), Dc is the depth of the contaminated soil (in meters), and ρ_s is the bulk density of the soil (in kg/m^3). The mass of contaminant can then extracted by:

$$M_{pollutant} = M_{soil} * C \qquad \text{Equation 2}$$

where M_{soil} is the mass of contaminated soil and C is the pollutant concentration (in percent). The area of the contaminated soil was derived from a digitized map of geo-stratigraphic assemblages divided up by zone. Depth was the average thickness of contamination for cores of the same assemblage type. In this area, the bulk density is approximately 1.3 kg/m^3 (Hughes, 1982). The mass of contaminated sediment (Equation 2), Zn, and Pb were calculated for each assemblage within each zone.

Method Validation

Accuracy and precision demonstrate the limits of instrumentation and provide a way to assess the error of the method. The precision of an analysis reports on the ability of the instrument to get the same results when repeatedly analyzing a sample. In this study, this was done by analyzing lab duplicates of samples. The accuracy of an analysis reports on the instruments ability to determine the actual value of the sample. This was done by analyzing a standard with known concentrations and comparing how close the value determined by the XRF was to the value reported for the standard.

The standard used in the first three batches was supplied by the manufacturer. The reported value of Pb was not accurate and lacked some elements. Therefore the standard was changed after 9/27/2008 to a U.S. Geological Survey soil standard GXR-1. The standard and lab duplicates were used to determine the accuracy and precision of each batch of XRF analyses, which were the result of not being able to analyze all samples in one session. Therefore, the error analysis can be used to identify errors between batches that might cause the need for samples to be reanalyzed. To do this, the measured XRF results were compared to actual values by calculating the relative percent difference (RPD):

$$RPD = ((M - A)/(Average\ (M, A)) * 100\% \qquad \text{Equation 3}$$

where *M* is the value measured value and *A* is the actual value. When determining accuracy for each batch, values determined by the XRF for the standard sample were averaged and used for *M* and the actual value reported in the standard by the USGS value for *A*. Determining precision was a two-step process: first, the RPD for each pair of duplicates was calculated (*A* was the initial analysis, *M* was the duplicate); and second, the average of all those values was calculated and used to determine a value for the analysis batch.

The results of the accuracy and precision assessment for Zn, Pb, Fe, Mn, and Ca are provided in Table 4 and Table 5. Negative mean values in the accuracy assessment indicate that the XRF measurements were below the actual value of the standard while positive error values indicate that the measurements were above the actual value. Zn and Fe were consistently under predicted, Mn and Pb were under predicted in all but one batch, and C (excluding one batch) was consistently over predicted. Zn had the smallest range of values (-1 to -9%), indicating that it tended to be the most accurately analyzed element while Mn had the largest range (-40 to 3%), signifying that it was the most inaccurately analyzed. Fe was the most precisely analyzed element with the smallest range of values while Mn was the least precisely analyzed with the largest range of values. Steps were taken to reduce analysis error, however, several factors could influence the accuracy and precision, including: the heterogeneity of the sediment in the sample bag, void space in the sample, moisture content, insufficient sample size, and cross contamination. Since error values in both the accuracy and precision assessment (excluding Mn) were below ±20%, the results were deemed acceptable and passed the quality assurance/quality control policy of the lab. However, it is reasonable for XRF values to be slightly less than those reported for the standards because standard analyses are based on total digestion while the XRF relies on surface activity only.

Table 4. X-ray fluorescence accuracy assessment. Values are the relative percent difference between the known concentrations of the standard and the concentrations determined by the XRF. Values crossed out were given incorrect standard concentration from the manufacturer of the standard and were therefore excluded. Values labeled "NA" indicate that a value from the manufacturer was not supplied for the standard or there were not enough values to calculate the average RPD for the batch.

Date Analyzed	Zn	Pb	Fe	Mn	Ca
4/3/2008	-2.4%	~~82.9%~~	-12.5%	NA	4.9%
9/25/2008	-2.3%	~~87.9%~~	NA	NA	11.6%
9/27/2008	-7.8%	~~87.9%~~	NA	NA	-1.9%
12/16/2008	-8.8%	-9.8%	-1.1%	-40.3%	5.7%
4/16/2009	-1.7%	-4.9%	-2.1%	2.8%	3.7%
4/21/2009	-2.9%	4.5%	-3.9%	-16.0%	3.6%
4/23/2009	-5.8%	-0.3%	-3.3%	-23.9%	3.3%
4/26/2009	-4.1%	-3.1%	-1.9%	-10.9%	7.3%
4/30/2009	-2.2%	-4.3%	-0.7%	-23.2%	5.1%
n batches	9	6	7	6	9
Mean	-4.3%	-3.0%	-3.7%	-18.6%	4.8%
Median	-1.7%	-3.8%	-2.1%	-19.6%	5.0%
Standard Deviation	2.6%	4.8%	4.0%	14.4%	3.6%
Mean +1 S.D.	-1.6%	1.8%	0.4%	-4.2%	8.5%
Mean -1 S.D.	-6.9%	-7.9%	-7.7%	-33.0%	1.2%

Table 5. X-ray fluorescence precision assessment. Values are the average relative percent difference for each batch between the initial analyses and the laboratory duplicate.

Date Analyzed	Zn	Pb	Fe	Mn	Ca
4/3/2008	-0.01%	0.01%	0.00%	0.01%	0.00%
9/25/2008	14.9%	-4.7%	1.9%	-3.9%	-6.6%
9/27/2008	-2.9%	0.3%	-2.4%	-9.2%	-8.8%
12/16/2008	13.3%	5.2%	-2.4%	-15.1%	14.7%
4/16/2009	7.4%	2.2%	-0.9%	-0.4%	3.6%
4/21/2009	5.3%	-2.3%	1.2%	4.8%	4.7%
4/23/2009	1.7%	-5.3%	2.2%	0.5%	-14.4%
4/26/2009	5.0%	-6.6%	-0.6%	-5.4%	-3.7%
4/30/2009	-1.4%	-2.3%	-2.1%	-5.2%	3.7%
n batches	9	9	9	9	9
Mean	4.8%	-1.5%	-0.3%	-3.8%	-0.8%
Median	5.0%	-2.3%	-0.6%	-3.9%	0.0%
Standard Deviation	6.3%	3.8%	1.8%	5.9%	8.7%
Mean +1 S.D.	11.1%	2.3%	1.5%	2.1%	7.9%
Mean -1 S.D.	-1.5%	-5.3%	-2.1%	-9.7%	-9.5%

CHAPTER 5

TEXTURAL AND GEOCHEMICAL CHARACTERISTICS OF FLOODPLAIN SEDIMENT

Results from geochemical and textural analyses are presented and discussed in this chapter. The chapter is divided into four sections: background Zn determination, floodplain sediment geochemistry, physical attributes of floodplain sediment, and distribution of Zn in floodplains. Establishing background Zn levels help to distinguish between natural and mining-enriched sediment. Sediment geochemistry will be the foundation for validating Zn as a tracer in this study. Zn-sediment relationships will be used to determine what type of sediment Zn is most associated with. Relating Zn concentrations to properties such as elevation, distance from channel, and distance downstream gives clues as to what controls Zn distribution within alluvial deposits.

Background Zn Concentration

Pearson Creek background data were used evaluate the natural geochemistry of the watershed (Figure 14). Nine samples from cutbanks along Pearson Creek upstream of the mining areas were analyzed with the XRF. These values were compared to values from 28 samples along the Upper James River upstream and out of the mining area (Figure 14). Background concentrations of Zn in Pearson Creek watershed averaged 54 ppm with a standard deviation of 14 ppm and for Turners Station along the James River averaged 40 ppm with a standard deviation of 8 ppm (Table 6). An upper limit was determined by adding 3 times the standard deviation to the mean value of the 9 Pearson Creek samples. All samples with concentrations of Zn greater than this value (97 ppm)

Table 6. Background Zn statistics from Pearson Creek, the James River near Turners Station, 7.5YR samples, and 10YR samples.

Location	*n*	Mean (ppm)	Geometric Mean (ppm)	Standard Deviation (ppm)	Coefficient of Variation (%)	Mean + 3X Standard Deviation (ppm)
Pearson Creek	9	54	52	14	26	97
James River near Turners Station	24	40	39	8	20	64
7.5YR Samples (<97 ppm)	17	41	38	16	38	88
10YR Samples (<97 ppm)	111	69	67	14	21	111

were considered to be anthropogenic-related and deposited since mining began in 1885. Results show that background sampling locations along upper Pearson Creek seem to be slightly more enriched with Zn than the James River at Turners Station. This could be from industrial inputs, urban effects, or the result of dissimilar geology between the two locations. For example, Pearson Creek has several faults in the upper part of the watershed that could contain minor deposits of Pb and Zn ore and elevate the background levels slightly (Figure 3).

In addition to comparing Pearson Creek to James River sediment, floodplain sediment samples with 7.5YR and 10YR color with concentrations below 97 ppm Zn were analyzed (see Chapter 6 for details on soil color dates). Samples with 7.5YR color were analyzed to see what background concentrations might have been between the Early and Late Holocene. Similarly, samples with 10YR color were analyzed to see what background concentrations might have between the Late Holocene and the initiation of mining. Results show that mean background concentration between the Early and Late Holocene (41 ppm) were lower than between the Late Holocene and the initiation of mining (69 ppm) and that current mean background concentrations fall between the two (54 ppm). Higher Zn concentration in the 10YR sediment implies that some enrichment occurred during the Late Holocene. This might have been due to natural weathering processes caused by incision into the mineralized zones located along the faults, which it does in several places upstream of the study area (Figure 11). Also, the mean Zn concentration in 7.5YR sediment is similar to the mean Zn concentration along the James River. This suggests that either backflooding of the James River might have been responsible for the formation of surfaces with 7.5YR sediment or a sufficient amount of time has allowed weathering processes to leach away the Zn.

Floodplain Sediment Geochemistry

Geochemical and textural data presented in this section are used to examine the magnitude of Zn, Fe, Mn, and Ca in floodplains along Lower Pearson Creek and relationships between Zn and Fe, Mn, and Ca. Metal-sediment relationships reveal how and where Zn is stored in floodplain sediments.

Metal Concentrations. X-ray fluorescence analysis results for Zn, Pb, Fe, Mn, and Ca are displayed in Table 7. The median Zn value indicates that in over half of the samples analyzed, Zn is present in concentrations exceeding background levels (77 ppm) and is more abundant than Pb, the other mining indicator. The large range of concentrations encompasses background (pre-mining) sediment, as well as highly contaminated mining and post-mining sediment. The source of high Ca concentrations is the limestone bedrock in the area primarily in the form of carbonate-rich mill wastes from nearby mining operations. In contrast, Fe and Mn sources are primarily related to natural chemical weathering.

Zn-Metal Relationships. Zinc concentrations in both contaminated and uncontaminated samples were plotted against Fe, Mn, and Ca to explore potential relationships. Due to its tendency to be highly mobile, a strong relationship with Mn might suggest that Zn is also mobile, while a strong relationship with Ca could imply that Zn is attached to tailings sediment and is relatively immobile. In contaminated and uncontaminated sediment, the vertical trend in the Fe-Zn plot (Figure 15) indicates Fe concentrations are relatively constant and that Zn is not associated with Fe. This is to be expected since Fe is not related to the mining waste sources. The same conclusion can be applicable to the vertical trend between Mn and Zn in contaminated sediment (Figure 16). However, the horizontal trend between Mn and Zn (Figure 16) in uncontaminated

Table 7. Metal concentrations in floodplain sediment along Pearson Creek.

Element	*n*	Min	Percentile			Max	Mean	Geometric Mean	Standard Deviation
			25th	50th	75th				
		ppm	ppm	ppm	ppm	ppm	ppm	ppm	ppm
Zn	382	18	72	192	666	12,395	600	230	1,151
Pb	347	11	25	69	147	4,768	190	64	404
Fe	382	12,683	16,789	18,115	19,540	25,560	18,160	18,037	2,123
Mn	378	34	928	1,152	1,288	5,870	1,131	965	566
Ca	382	1,107	3,563	9,355	18,794	181,893	16,479	8,829	23,727

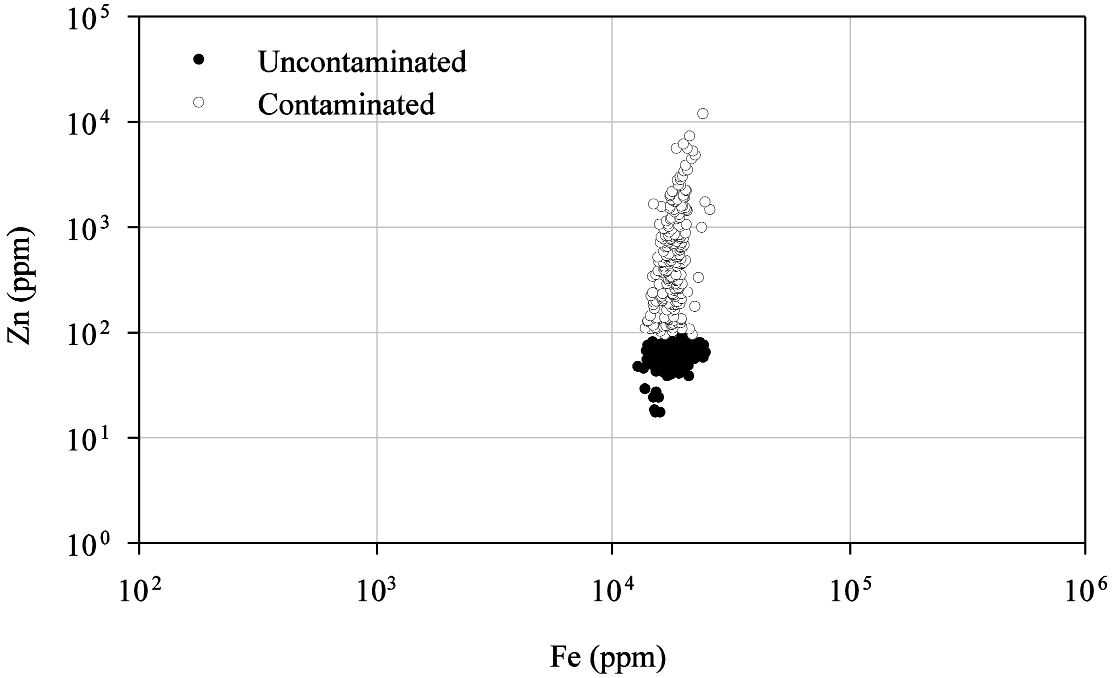

Figure 15. Zn vs. Fe in contaminated and uncontaminated sediment.

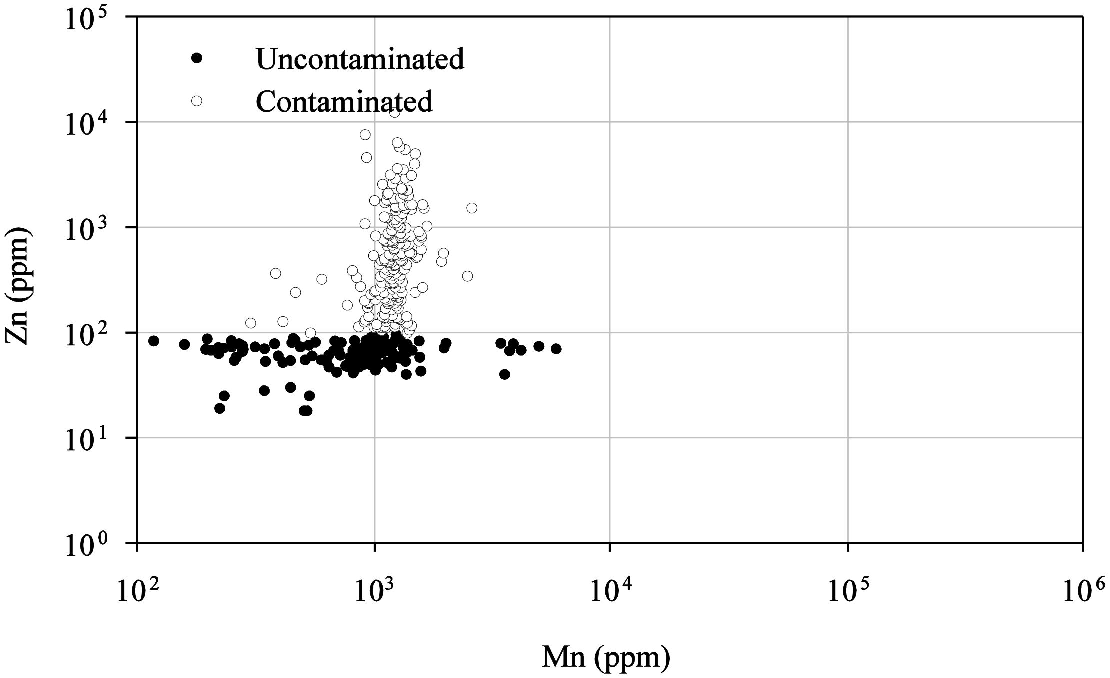

Figure 16. Zn vs. Mn in contaminated and uncontaminated sediment.

sediment can be explained by the high mobility of Mn in a saturated environment. Field observations confirm that Mn staining is present in these sediments and as coatings on gravel from lower floodplain deposits. Also, the strong positive relationship between Zn and Ca in contaminated samples demonstrates that Zn is primarily associated with calcium carbonate rock and fine sediment as sphalerite or sorbed forms (Figure 17). Uncontaminated sediment is within many of the same gleyed and deep samples that Mn depletion occurs and suggests Ca is precipitating out of Ca-rich groundwater during fluctuations in groundwater elevation (Figure 17).

Physical Attributes of Floodplain Sediment

Soil Color. Four broad soil colors were observed at Pearson Creek: 10YR, 7.5YR, 10YR 7/1 (mining-related), and gleyed (chroma <2). Soils with 10YR color were interpreted to be A, Bw, and C horizons up to 3 m thick. Sediment in the agricultural field on the eastern side of the valley is predominantly 7.5YR with a thin 10YR plow horizon on top. Mining-related sediment (10YR7/1) is typically within 1 meter below the surface and was discovered as both laminations and layers up to 1 meter thick. Dark gray, gleyed sediment with abundant redoximorphic features (Fe and Mn staining) was present at the bottom of cores that reached or went below the water table.

Sediment color may be used for interpreting the age of the deposit in the Ozarks. Sediments along the Pomme de Terre River with characteristics similar to those found at Pearson Creek were dated using ^{14}C by Brakenridge (1981). Brakenridge found that 10YR4/3 sediment in the Pippens formation, similar to the deeper 10YR sediment at Pearson Creek, was recent to late Holocene in age (0-1,600 yr B.P.). The 7.5YR sediment in the Rodgers formation, similar to the sediment found in the agricultural field

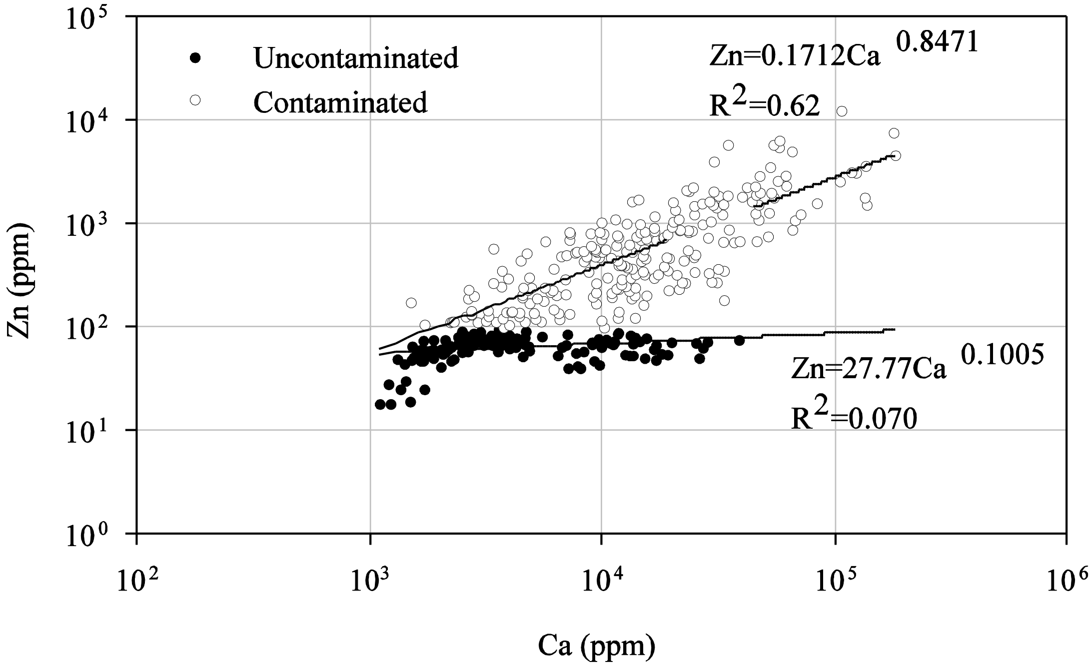

Figure 17. Zn vs. Ca in contaminated and uncontaminated sediment.

at Pearson Creek, was early to late Holocene in age (11,500-1,600 yr B.P.).

Sediment Texture. Sediment was classified into sand (2000-62.5µm), silt (62.5-3.9µm), and clay (<3.9µm). More than 92% of the samples were classified as silt loams on a USDA soil texture diagram, with loam, sandy loam, and sand making up the remainder (Figure 18). The dominance of silt loam is reasonable since all but the tailings tributary samples are located within the Cedargap and Dapue soil series, which are classified as gravely silt loam and silt loam, respectively (NRCS, 2008). Vertical profiles of sand, silt, and clay also show a general lack of sand. Three cores (Site 4A: 7 m, 25.5 m; Site 5: 0 m) display a fining upward sequence (Figure 19) and five cores (Site 2: 66 m; Site 3A: 36.4 m, 91.5 m, and 108.5 m) exhibit a slight coarsening upward trend (Figure 20). Fining upward trends are characteristic of fluvial environments where floodplains are formed by lateral and vertical accretion due to the lateral migration of the channel. Coarse material present at the base of the sequence usually represents the elevation of a previous channel bed or a bar. Floods deposit sediment on top of the bar, increasing the height of the surface. Progressively finer sediment is deposited on top of the surface as the flow required to inundate the surface increases. Coarsening upward sequences could be the result of gravel splay deposition on top of previously deposited fine-grained floodplain sediment or changes in sediment source. All remaining cores have occasional small peaks or drops in sand but are mostly uniform. The uniformity of the samples is likely the result of the system being dominated by a bi-modal source of sediment supply, either gravel or fines. Fines (silt and clay) are found in overbank deposits and back swamp environments at Sites 1A and 1B but are generally lacking in active bed sediment. The active channel bed is composed of gravel and very little sand, which is not surprising considering the surrounding geology contains only very minor amounts of sand and no

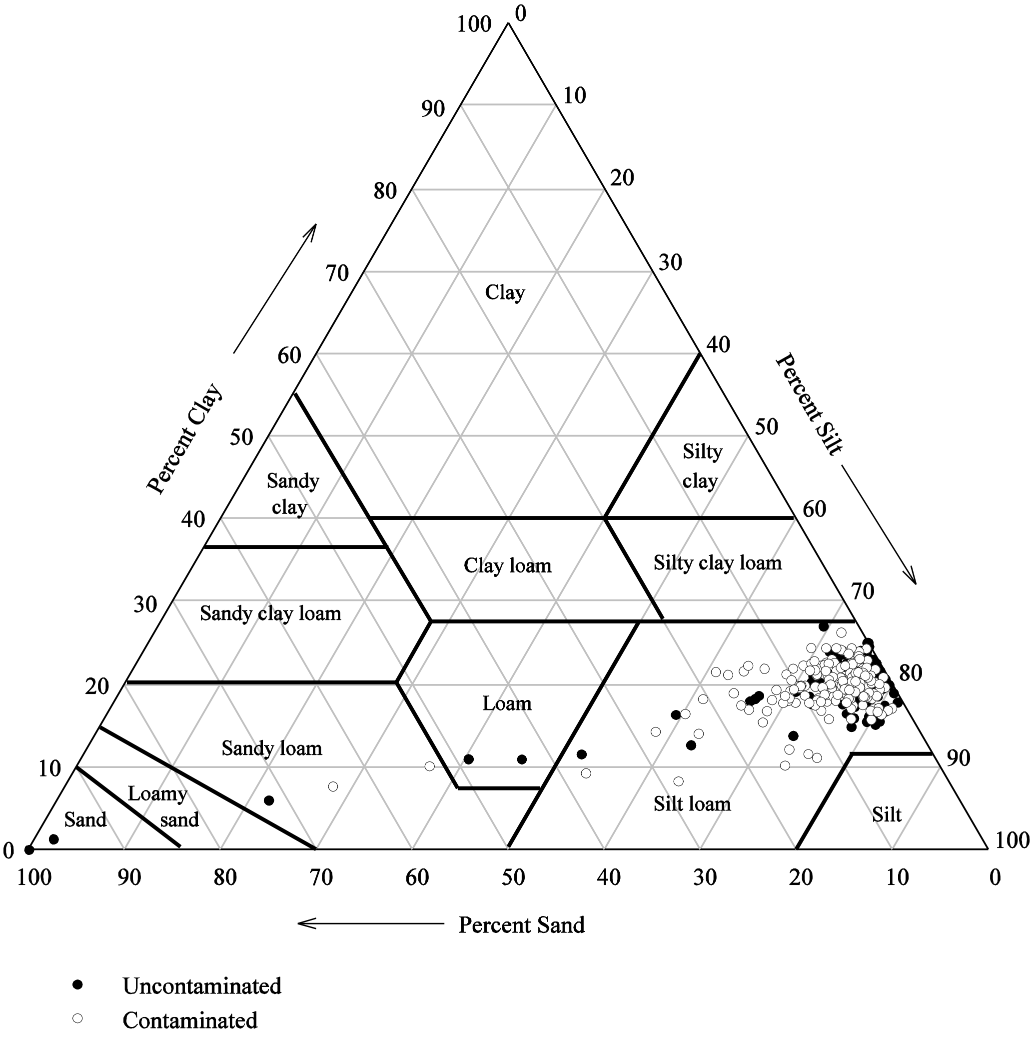

Figure 18. Sediment texture data from Pearson Creek plotted on a texture classification diagram. Modified from Figure 3-16 of Soil Survey Division Staff (1993).

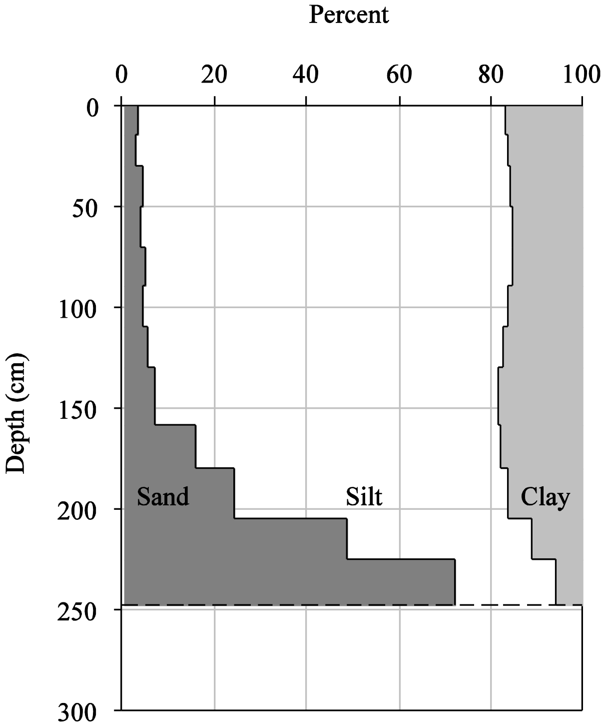

Figure 19. Example of a fining upward sequence from Site 4A at 7 m.

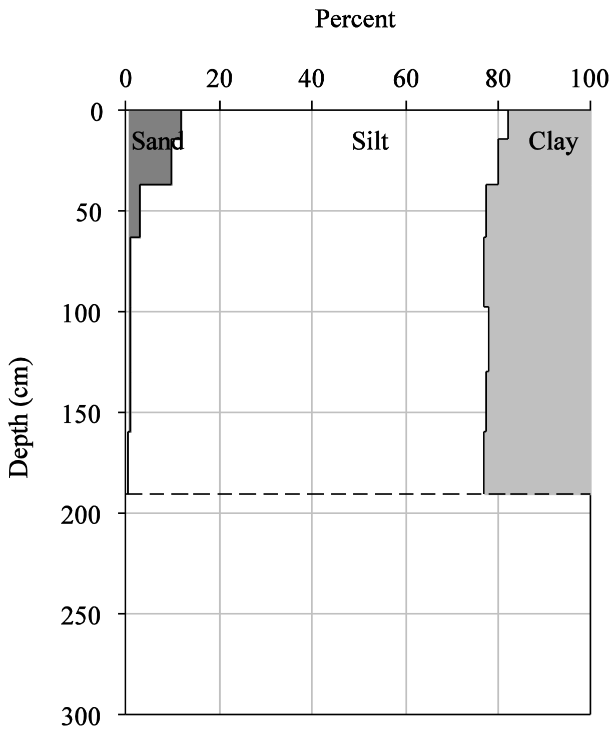

Figure 20. Example of a coarsening upward sequence from Site 3A at 108.5 m.

other significant sources of sand exist in the watershed. Therefore, the only sediment available to be deposited on floodplains during floods is silt and clay.

Sediment-metal Relationships. It is important to understand how Zn is associated with sediment size fractions in environmental assessments as it gives clues to source, geochemical behavior, and physical mobility (Leenaers, 1989). Zn was plotted against three grain size fractions: sand (2000 - 62.5 μm), silt (62.5 - 3.9 μm), and clay (<3.9 μm). Sand percent (Figure 21) in contaminated sediment has a weak positive relationship with Zn (R^2=0.40) while contaminated silt and clay-sized sediment have no relationship with Zn (Figure 22, Figure 23). Pavlowsky (1995) found a strong relationship between Zn concentration and sand percent; however, the results presented here show a weak correlation, likely the result of waste from the milling process being introduced into the system. Consequently, it appears that in this system, grain size does not play a major role in the distribution of Zn contamination.

Distribution of Zn in Floodplains

Soil Core Trends. In these cores, trends are interpreted from the bottom-up by noting high or low Zn concentrations. Zinc concentrations typically start below background, increase sharply, and then gradually decrease up to the surface (Figure 24). The depletion of Zn above the peak Zn concentration could be caused by sediment mixing, reduced flood inundation due to vertical accretion on banks or channel widening, a reduction of contaminated sediment influx following the cessation of mining, or any combination thereof (Knox, 1987; Lecce and Pavlowsky, 2001). The sharp increase in Zn concentration is indicative of the barrier between mining-influenced sediment and

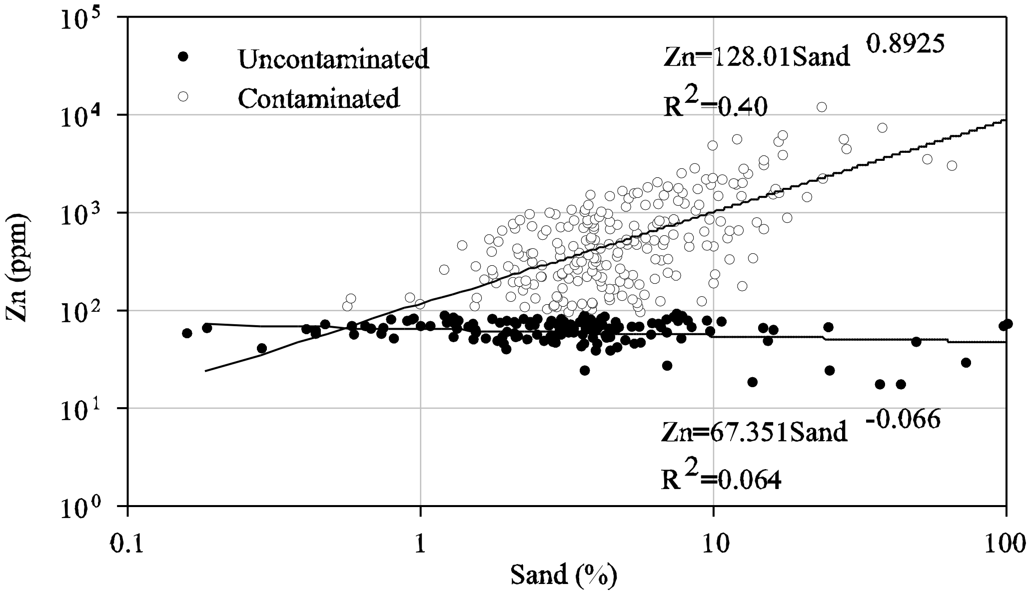

Figure 21. Zn vs. sand in contaminated and uncontaminated sediment.

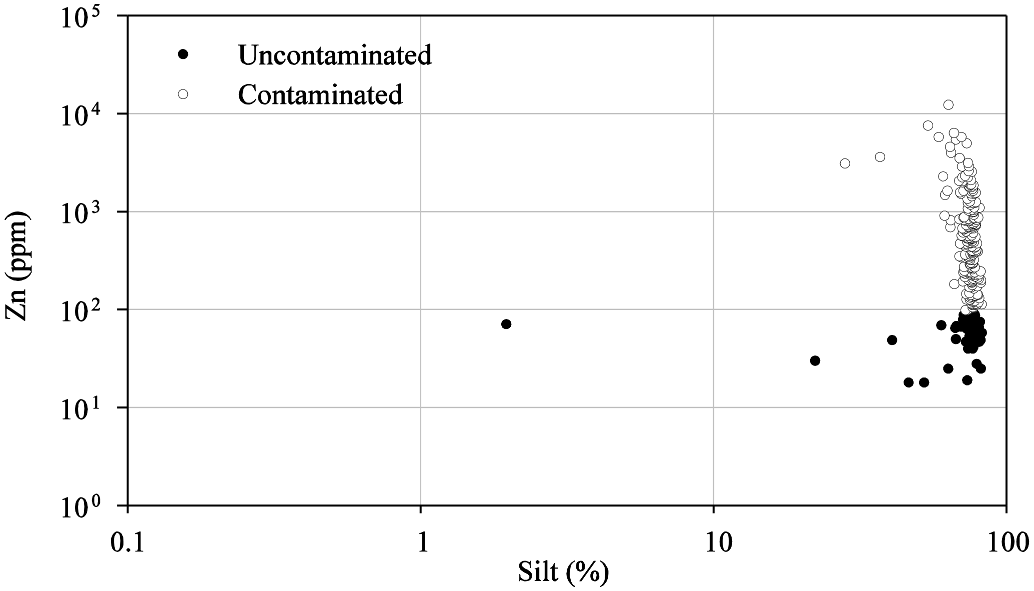

Figure 22. Zn vs. silt in contaminated and uncontaminated sediment.

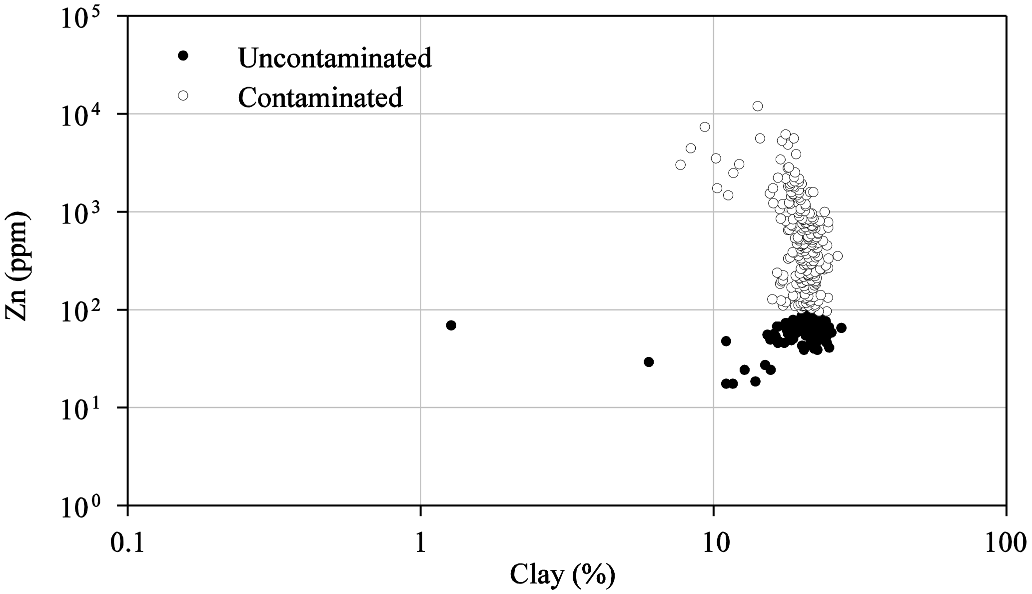

Figure 23. Zn vs. clay in contaminated and uncontaminated sediment.

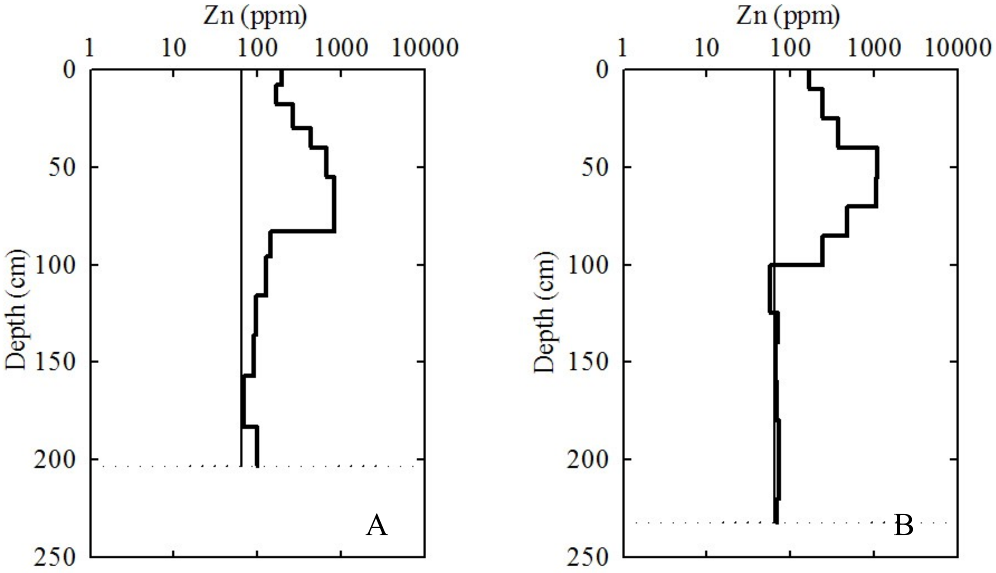

Figure 24. Example of Zn in the down-core direction. (A) Site 1B at 107 m showing possible effects of core extraction contamination and (B) Site 3A at 58 m illustrating a core with very little core extraction contamination. Zinc (thick black line), three times the standard deviation of the average background concentration (thin black line), and bottom of the core (dotted line) are shown.

sediment that was deposited prior to mining. Gradual or drawn out decreases in Zn in the down-core direction are the result of vertical migration of Zn, local inputs by mine diggings (Lecce and Pavlowsky, 2001), weathering of ore outcrops, or Oakfield contamination. Because Zn in this area is not very mobile, vertical migration of Zn would be low. Sampling errors occur for two reasons during sampling: (1) core extraction and (2) sample interval selection. During core extraction, uncontaminated samples located stratigraphically below contaminated samples must be pulled up through contaminated portions of the core hole. The Oakfield barrel is open and can scrape off contaminated soil and lead to cross-contamination. Sampling intervals were based primarily on physical differences present in the core. It is possible in cores that show very little physical differentiation that the point between the initial Zn and uncontaminated sediment was mistakenly located in the middle of the core sample. This would effectively mask the transition between contaminated and uncontaminated sediment by diluting the contaminated sediment with the uncontaminated sediment directly beneath it and result in an overall lower Zn concentration. Early mining operations would have also introduced contaminated sediment into the stream at volumes and concentrations lower than during the peak mining period since the scale of mining production was much lower. The increasing input of mine waste during larger scale mining operations would be reflected in the floodplain stratigraphy as a gradual increase of Zn up to the peak concentration. While there is no direct evidence for early small-scale mining operations in the immediate area or upstream, Schoolcraft noted that the local natives were mining galena from the stream and smelting it to make bullets when he visited in 1819 (Rafferty, 1996). Even though Pb and Zn were in the same deposits, processing techniques for Zn were not available during the early mining, so if an early mining signal did exist, it would be expressed by a slight increase in Pb stratigraphically below the initial contamination of Zn. However, there are not any deviations of note between Pb and Zn.

The lowest concentrations of Zn were found in gleyed sediment or gravel at the bottom of cores or in the upper terrace surface. The highest concentration of Zn in the study area (12,395 ppm) was found at a cutbank exposure of an historic point bar deposit just south of Site 1B (Figure 13). The sediment at this location is very uniform in size with no discernable laminations or structure present, suggesting that it might have been deposited over a very short amount of time, perhaps one flooding event or following a tailings dam breach. The location suggests that sources upstream of the current study area were contributing significant amounts of mining-related sediment to the system.

Valley Distribution. As stated previously, work by others have found that Zn concentrations tend to be highest near abandoned mine sites and decrease with distance downstream (Lewin and Wolfenden, 1978; Bradley and Cox, 1986; Graf, 1996; Carlson, 1999; Lecce and Pavlowsky, 2001; Trimble, 2001). At Pearson Creek, there is a lot of variability in Zn in the downstream direction, however, a general decreasing trend can be observed with a small increase where the mining tributary enters (Figure 25). The mean of the upper 50 cm was plotted to show the concentrations of recent sediment deposits. However, there is little difference between the mean and the mean of the upper 50 cm.

Distance from Thalweg. Plots of Zn concentration and distance from the thalweg were used to see how much of a role distance played in the distribution of Zn across floodplains. Zinc concentrations were typically highest close to the thalweg and decreased with distance away from it (Figure 26). However, cores close to, as well as far from, the channel can have high or low Zn concentrations. This is likely because the

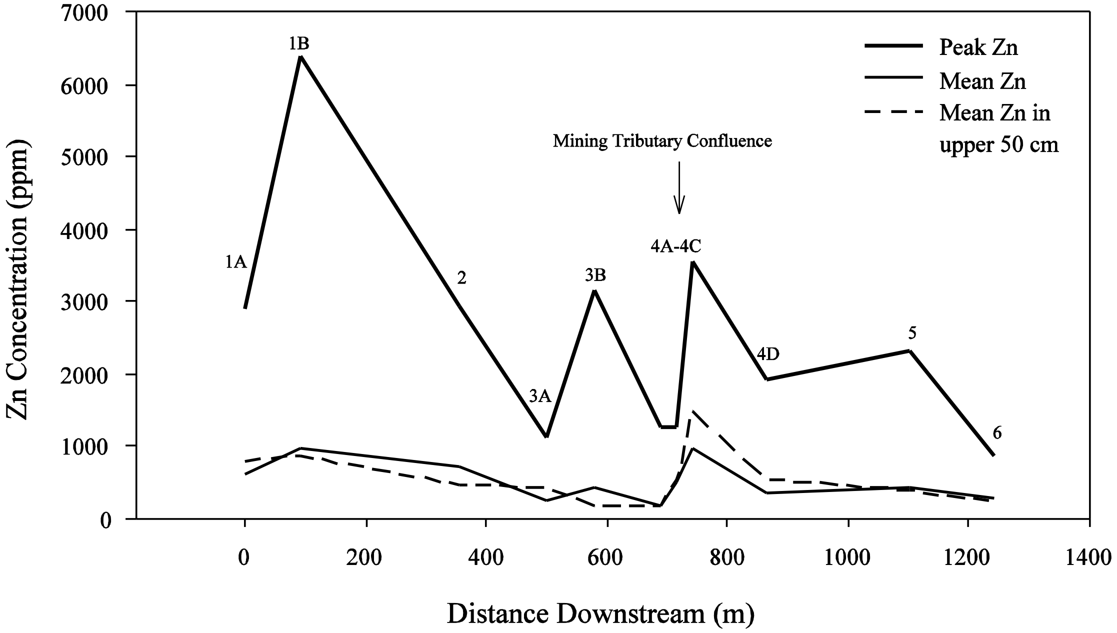

Figure 25. Downstream distribution of Zn. There is a general decrease downstream in Zn concentrations of the peak, mean, and mean in the upper 50 cm.

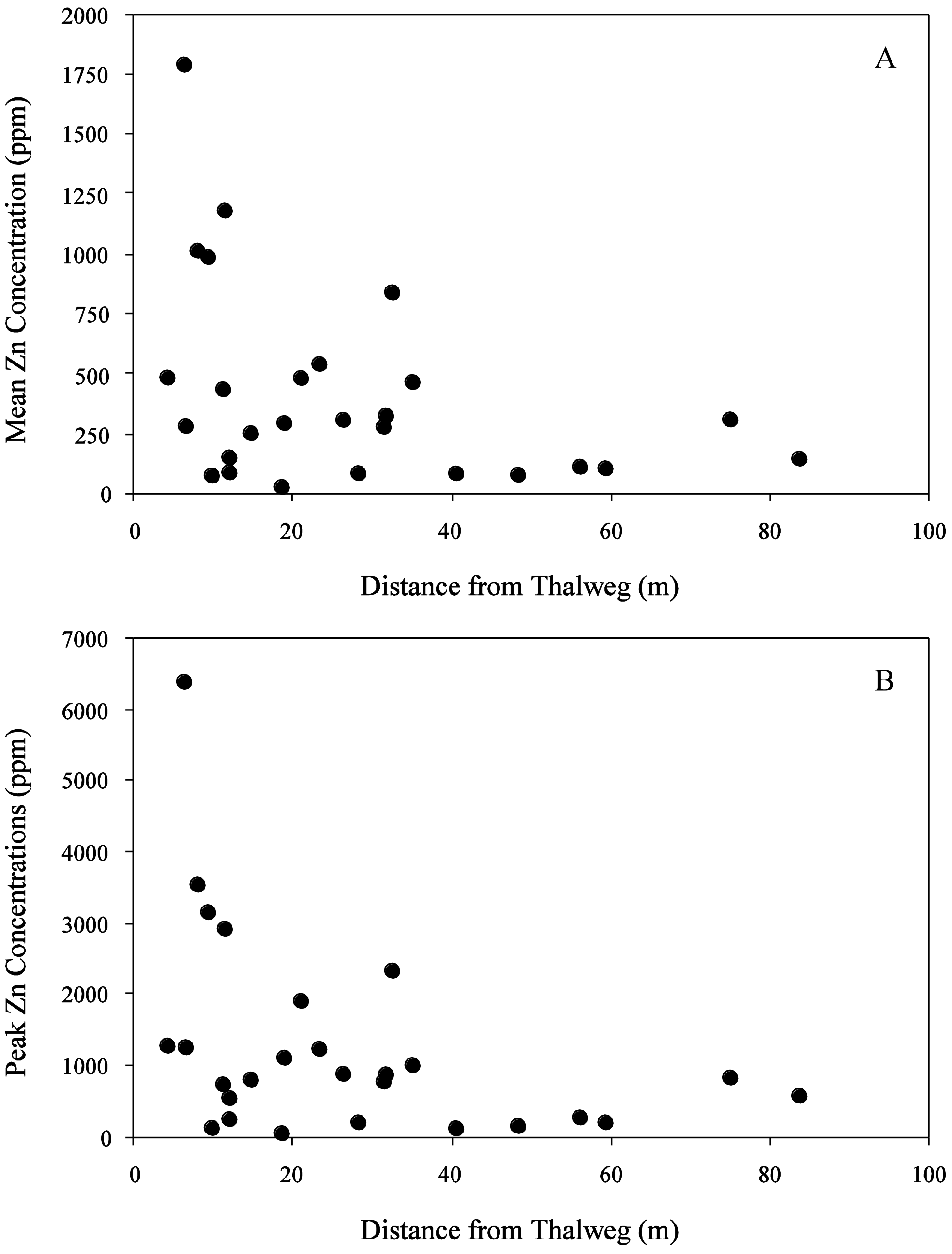

Figure 26. Zn concentration vs. distance from thalweg for the mean (A) and peak (B) Zn concentration.

spatial distribution of Zn across floodplains is complex. Brewer and Taylor (1997) suggest that the complexity is the result of patterns, rates, and timing of deposition tied to the state of the stream at different time periods. Lecce and Pavlowsky (2001) found similar results in cross-valley cores in the Blue River watershed in Wisconsin. They explained that, in addition to floodplain topography, cross-valley distribution of contaminated sediment is determined by the size of the sediment being transported, surface roughness, and available storage space (i.e. wide valleys).

Elevation above Thalweg. Plots of Zn elevation and surface elevation above the thalweg were used to see how much of a role surface elevation played in the distribution of Zn within floodplains. As the surface elevation increases, depths to initial and peak Zn concentrations tend to decrease (Figure 27). High surfaces close to the channel tend to have very little contamination present and, as a result, cause scattering of the data.

The distribution of Zn contamination at any location is largely determined by its distance from and elevation above the thalweg. Surface elevation above the thalweg, core distance from the thalweg, and thickness of Zn contamination data were used to create a three dimensional surface and illustrate some general trends in the data (Figure 28). The 3-D surface shown in the graph indicates that the thickest contamination is located within ~20 m of the channel and on low surfaces (<2.5 m). This trend marks recent channel migration and backfilling on the inside of meander bends to the depth of the bed. Thicker packages of contaminated sediment located between 60 and 80 m on the figure are from cores located at Sites 1A and 1B. At both of these sites, the channel is located on the east side of the valley with a low, wide surface extending to the bluff on the west side of the valley. The width of the low surface is greater in these areas than at sites where the channel is located in the center of the valley and, therefore, the distance of

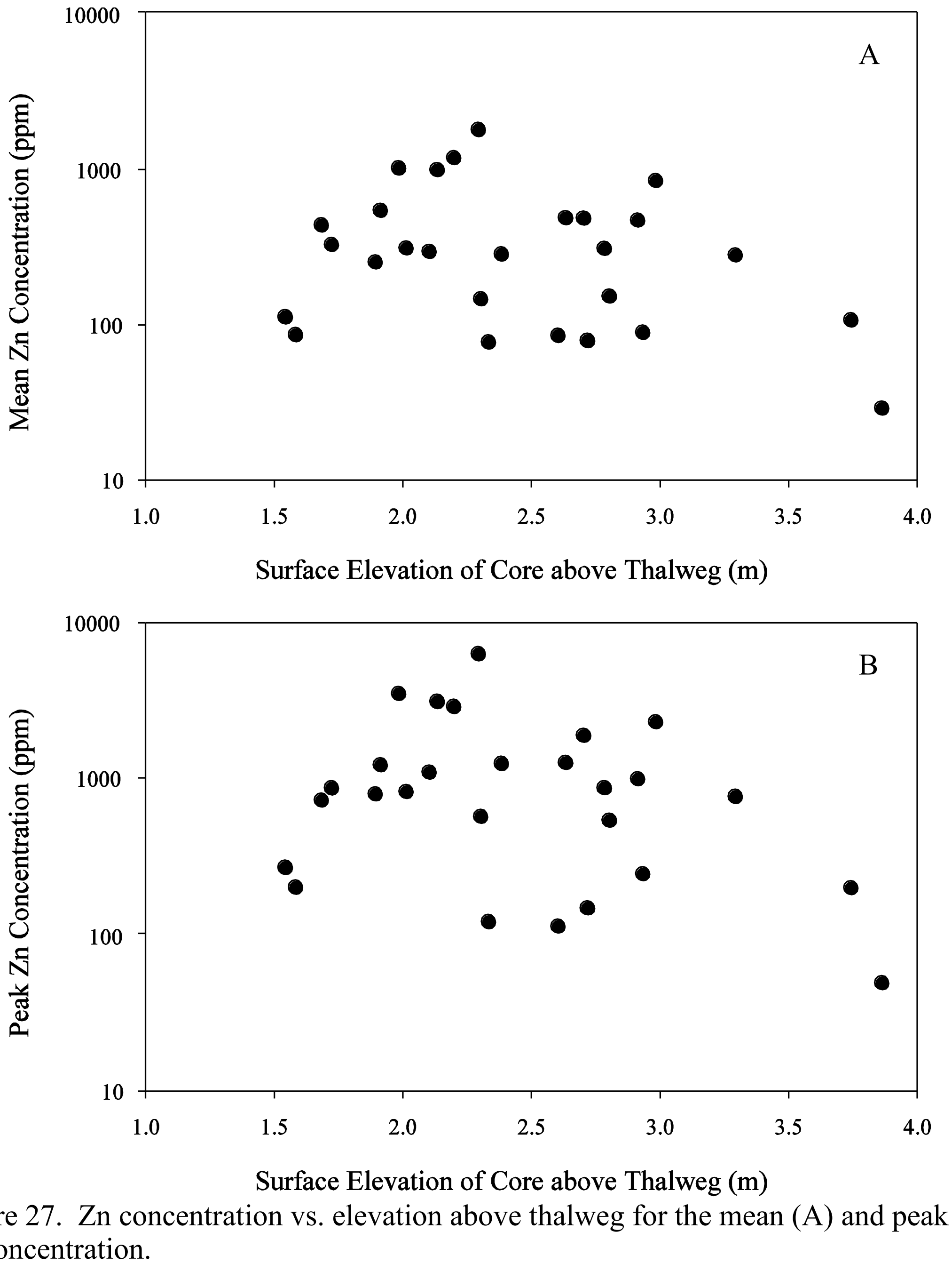

Figure 27. Zn concentration vs. elevation above thalweg for the mean (A) and peak (B) Zn concentration.

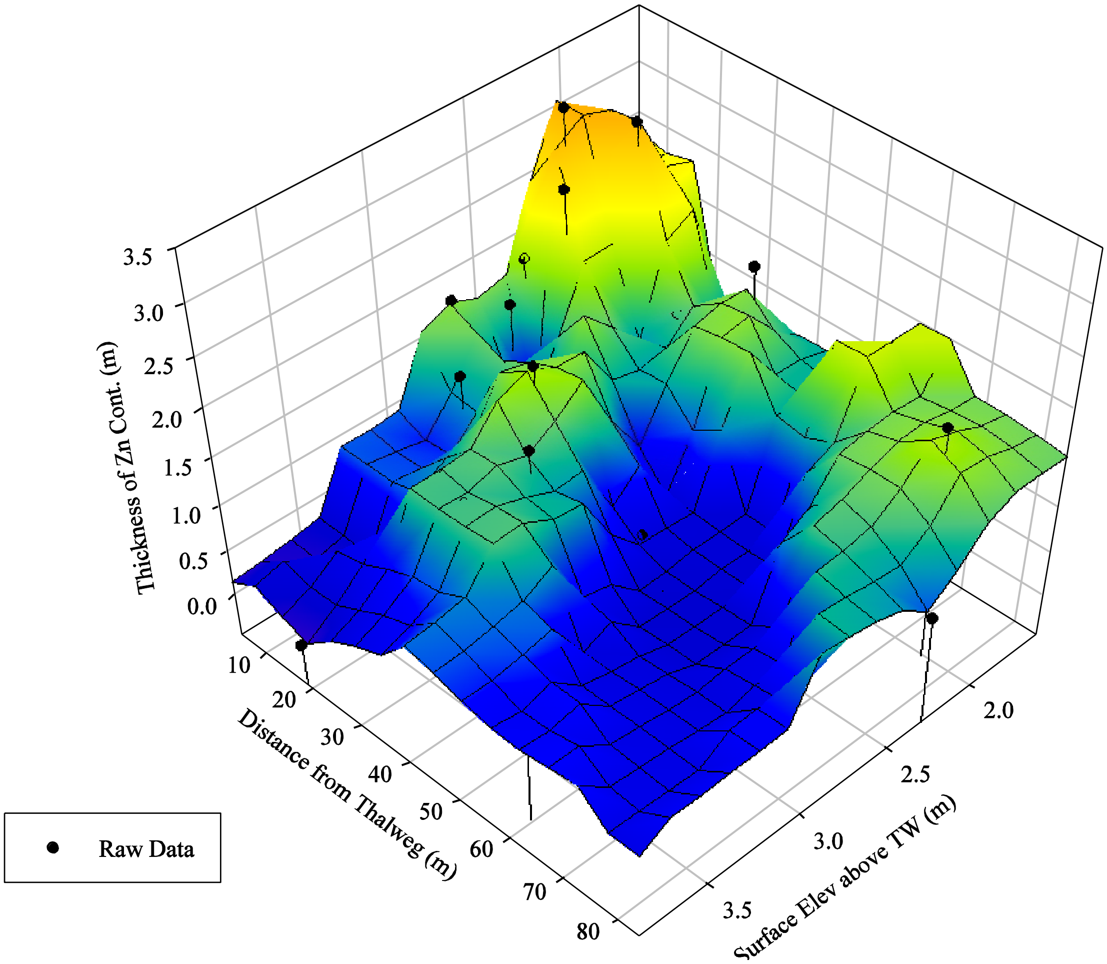

Figure 28. Thickness of Zn contamination vs. surface elevation and distance from thalweg. Generally, the thickness of Zn contamination decreases as both distance and elevation above the thalweg increases. Raw data (black dots) are plotted to illustrate some of the error caused during smoothing of the dataset.

cores on comparable surfaces at those other sites is less. The absence of data greater than 3.0 m above the thalweg and 60 m from the channel is due to the fact that low surfaces were generally limited to within 50 m of the channel. High surfaces close to the channel are due to meandering of the stream eroding into them. They contain little contaminated sediment which is likely due to the fact that their elevation above the channel prevents frequent inundation, as explained by Brewer and Taylor (1997).

CHAPTER 6

GEO-STRATIGRAPHIC ASSEMBLAGE TRENDS AND GEOMORPHIC EVOLUTION

Data presented thus far have focused on physical, spatial, and geochemical relationships among core samples. This chapter focuses on similar comparisons among geo-stratigraphic assemblages. This chapter also provides information managers need to know to locate the contaminant (in this case Zn). First, general geomorphologic characteristics of Lower Pearson Creek are presented and used to distinguish the difference between background sites and study area sites. Second, geo-stratigraphic assemblages are presented and used to describe the across-valley and downstream distribution of Zn. Third, sedimentation rates determined from Zn stratigraphy are used to estimate the relative degree of anthropogenic impact to the watershed. Fourth, an account of the fluvial geomorphic evolution at each site will be presented. Fifth, conceptual diagrams generated from geo-stratigraphic assemblages at cross-sections are used to describe the general geomorphic evolution along lower Pearson Creek. Last, the storage of contaminated sediment, Zn, and Pb is presented in order to address the environmental impact of historical mining within the study area.

General Geomorphology

The valley floor of lower Pearson Creek at the study area is composed of floodplains and terraces. Agricultural fields dominate the eastern side of the valley and are dissected by a small tributary. Gravel bars are common along the channel margins of each site. Wide floodplains close to the channel are not common. Instead, in-channel landforms are typically low, narrow surfaces and manifest themselves at sites 4D, 5, and 6. A buried sewage line trending NNE is located along the western side of the valley (Figure 29). The sewer line follows a flood chute located along the bluff on the west side of the valley between Sites 3A and 4C and crosses just downstream of Site 2. Shallow refusal depths along the flood chute are expressed in cross-sections at Sites 2, 3A, 3B, and 5 were unable to be sampled due to the aggregate put in place to protect the sewer line during installation.

Geo-stratigraphic Assemblages

Geo-stratigraphic assemblage is defined as a stratigraphic arrangement of sediment with unique geochemical and physical properties related to the hydro-geomorphic conditions dominant at the time of deposition. Zinc, soil color, refusal, and floodplain geomorphology data were used to identify geo-stratigraphic assemblages. As was shown in the previous chapter, no marked down-core relationship between texture exists and its use in characterizing cores was very limited. When examining down-core relationships, three vertical stratigraphic patterns were prominent: terrace veneer, floodplain drape, and channel fill. Each core was able to be categorized into one of these three geo-stratigraphic assemblages. Terrace veneers of two different ages were found, however, both are capped with a thin layer (<50 cm) of slightly contaminated 10YR Historical sediment. The Historical 10YR on the younger terrace veneer is underlain by uncontaminated 10YR late Holocene sediment (Figure 30). The Historical 10YR on the older terrace veneer is underlain by uncontaminated 7.5YR early to middle Holocene sediment (Figure 31). Present on the older terraces is a dense 7.5YR silty layer (Bt horizon) approximately 75 to 100 cm below the surface. Data from the two types of

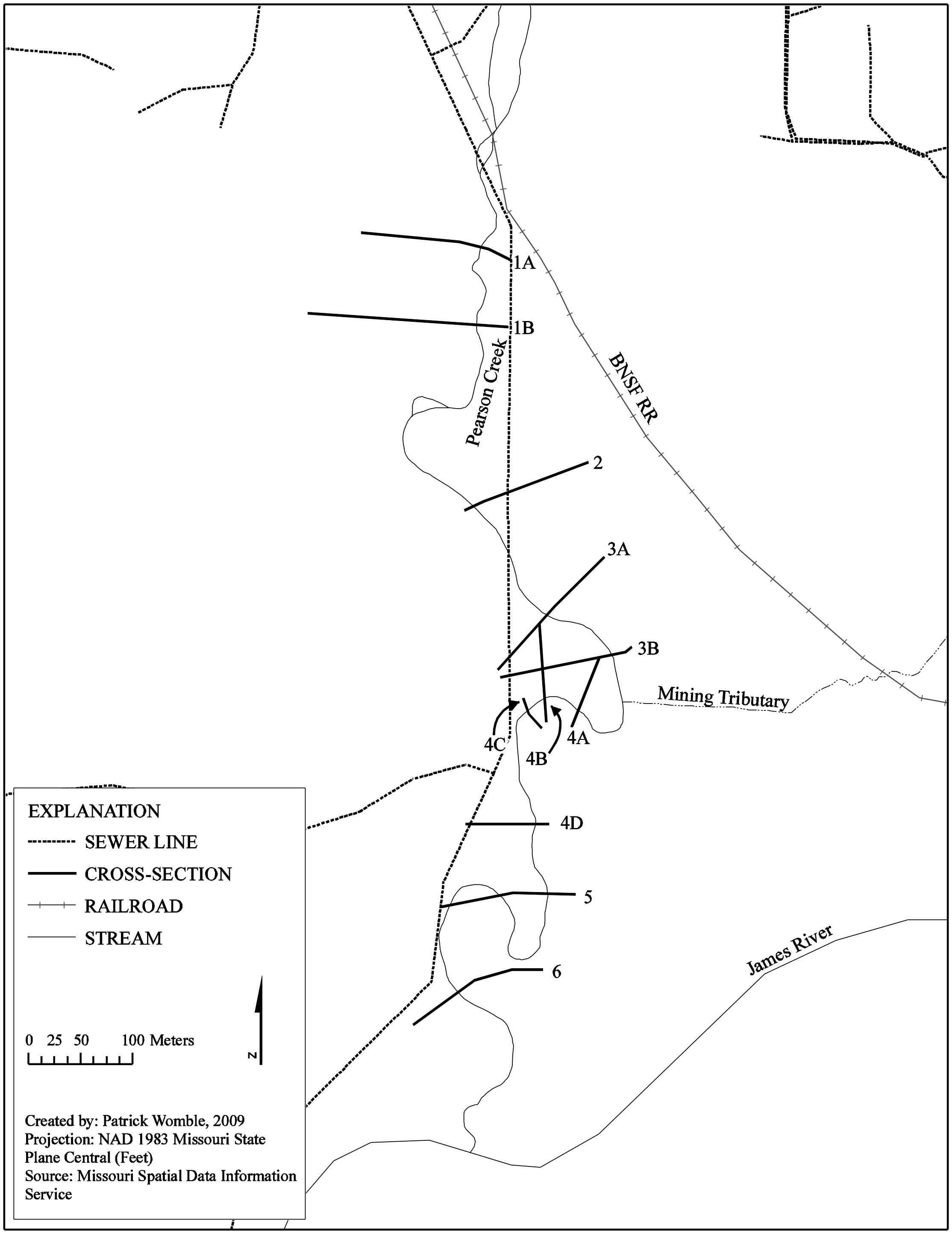

Figure 29. Location of sewer line in relation to cross-sections.

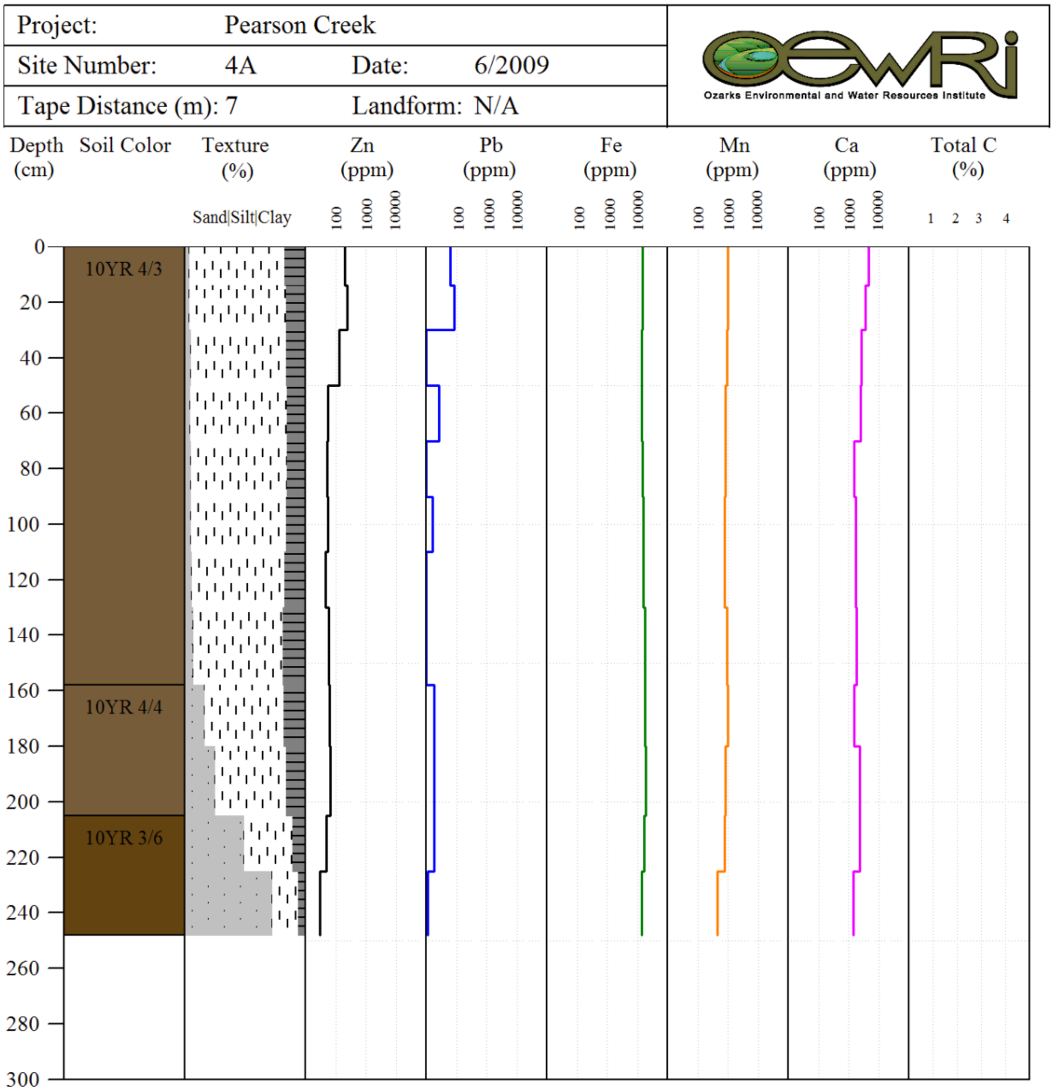

Figure 30. Stratigraphic log example of a 10YR terrace veneer assemblage at Site 4A (7 m).

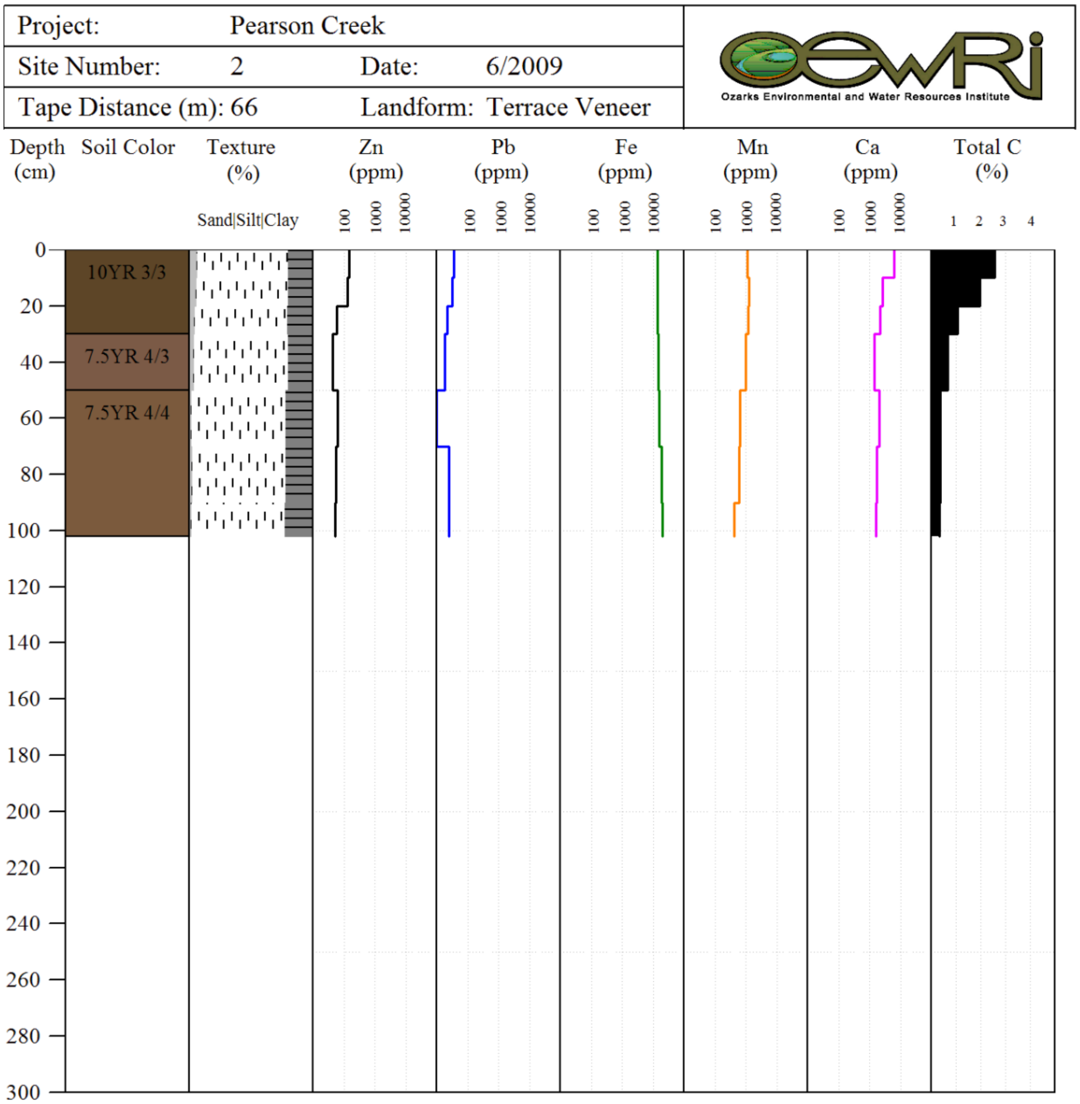

Figure 31. Stratigraphic log example of a 7.5YR terrace veneer assemblage at Site 2 (66 m).

terraces were combined to create a larger sample population due to the low number of samples collected on terraces. Floodplain drape assemblages, the most common in the study area, consist of approximately 1 m of contaminated 10YR sediment over uncontaminated 10YR sediment (Figure 32). Channel fill assemblages are fully contaminated 10YR sediment that can extend below the current stream bed and contain laminations of mining sediment approximately 1 m below the surface (Figure 33).

Trends among geo-stratigraphic assemblages were identified using Zn data as well as median distance from and elevation above the thalweg from core data. Summary statistics for Zn content in each geo-stratigraphic assemblage show that Zn concentrations in all categories are lowest in terrace veneer assemblages and highest in channel fill assemblages (Table 8; Figure 34A). Terrace veneer assemblages tend to be farthest from and highest in elevation above the channel, channel fill assemblages are closest to and lowest in elevation above the channel, and floodplain drape assemblages fall between the two (Figure 34B and Figure 34C).

The longitudinal profile of average geo-stratigraphic assemblage elevations is shown in Figure 35. As stated above, the average surface elevation of each assemblage type increases from Channel Fill to Floodplain Drape to Terrace Veneer (Figure 34C). However, the longitudinal profile shows two locations where Channel Fill assemblages are higher in elevation than Floodplain Drape assemblage. This is due to Channel Fill assemblages in these areas having levees (natural or man-made) capping them, which are at similar or slightly higher elevations than the adjacent Floodplain Drape surfaces. Also, where sites have more than one of the same types of assemblage (e.g. Site 3A), an average elevation was computed. Extremes in elevation would draw up or down the elevation of the point plotted in the longitudinal profile.

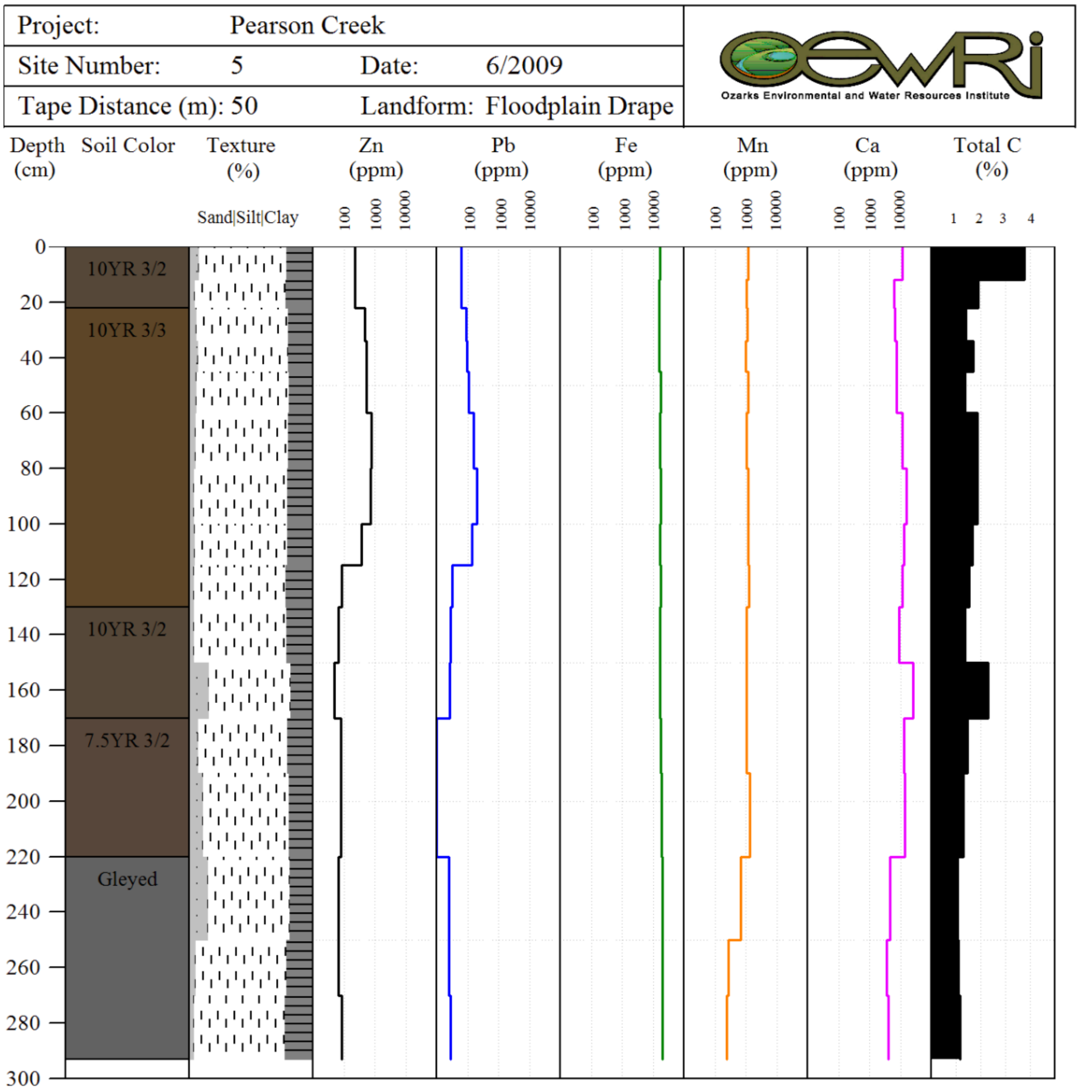

Figure 32. Stratigraphic log example of a floodplain drape assemblage at Site 5 (50 m). The bump in carbon at the contact between the 10YR and 7.5YR sediment suggests that it might be a late Holocene buried horizon.

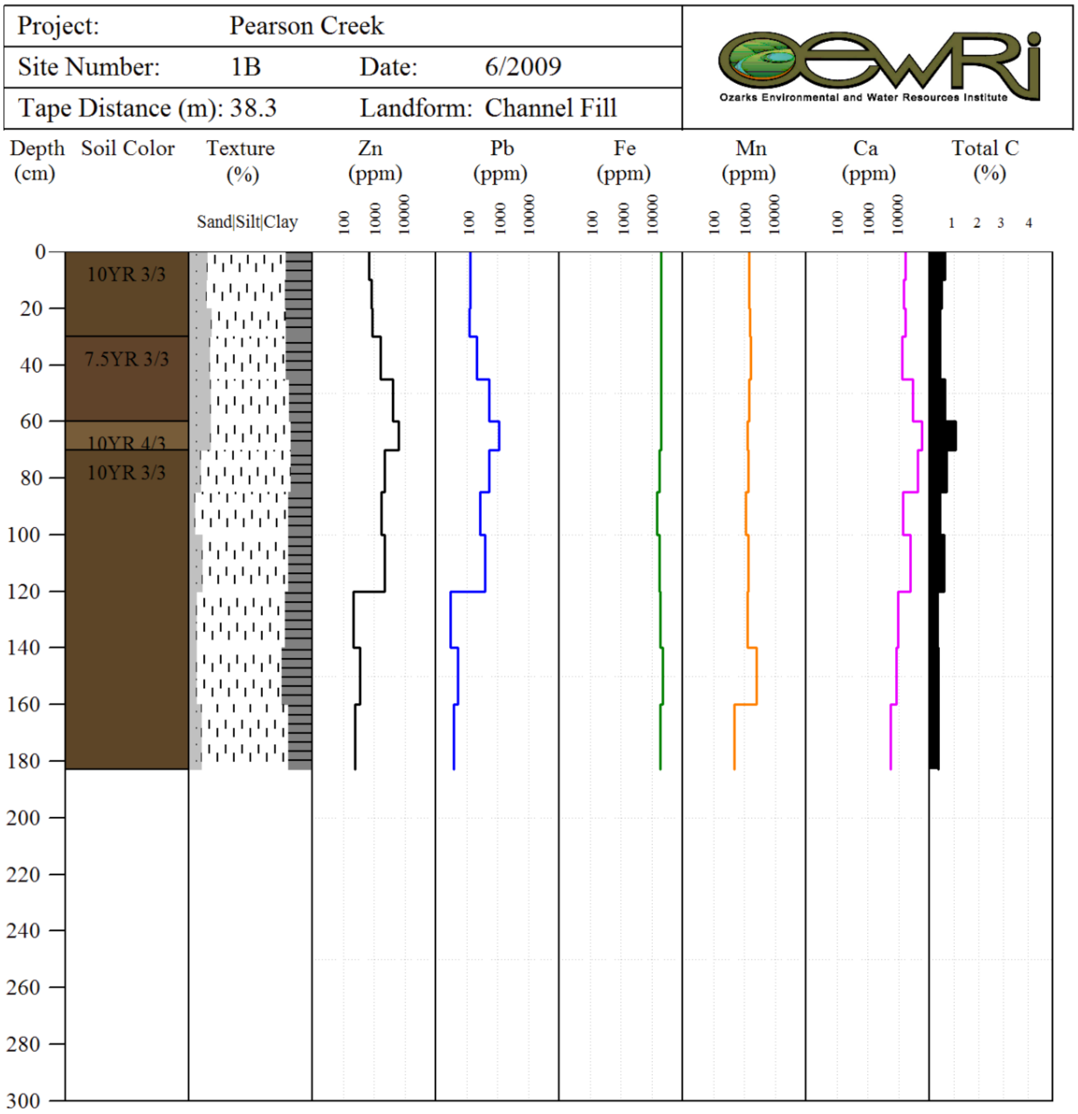

Figure 33. Stratigraphic log example of a channel fill assemblage at Site 1B (38.3 m). The 7.5YR sediment located near the top of the core could be from eroded colluvial and hillslope sources or the result of remobilized alluvial sediments. Regardless of its source, its stratigraphic position indicates that it is not Holocene in age.

Table 8. Summary statistics of Zn content for geo-stratigraphic assemblages. Note that for all statistics, values increase from terrace veneer to channel fill.

Assemblage	*n*	Min	Max	Mean	Median	Standard Deviation	Percentile	
							10th	90th
Terrace Veneer	71	18	270	85	66	55	41	164
Floodplain Drape	77	40	3,539	396	139	522	59	1,036
Channel Fill	227	179	12,395	1,441	697	1,910	288	3,012

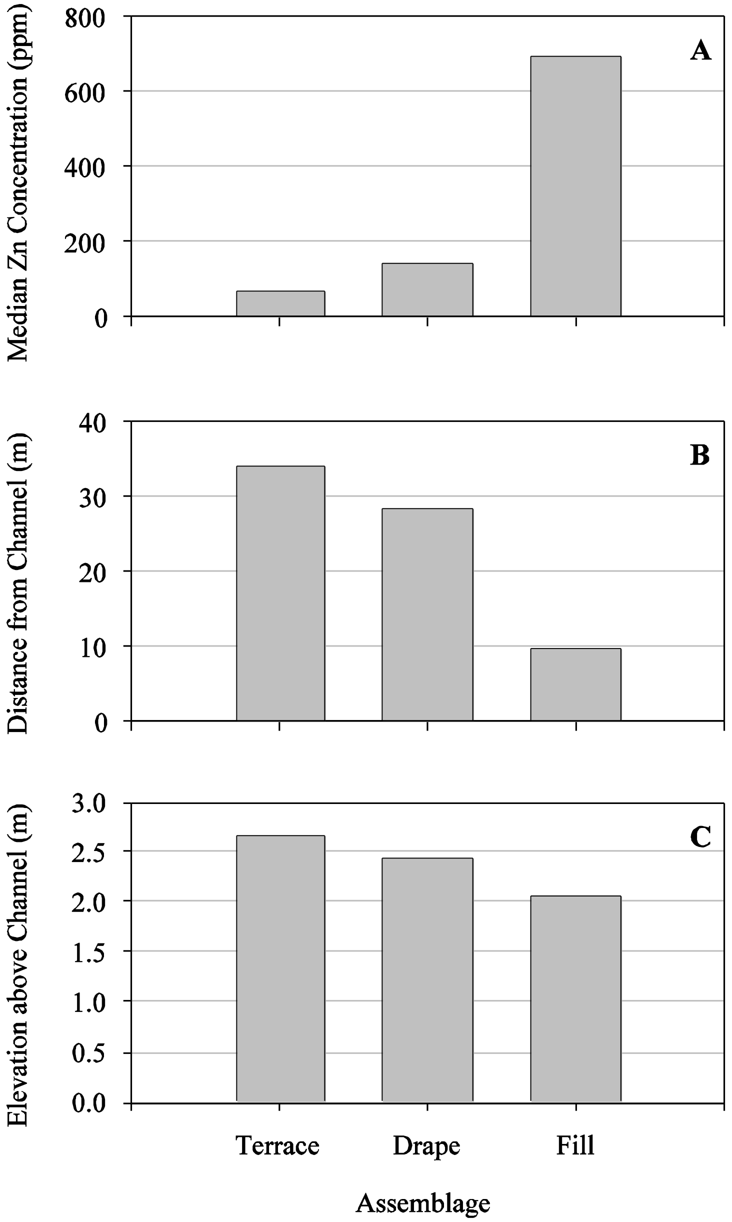

Figure 34. Spatial trends in geo-stratigraphic assemblages. (A) Median Zn concentration, (B) distance from thalweg, and (C) elevation above thalweg. Trends indicate that terrace veneer assemblages tend to have the least amount of Zn, be farthest from the channel, and be highest in elevation. Conversely, channel fill assemblages have the highest Zn concentrations, be closest to the channel, and lowest in elevation. Floodplain drape assemblage values fall between terrace veneer and channel fill values.

At Site 1A and 1B, the elevations of all three assemblages are within 0.39 m of each other. Downstream, at Site 6, the Terrace Veneer assemblage is 2.1 m higher in elevation than the Channel Fill assemblage. Differences between assemblage elevation upstream (Sites 1A and 1B) and downstream (Site 6) can be attributed to the fact that upstream sites lack the presence of active floodplains, whereas downstream, the Channel Fill assemblage is the active floodplain.

Elevation from refusal to the Terrace Veneer increases in the downstream direction (Figure 35). The wedge of sediment is likely the result of a base level rise in the James River at the confluence. An increase in the elevation of the channel bed at the confluence would force water further upstream during flooding, encouraging deposition in the transition zone where flowing water from Pearson Creek met the backflooded water of the James River. Furthermore, base level rise would decrease the slope of the channel, which promotes deposition.

Anthropogenic Influence on Sedimentation Rates

Sedimentation rates, calculated using time references and sediment tracers, can provide insight into how human land use changes have affected the watershed. High sedimentation rates signify the addition of more sediment into the system. The source of which is usually from an erosional process induced by upstream land use changes such as construction, mining, logging, or agricultural practices (Lewin et al., 1977; Knox, 1977, 1987, 1989; Trimble and Lund, 1982; Magilligan, 1985; Jacobson and Primm, 1994). The mean mining-era sedimentation rate at Pearson Creek was 2.20 cm/yr and the mean post-mining sedimentation rate was 0.64 cm/yr. Mining-era sedimentation rates ranged from 0.19 cm/yr in a terrace veneer assemblage (Site 5, 0 m) to 6.30 cm/yr in a channel

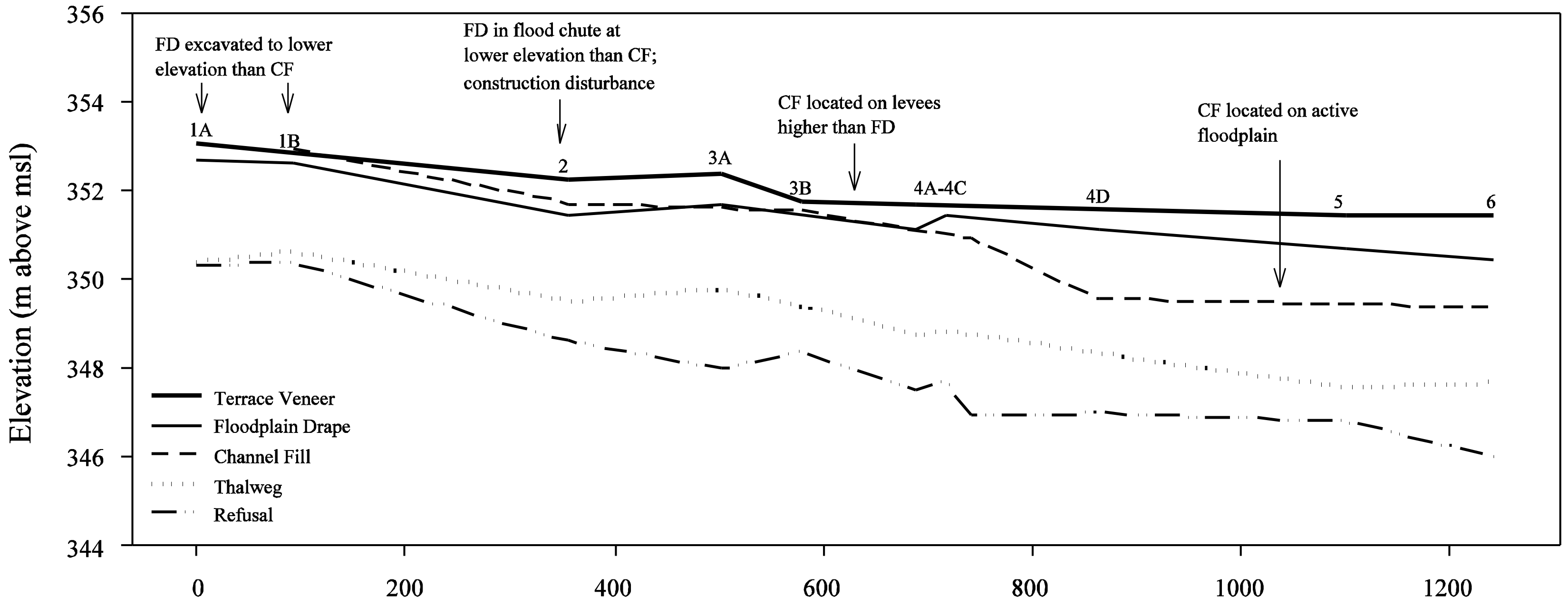

Figure 35. Longitudinal profile by geo-stratigraphic assemblage (FD= Floodplain Drape; CF= Channel Fill).

fill assemblage (Site 2, 102.9 m) (Table 9). Post-mining rates ranged from 0.05 cm/yr in a terrace veneer assemblage (Site 5, 0 m) to 2.08 cm/yr in a channel fill assemblage (Site 6, 76.1 m). Sedimentation rates by geo-stratigraphic assemblage, shown in Figure 36, also show lower post-mining sedimentation rates. Sedimentation rates are highest in channel fill assemblages and lowest in terrace assemblages.

Similar studies in the Driftless Area (Knox, 1987; Lecce and Pavlowsky, 2001), the North Carolina Piedmont (Lecce et al., 2008), and the Ozarks (Carlson, 1999) found comparable sedimentation rates and trends (Figure 37). As at Pearson Creek, every study reported lower sedimentation rates during the post-mining period. Lower post-mining sedimentation rates would point to mining operations as the cause, but this is not the case. In the Driftless Area of Wisconsin, Knox (1987) explained that mining operations have little impact on sedimentation rates and that high sedimentation rates during the mining period were more likely due to simultaneous row-crop farming practices in the region. Therefore, it is probable that a large portion of sediment considered to be contaminated does not have a purely mining-related source but is instead a combination of upland soil and mining waste erosion.

Knox (1987) and Trimble and Lund (1982) further suggest that the decrease in sedimentation following the mining period has little to do with the cessation of mining but rather land use changes and better land management practices. Mining at Pearson Creek (1885-1912) was occurring during the same time that row-crop farming (1870s-1940s) was the dominate land use class in Greene County (Figure 8). This suggests that, similar to Knox's study, sediment erosion from agricultural fields was the major source of high sedimentation rates during the mining period.

Table 9. Mining, post-mining, and total sedimentation rates per core.

Site	Core m	Mining cm/yr	Post-mining cm/yr	Total cm/yr
1A	107.5	1.67	0.31	0.61
1B	38.3	4.19	0.73	1.49
1B	107.0	4.44	0.86	1.65
2	66.0	0.37	0.10	0.16
2	91.0	3.96	0.31	1.11
2	102.9	6.30	0.90	2.08
3A	36.4	0.56	0.26	0.33
3A	58.0	1.67	0.57	0.81
3A	91.5	2.22	0.52	0.89
3A	108.5	1.30	0.52	0.69
3B	11.0	0.67	0.16	0.27
3B	30.2	5.00	1.93	2.60
3B	48.0	0.56	0.16	0.24
3B	77.0	1.59	0.13	0.45
4A	7.0	1.33	0.15	0.41
4A	25.5	3.33	0.57	1.18
4B	29.5	2.33	1.11	1.38
4C	13.0	1.78	0.77	0.99
4D	0.0	2.22	0.78	1.10
4D	33.0	2.41	0.89	1.22
4D	47.0	1.78	0.52	0.80
5	0.0	0.19	0.05	0.08
5	50.0	2.59	0.63	1.06
5	103.0	3.22	0.66	1.22
6	28.0	1.11	0.31	0.49
6	61.0	2.59	1.25	1.54
6	76.1	-	2.08	1.35

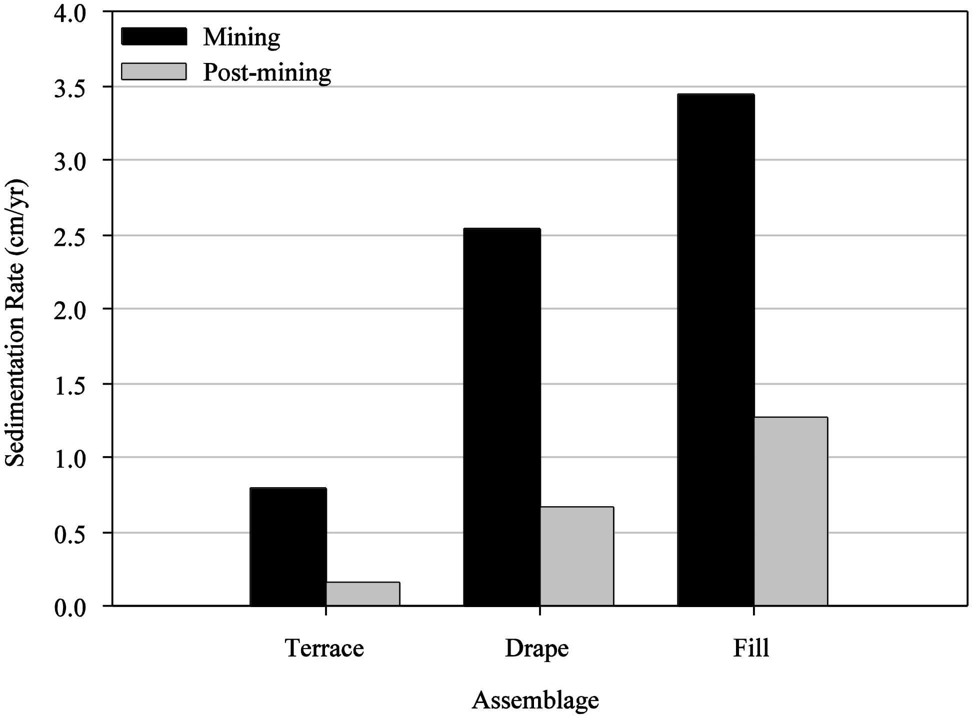

Figure 36. Average sedimentation rates for alluvial assemblages. Sedimentation rates are highest in channel fill assemblages and lowest in terrace assemblages. Post-mining sedimentation rates are lower than mining sedimentation rates for all assemblages.

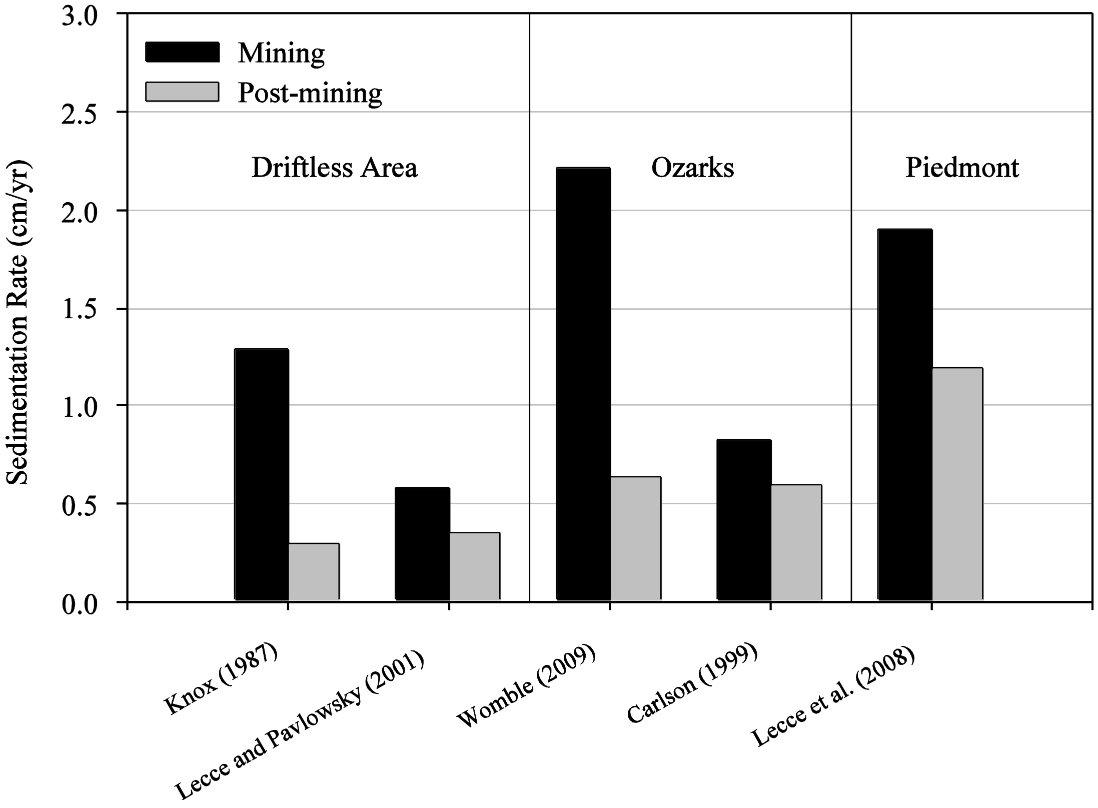

Figure 37. Average sedimentation rate compared to other studies. Mining sedimentation rates are higher than post-mining rates in all studies and rates at Pearson Creek are of the same magnitude as previous studies.

Geomorphic Evolution

Geomorphic Evolution by Site. The geomorphic evolution of each site was interpreted using down-core profiles of soil color and Zn concentration. Site 1A is located in the upper most portion of the study area (0 m) where the valley floor is low and wide (Figure 13). Prior to mining, the channel appears to have been in approximately the same location as it is currently. However, the tributary that enters Pearson Creek at the railroad bridge was likely entering further downstream and to the west of the present day main channel. Prior to the mining period, a large bar formed between the two channels, possibly due to an increase in sediment supply from the upper watershed due to increased soil erosion (Figure 38A). The bar might have filled in the tributary channel, forcing the confluence upstream. Following the construction of the bar, contaminated mining sediment began accumulating on top of it, building a new floodplain. The presence of large trees (possibly 100 years old) on top of this surface suggests that it has been stable since mining ended (tree cores are needed to confirm this). Currently, deep excavation scars from topsoil mining created after the mining period on the floodplain provide pathways for flood waters to exploit (Figure 38A). Consequently, as the flow clears the bridge, it combines with the tributary flow and spreads out across the excavated floodplain, removing and depositing material during subsequent flooding events.

Site 1B is located at 91 m on the longitudinal profile, just downstream of Site 1A. The valley here is still wide and topsoil mining scars are present. However, the geomorphic evolution is slightly different. Completely contaminated cores at 38.3 m and 107 m suggest that the channel migrated east across the valley floor during the mining period, in-filling with sediment along the way (Figure 38B). Following mining, overbank

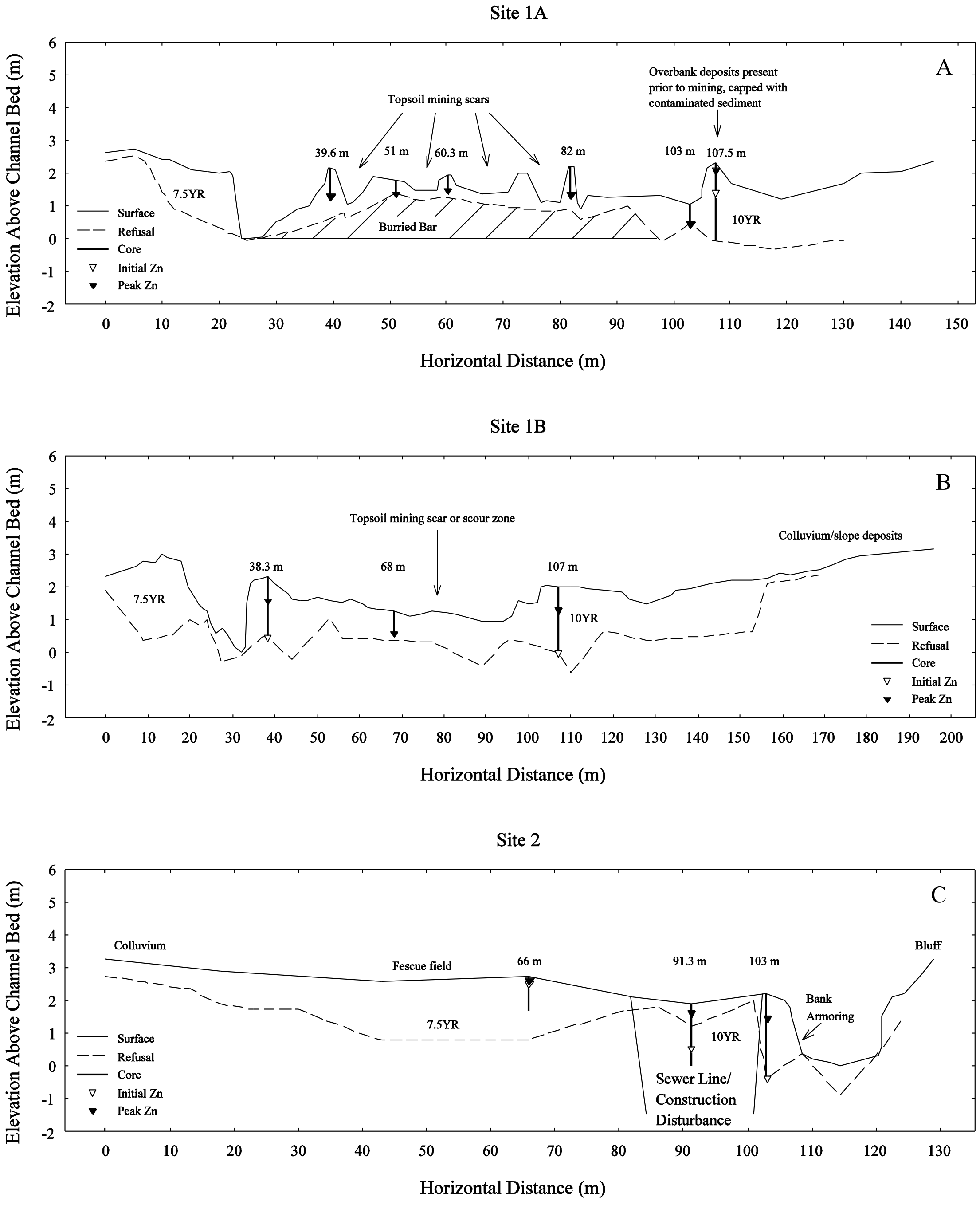
Site 1A

Site 1B

Site 2

Figure 38. Cross-sections at (A) Site 1A, (B) Site 1B, and (C) Site 2. Figures are oriented looking downstream.

flooding deposited silty-material, increasing the height of the surface. Topsoil mining followed, removing much of this sediment.

Site 2 is located at 357 m on the longitudinal profile, downstream and around a meander from Site 1B. The channel here is relatively straight and pinned up against the bluff on the west side of the valley (Figure 13). Contaminated sediment east of the current channel indicates that the channel has migrated to the west since mining began (Figure 38C). A thin layer of contaminated sediment is present in the field, deposited during large flooding events since mining. Slope erosion of the bluff is contributing coarse material to the channel. However, the primary source of channel material appears to be from remobilized bar or splay deposits upstream. Colluvial slope deposits, notable by shallow refusal depths and 7.5YR sediment, are present on the east side of the valley (Figure 38C).

Site 3A is located 501 m on the longitudinal profile at the beginning of a large meander bend (Figure 13). The same fescue field at Site 2 is present on the east side of the valley at Site 3A (Figure 39A). Contamination is present in the top 1 meter of cores at 58 m, 91.5 m, and 108.5 m, indicating that 1 meter of sediment has been deposited since mining began. In addition, large refusal depths in the center of the channel indicate that the channel has aggraded as well. There is no evidence for horizontal channel activity due to the absence of contamination at or below the depth of the current channel bed elevation.

Sites 3B, 4A, and 4B, located at 579 m, 689 m and 717 m, respectively, have nearly identical geomorphic histories. Site 3B is oriented across the valley (east-west) and located just upstream of where the mining tributary enters Pearson Creek (Figure 13). Sites 4A and 4B are oriented along the valley (approximately north-

Site 3A

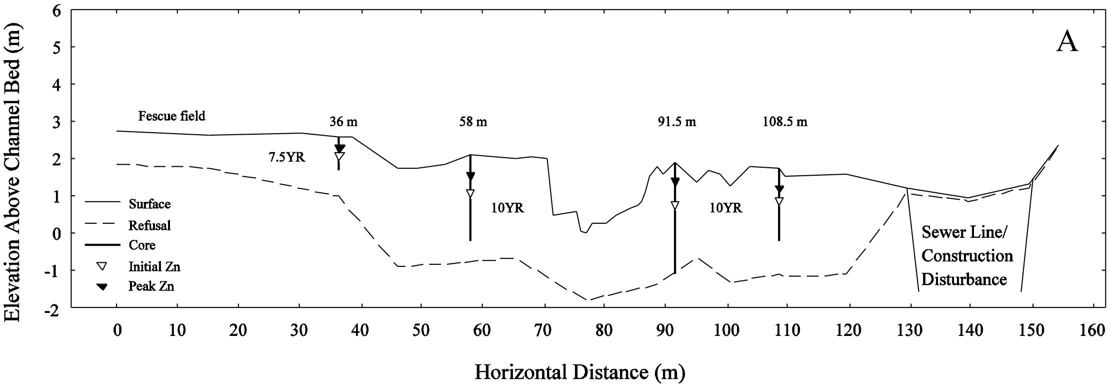

Site 3B

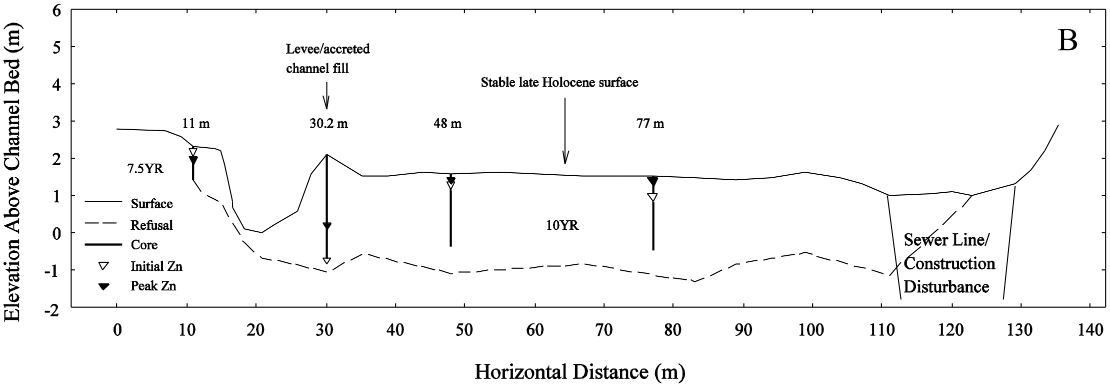

Figure 39. Cross-sections at (A) Site 3A and (B) Site 3B. Figures are oriented looking downstream.

south) just downstream of the mining tributary (Figure 13). All cross-sections dissect the same surface. The higher uncontaminated surface is an early to middle Holocene terrace at Site 3B and a late Holocene to historical terrace at Sites 4A and 4B (Figure 39B, Figure 40A, and Figure 40B). The lower surface in the center of each cross-section is late Holocene to historical in age and is contaminated near the top of the core profiles, indicating that the surface has encountered some vertical accretion. Cores located near the channel on the levees of all three sites indicate that some limited channel migration or contraction has occurred since mining began (as much as 7 m at Site 3B).

Site 4C is located at 742 m on the longitudinal profile up against the bluff. The geomorphic evolution here is similar to Site 3A with the exception that the channel here has migrated since mining ended. There is approximately 1 meter of contaminated sediment present on the east side of the channel, suggesting that it has been stable (Figure 40C). Contaminated bank samples from the west side of the channel indicate that it has been built since mining ceased. It is possible that the channel was located to the west of its current position and has migrated east since mining, filling-in with contaminated sediment as it did so.

Site 4D is located at 863 m on the longitudinal, just upstream of a large meander s-curve. The fescue field is present on the east side of the valley, followed by a very wide channel with a low bar, high bar, and floodplain (Figure 41A). A small tributary enters the channel just upstream and supplies a small amount of fresh gravel that forms small splays on top of Site 4Ds bar complex. The east side of the channel is currently being undercut and large woody debris in the channel has promoted scour upstream and shadow bar growth downstream. The west side of the valley is composed of another surface at a similar elevation to the fescue field. Both of these surfaces, represented

Site 4A

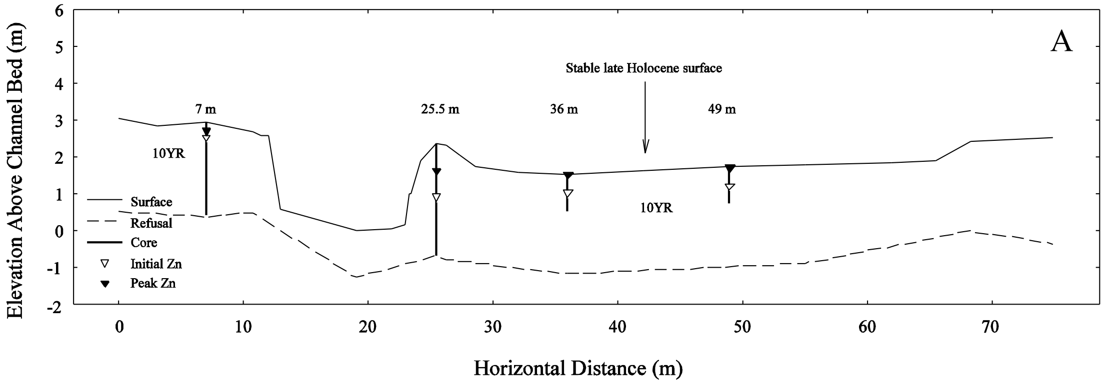

Site 4B

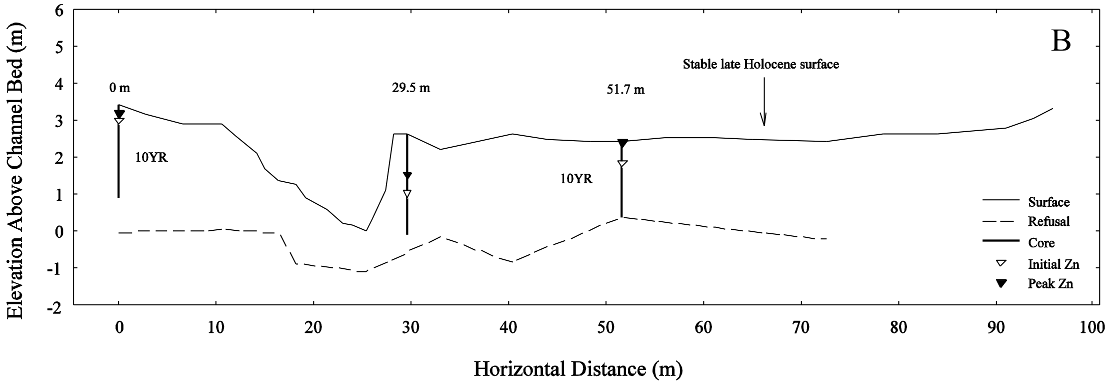

Site 4C

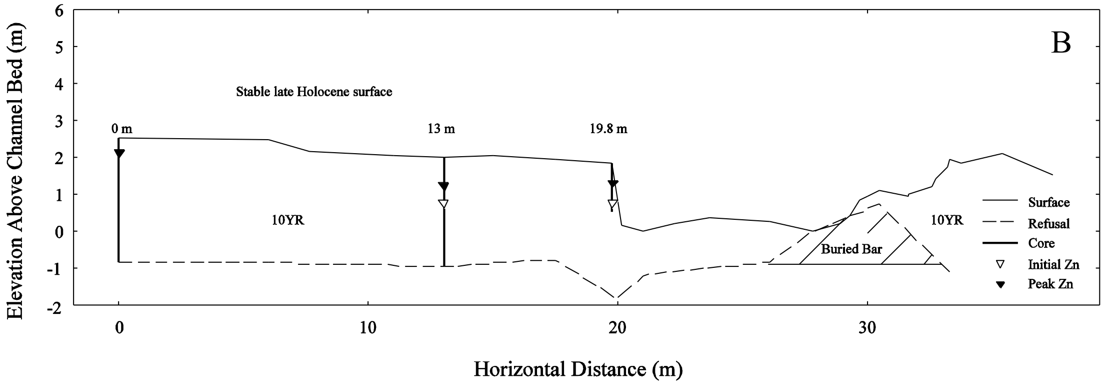

Figure 40. Cross-sections at (A) Site 4A, (B) Site 4B, and (C) Site 4C. Note the scale difference at Site 4C. Figures are oriented looking downstream.

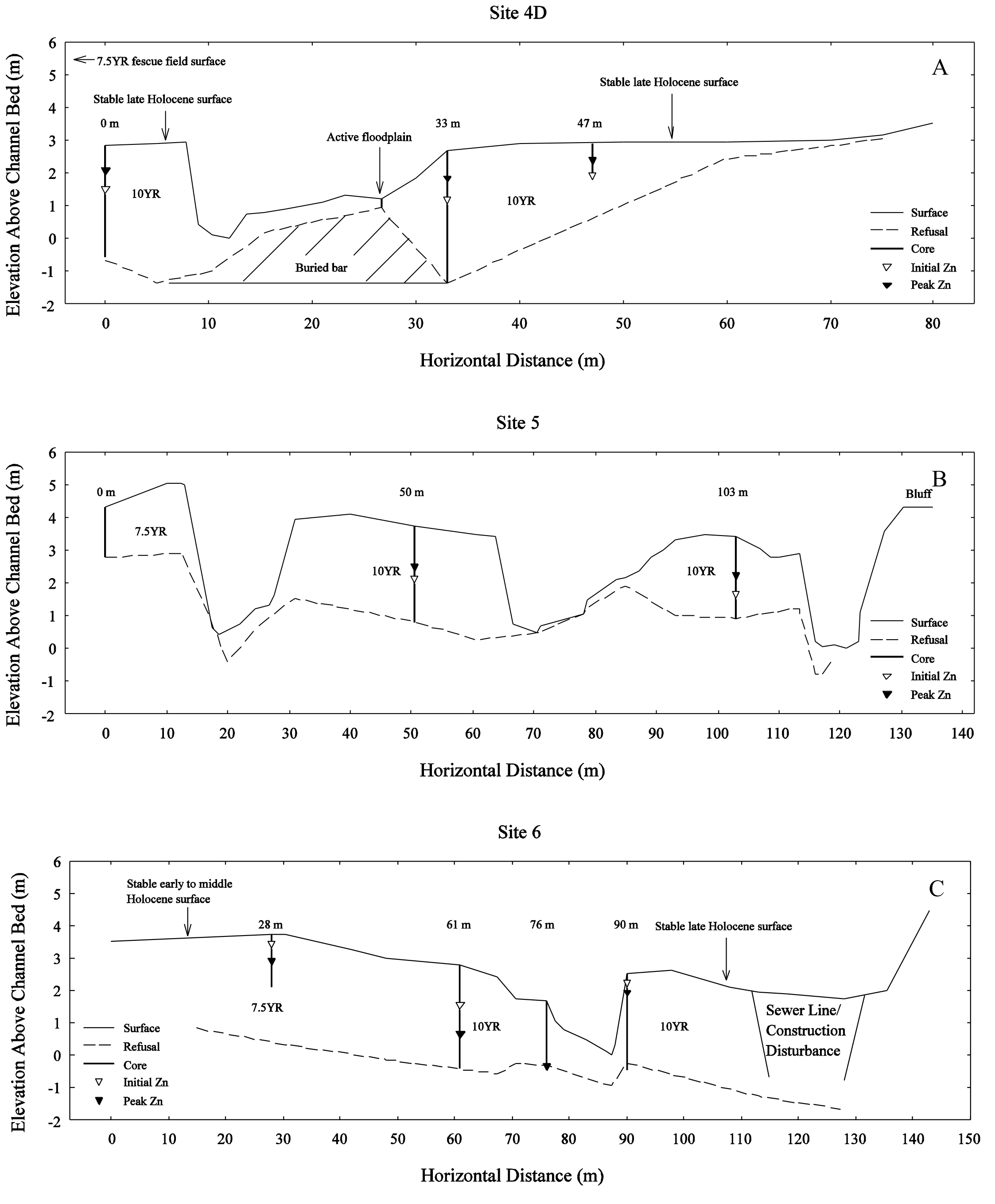
Site 4D

Site 5

Site 6

Figure 41. Cross-sections at (A) Site 4D, (B) Site 5, and (C) Site 6. Figures are oriented looking downstream (south).

by cores at 0 m and 47 m, are contaminated to a depth of approximately 1 meter, indicating that they were present prior to mining. The lower surface represented by the core at 33 m has a similar history and comparable amount of contaminated sediment on top of it, suggesting that it too was present prior to the mining period. At this site, approximately 1 meter of bed aggradation has occurred, evidenced by the ~1 m depth to refusal in the channel. It can be surmised, then that the channel configuration was similar prior to mining and simply increased in elevation.

Site 5 intersects the stream three times at 935 m, 1,103 m, and 1,147 on the longitudinal profile around a large meander s-curve (Figure 13). The fescue field is located on the east side of the valley, followed by two point bar complexes separated by channels, and a final channel pinned up against the bluff on the west side of the valley (Figure 41B). The point bar closest to the field terrace is building in the down-valley direction while the second is building in the up-valley direction. The fescue field surface is uncontaminated whereas the two other surfaces at 50 m and 103 m are contaminated to a depth of 1.5 m each.

Site 6 is located at 1,243 m on the longitudinal profile on the outside of a meander bend, just downstream of Site 5 (Figure 13). The fescue field on the east side of the valley is the highest surface present. From the field, two lower surfaces step down toward the channel (Figure 41C). High and low bars are located on the east side of the channel. A surface lower in elevation than the field, is located on the west side of the valley, extends to the bluff, and is currently being eroded and undercut. Cores in the field (28 m) and lower surface on the west side of the channel (91 m) are contaminated to a depth of 60 cm, indicating that the surfaces were present and stable prior to mining. The presence of 7.5YR sediment on the upper surface indicates that it is older (early to middle

Holocene) than the lower 10YR surface (late Holocene to historical). The core at 61 m is contaminated to a depth of 1.70 m whereas the core at 76.1 m is completely contaminated. The uncontaminated portion of the core at 61 m suggests that it was present prior to mining. However, the peak Zn concentration found in the core at 76.1 m is lower than in the core at 61 m, suggesting that the surface at core 76.1 m was constructed since mining ceased, likely due to lateral migration of the channel west.

General Evolution Model. Conceptual diagrams are used to show the arrangement of geo-stratigraphic assemblages and how they relate to the geomorphic evolution of Pearson Creek. The age of deposits and timing of geomorphic events is described as the pre-mining, mining, and post-mining periods. The pre-mining period (prior to 1885) involved sedimentation of uncontaminated (below background) sediment, soil development on higher surfaces, and narrower channels. During the mining period (1885-1912), sediment with Zn concentrations exceeding background was deposited, channels widened, and lateral migration began. However, it is likely that increased channel activity (widening and migration) would have begun just prior to mining due to the conversion of the watershed to agricultural land uses. Initial land use changes, occurring as early as the 1830s, would have increased the magnitude and frequency of floods and caused channel widening, alluviation, and bed aggradation (Knox, 1977; Lecce, 1997). The post-mining period (1912-present) signifies the time when Zn levels in sediment being deposited dropped below the peak concentration but were still above background. Sources of post-mining sediment could include: remobilized contaminated deposits, construction sites, industry, and eroding tailings piles. Following the development of conceptual diagrams, patterns between sites show that diagrams could be grouped into three dominant zones (Figure 42). It can be seen that these zones seem to

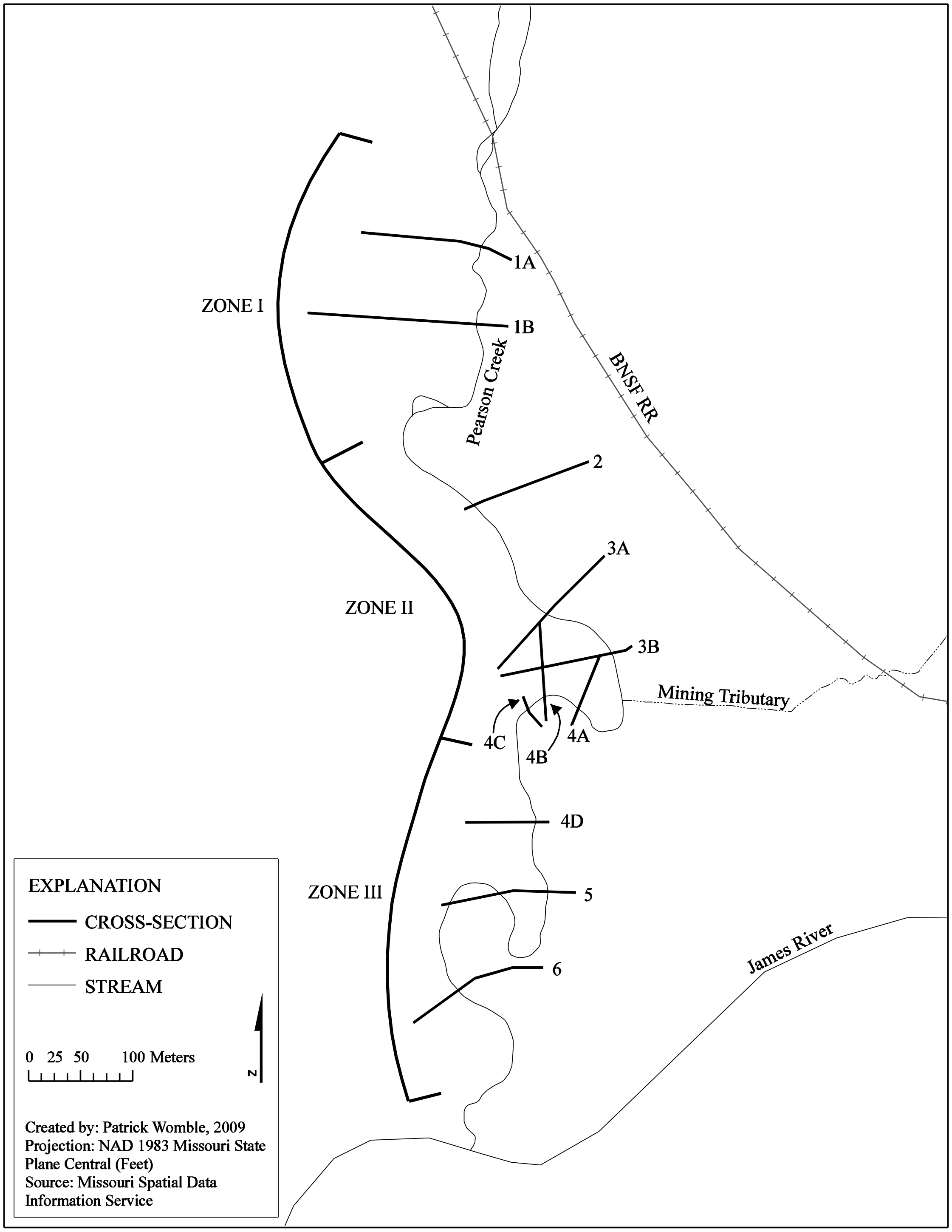

Figure 42. Distribution of zones determined from conceptual diagrams.

coincide with changes in the planform of Pearson Creek. The stream in Zone I is relatively straight (sinuosity= 1.1) whereas in Zones II and III, the stream is more meandering (sinuosity= 1.8). Conceptual diagrams from sites best representing each zone will be used to describe the general geomorphologic evolution of lower Pearson Creek.

Zone I. The conceptual diagram for Zone I, represented by Site 1B, shows a early to middle Holocene terrace veneer assemblage on the east side of the valley, a scoured and excavated channel fill assemblage in the middle of the valley, and a floodplain drape sediment assemblage on the west side of the valley (Figure 43A). The pre-mining period involved the construction of the 7.5YR terrace. During, or just prior to, the mining period, a disturbance (likely the result of increased sediment supply due to hillslope erosion caused by land use changes) caused the channel to fill in with sediment and push the site of the confluence between the small tributary near the railroad bridge and Pearson Creek closer to the bridge, transforming the west side of the valley into a backswamp. The channel fill assemblage confirms this. Some time following the mining period, the area was known to have undergone some limited topsoil mining in the channel fill assemblage sediment. Fully contaminated sediment and the presence of large trees on top of pendants left behind by topsoil mining suggest that the surface was stable following Zn mining and prior to soil removal. Gravel and fines are currently being deposited in this area as floods exploit the sites of excavation.

Zone II. The conceptual diagram for Zone II, represented by Site 3B, has terraces on both sides of the channel which imply that this area was relatively stable prior to and since the mining period (Figure 43B). The 7.5YR terrace veneer assemblage indicates that the surface was built during early to middle Holocene, while the lower 10YR terrace

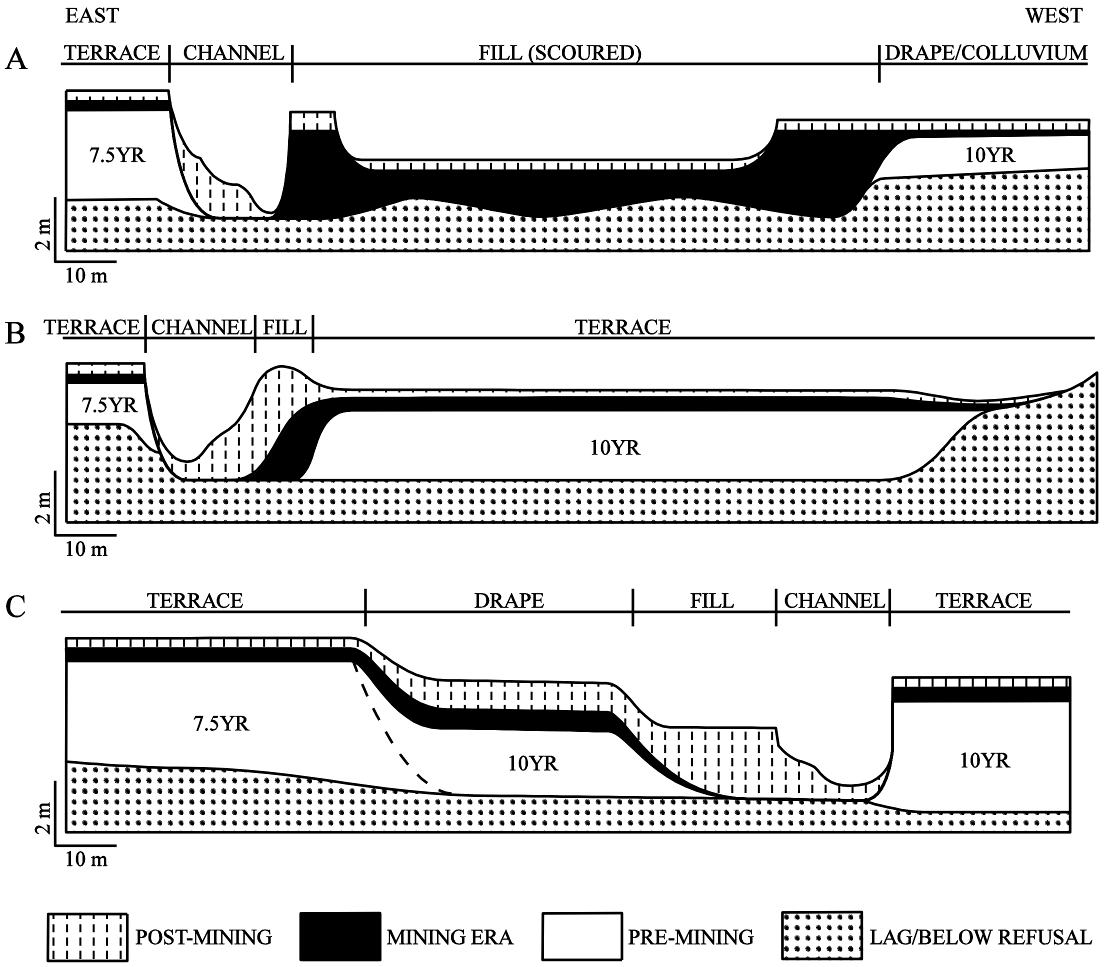

Figure 43. Floodplain models. Conceptual diagrams of (A) Zone I at Site 1B, (B) Zone II at Site 3B, and (C) Zone III at Site 6. Figures are oriented looking downstream.

on the west side of the valley indicates that lateral migration occurred at some point during the late Holocene. A thin channel fill assemblage on the west side of the channel indicates that the channel has contracted or migrated slightly to the east and subsequently filled in with sediment since mining began. This trend is observed at Sites 3B, 4A, and 4B. At Site 2, the channel has moved toward the west. As evidenced by the terrace assemblages, vertical accretion on overbank surfaces has dominated in this zone since mining began. Local variability is observed at Sites 3A and 4C and is related to where they are in relation to the meander bend. These sites saw no lateral migration during the mining period. However, similar to the other sites, vertical accretion has dominated since mining began.

Zone III. The conceptual diagram for Zone III, represented by Site 6, has all three assemblages present on the east side of the valley, stepping down in elevation towards the channel (Figure 43C). This zone has had a significant amount of both vertical and lateral accretion since mining began. During the early to middle Holocene, the 7.5YR terrace was constructed. Following this, during the late Holocene to historical period, the 10YR terrace was built. During the mining period, the floodplain drape sediment was deposited, responding to the increased sediment supply due to land use changes. Vertical accretion was dominant at this time. The post-mining period has seen primarily lateral migration at work, as evidenced by the large accumulation of post-mining sediment at Sites 4D and 6 and active point bars at Site 5. The thickness of post-mining sediment appears to be greater in the deposition zone than in other zones and could be the result of frequent backflooding from the James River. Where affected, backflooding creates an area of decreased velocity where flow from Pearson Creek collides with the stagnant backflood waters. The sudden decrease in velocity causes sediment to drop out of suspension onto flooded surfaces. Therefore, more sedimentation would be present in areas that are more frequently subjected to backflooding, such as Sites 4D, 5, and 6 on Pearson Creek. Additionally, a decrease in slope, possibly due to a base level rise of the James River induced by land use change, would promote increased meandering of the stream and deposition of post-mining sediment in the channels.

A timeline of land use and geomorphic change is presented in Table 10. It reports the most prominent geomorphic changes and dominant sedimentation processes occurring during the pre-mining, mining, and post-mining periods in each zone as well as the land use history in the watershed. Pre-mining geomorphic processes were dominated by vertical accretion of uncontaminated sediment and the construction of 7.5 and 10YR terraces. Mining period geomorphic processes included channel adjustments (migration, widening), bed aggradation, and were dominated by both vertical and lateral accretion. Post-mining geomorphic processes have been dominated by vertical accretion with some limited lateral accretion in Zone II and a significant amount of lateral accretion in Zone III.

A lag exists between when land use changes begin and when the effects from them to appear downstream (Knox, 1977) and it is possible that when land use changes prior to mining occurred, the channel responded by getting wider and deeper. If the peak effects of land use change (increased sediment yield and runoff) coincided with mining, the input of sediment would have caused the channel to contract and the bed to aggrade. This is supported by the presence of contaminated sediment along the channel margins and below the current bed at the 103 m core at Site 2 and the 30.2 m core at Site 3B. A similar pattern, however in post-mining sediment, was found at Site 6. Aggradation at this site could be related to base level rise of the James River following the construction

Table 10. Timeline of land use history and geomorphic change.

Zone	Pre-Mining (Holocene to 1885)	Mining Era (1885-1920)	Post-Mining (1920-Present)
Watershed	– Land clearing for farming – Row-crop farming dominant	– Row-crop on the decline, pasture farming on the rise	– Pasture farming dominant – Soil conservation practices implemented
Zone I	– Early to middle Holocene construction of 7.5YR terrace – Disturbance-induced bar constructed in center of valley – Channel to or near its current position just prior to mining – Vertical accretion dominant	– Construction of floodplain on bar during high flows – Lateral migration dominant	– Removal of sediment by scour or excavation – Erosion and migration toward the east bank – In-channel deposition dominant
Zone II	– Early to middle Holocene construction of 7.5YR terrace – Lateral construction of late Holocene to historical 10YR terrace – Vertical and lateral accretion occurring	– Little contamination deposited on surface – Limited channel widening – Channel bed aggradation (~1.5-2 meters) – Vertical accretion more dominant than lateral accretion	– Vertical accretion on stable terrace surfaces – Vertical accretion dominant early on – Lateral accretion more recent
Zone III	– Early to middle Holocene construction of 7.5YR terrace – Late Holocene to historical construction of 10YR terrace – Vertical accretion dominant	– Vertical accretion of contaminated sediment on overbank surfaces – Channel bed aggradation (~1.5-2 meters) – Vertical accretion dominant	– Formation and extension of point bars – In-filling of channels with post-mining sediment – Lateral accretion dominant

of Lake Springfield or in-channel deposition from an increase in sediment supply due to land use changes.

Contaminant Storage in Floodplain Deposits

In this section, the distribution of mass storage of contaminated sediment, Zn, and Pb is evaluated. Previous work showed that the concentration of Zn is dependent on elevation above the thalweg, distance from the thalweg, and distance downstream from mining sources (Figure 25; Figure 28). The lateral distribution of Zn concentrations along floodplain transects was explored by examining geo-stratigraphic assemblage trends (Table 8; Figure 34). These trends shed light on the intensity of Zn stored in alluvial deposits but not the total mass storage.

The first step to understanding the volume of storage involves the mapping of different geo-stratigraphic assemblages in the study area (Figure 44). The second step is to use core information to estimate the thickness of contamination for each assemblage by zone (Table 11). The third step involves the calculation of mass storage (Equations 1, 2; Table 11). Finally, spatial patterns of storage are plotted (Figure 45).

Storage of contaminated sediment, Zn, and Pb is similar between all three Zones (Table 11). In Zone I, Channel Fill assemblages store more contaminated sediment, Zn, and Pb than either Terrace Veneer or Floodplain Drape assemblages. Zinc and lead storage patterns in Zone II are similar to those found in Zone I, however at lower magnitudes. Storage of contaminated sediment in Floodplain Drape and Terrace Veneer assemblages is greater in magnitude than in Zone I. This is because Terrace Veneer assemblages on either side of the stream limit the amount of available storage by limiting the amount of lateral migration in the stream more than in Zone I or Zone III. Therefore,

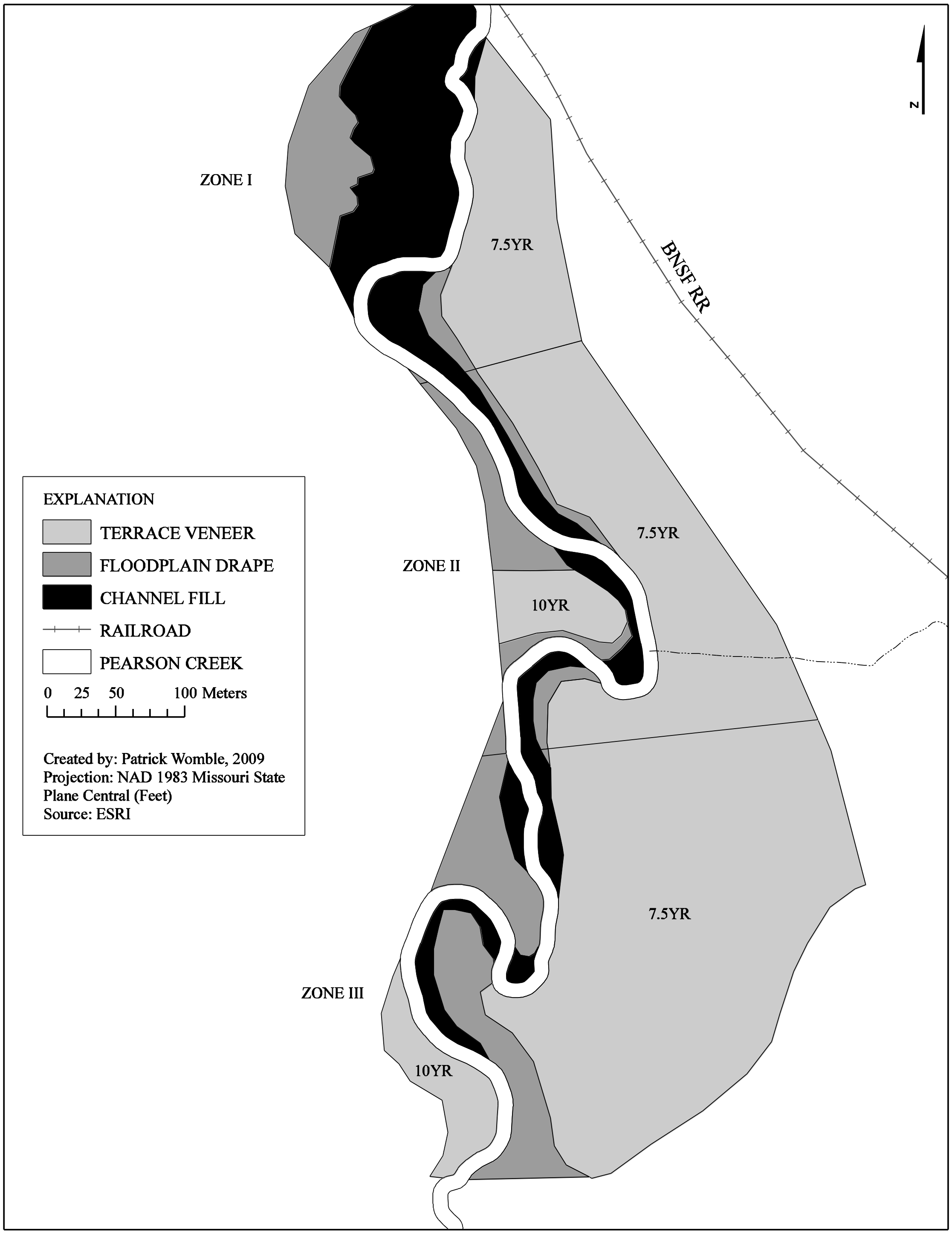

Figure 44. Spatial distribution of geo-stratigraphic assemblages.

Table 11. Summary of contaminated sediment, Zn, and Pb storage. TV=Terrace Veneer; FD= Floodplain Drape; CF= Channel Fill.

			Contaminated Sediment			Zinc		Lead	
Zone	Assemblage	Area (m^2)	Depth (m)	Volume (m^3)	Mass* (Mg)	Concentration (%)	Mass (Mg)	Concentration (%)	Mass (Mg)
	TV	14,734	0.38	5,599	7,278	0.016	1.1	0.005	0.4
I	FD	6,941	0.91	6,316	8,211	0.033	2.7	0.009	0.7
	CF	17,078	0.86	14,687	19,093	0.156	29.8	0.031	5.9
	Total	38,752		26,602	34,582		33.7		7.0
	TV	32,293	0.38	12,271	15,953	0.016	2.5	0.005	0.8
II	FD	6,525	1.25	8,124	10,561	0.054	5.7	0.017	1.8
	CF	4,167	2.33	9,696	12,604	0.130	16.4	0.042	5.3
	Total	42,985		30,091	39,118		24.6		7.9
	TV	61,245	0.43	26,540	34,502	0.039	13.4	0.005	1.6
III	FD	11,647	1.42	16,500	21,450	0.067	14.4	0.022	4.8
	CF	4,319	2.00	8,639	11,231	0.044	4.9	0.009	1.0
	Total	77,212		51,679	67,183		32.7		7.4
	Grand Total	158,950		108,372	140,883		90.9		22.3

* See Equations 1 and 2 in Chapter 4.

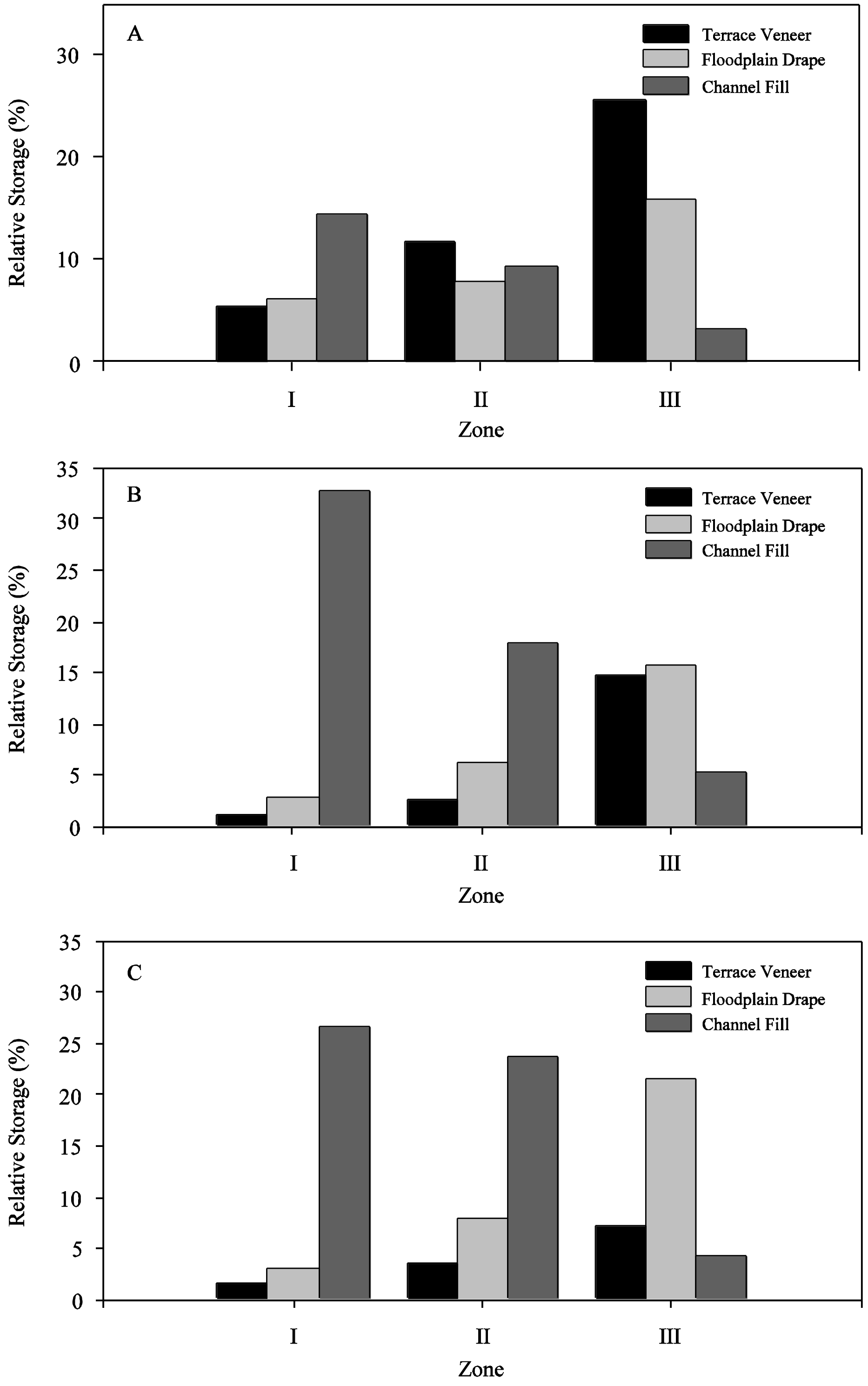

Figure 45. Relative storage by zone. (A) Contaminated sediment, (B) Zn, and (C) Pb relative storage. Relative Storage (%)= (Component Storage/Total Floodplain Storage)*100.

contaminated sediment introduced by the mining tributary (Figure 13) would be washed downstream into Zone III and out into the James River. In Zone III, the Floodplain Drape assemblage is the site of the most storage (Figure 45).

In order to see how storage is distributed within geo-stratigraphic assemblages, the total mass storage of each component (contaminated sediment, Zn, Pb) within each assemblage was divided by the total mass storage of that component for the entire study area. The results indicate that for Zn and Pb storage increases from Terrace Veneer → Floodplain Drape → Channel Fill assemblages (Figure 46). In fact, Channel Fill assemblages store approximately 50% of the total Zn (51.1 Mg) and 55% of the Pb (12.2 Mg) in the study area. Furthermore, approximately 33% of the Zn (29.8 Mg) and 26% of the Pb (5.9 Mg) stored in the entire study area is located within the Channel Fill assemblage in Zone I alone. This is due to the low, wide floodplains present as a result of topsoil mining and subsequent scouring. For contaminated sediment, storage increases from Floodplain Drape to Channel Fill to Terrace Veneer. This likely skewed by the large area used for the Terrace Veneer assemblage in Zone III in the calculations.

Since the Channel Fill assemblage in Zone I was excavated during topsoil mining (sometime after mining ceased), it might be helpful to calculate the storage values of the area prior to topsoil mining. To do this, the maximum thickness of contamination in the Channel Fill assemblages within Zone I (1.83 m at Site 1B) was used. The resulting pre-topsoil mining storage calculation doubled the Channel Fill assemblage values for contaminated sediment, Zn, and, Pb. These results indicate that prior to topsoil mining, over half of the total Zn and nearly half of the total Pb in the study area would have been stored in the Channel Fill assemblage in Zone I. This is significant because this area would have been a large source of potential pollution if topsoil mining had not occurred.

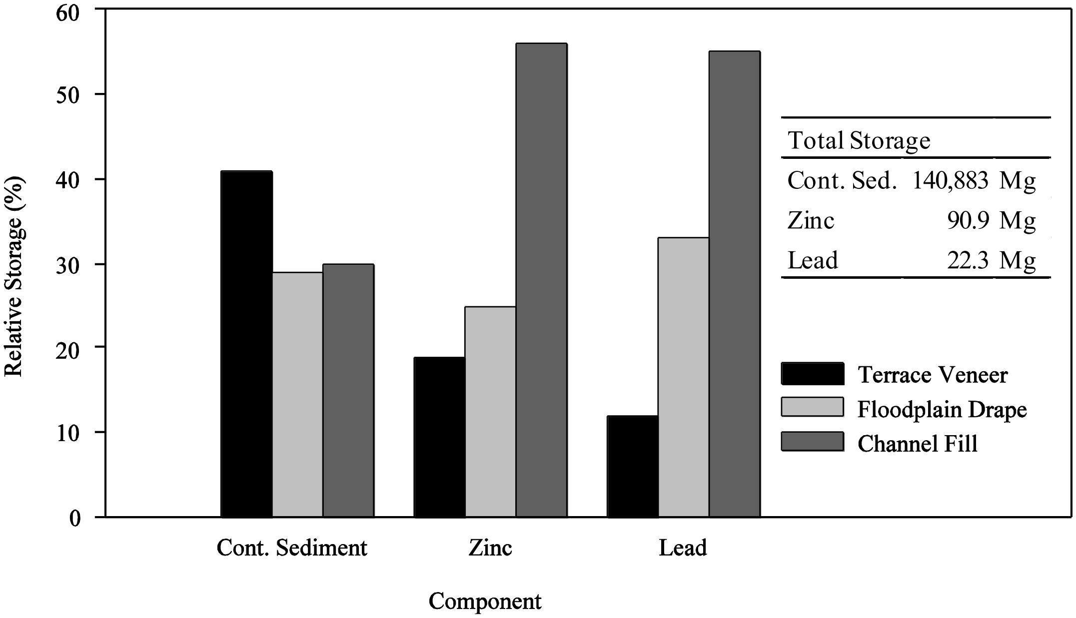

Figure 46. Distribution of relative storage by geo-stratigraphic assemblage for contaminated sediment, Zn, and Pb.

Storage values for the Terrace Veneer assemblage is unusually high in Zone III due to the large area that was mapped. The large areal extent of the Terrace Veneer assemblage within Zone III draws up the perceived storage value in Zone III higher than is likely present (Figure 46). The Terrace Veneer on the eastern side of the valley, closest to the James River, has not been cored to determine actual values of contaminant storage. Instead, to keep the calculations simple, it was assumed that this area was contaminated equally throughout. However, since contamination decreases with distance from Pearson Creek, it is likely that there is very little contamination on the eastern side of the valley, which would result in smaller storage values. This area could be further sampled to improve on these results.

Mass storage values can be used for determining what percent of the total mining production is stored in floodplain deposits. Total documented production in Pearson Creek for Zn was 21,150 Mg and for Pb was 5,229 Mg (Thomson, 1986). Results indicate that 0.43% of both Zn and Pb are currently stored in the study area. These values only represent a portion of the total storage in alluvial sediment in areas affected by the mines. For example, it is known that areas upstream of the current study area were affected by historical mining practices and that Zn is present in alluvial sediments along the James River downstream of Pearson Creek and in Lake Springfield. Incorporating these areas would provide a better estimate of the total amount of Pb and Zn introduced into alluvial sediment as a result of mining operations along Lower Pearson Creek.

CHAPTER 7

SUMMARY AND CONCLUSIONS

The purpose of this study was to develop a history of geomorphic responses to land use change along lower Pearson Creek by (1) determining the magnitude and across-valley distribution of mining-contaminated sediment; and (2) using floodplain sedimentology and trace-metal dating to determine recent and historical geomorphic changes. The broader goal was to increase the understanding of how streams in the Ozarks have responded to historical land use change and how they store mining-related sediment. To complete this study, soil cores were extracted from alluvial deposits along cross-sections and analyzed for physical and geochemical properties. Results of the analyses were used to correlate stratigraphic similarities and identify across-valley Zn trends.

The results of this study reveal that alluvial deposits along lower Pearson Creek are contaminated with Zn (Table 7) and were influenced by post-settlement land use change. The mean Zn concentration of all samples was 600 ppm while the median concentration was 193 ppm, ~8 and ~2.5 times background level, respectively. In general, the thickness of Zn contaminated sediment decreases with distance away from and height above the channel. Sedimentation rates from 1885 to 1912 ranged from 0 cm/yr to 4.79 cm/yr and from 1912 to 2008 ranged from 0 cm/yr to 2.08 cm/yr. High sedimentation rates during the mining period were probably due to combined impacts of mining operations and row crop farming. The reduction in post-mining sedimentation rates is likely due to better soil management practices and conversion from row crop farming to pasture farming.

Three unique geo-stratigraphic assemblages were identified during this study: terrace veneer, floodplain drape, and channel fill. Terrace veneer assemblages are characterized by <50 cm of slightly contaminated sediment overly uncontaminated (<77 ppm) 7.5YR (early to middle Holocene) or 10YR (late Holocene to historical) sediment and signify older floodplains that have since been abandoned by Pearson Creek. Floodplain drape assemblages consist of approximately 1 m of contaminated 10YR sediment overlying uncontaminated 10YR sediment. Channel fill assemblages are made of up fully contaminated 10YR sediment that has been deposited since mining began. They indicate sediment was deposited in the channel during channel migration or contraction of the channel margins. Terrace veneer assemblages are generally located farthest from and highest above the channel, while channel fill assemblages are located nearest to the channel in both elevation and distance (Figure 34). Zn concentrations increase from terrace veneer assemblages to channel fill assemblages (terrace veneer < floodplain drape < channel fill) (Table 8). Zinc concentrations also decrease in the downstream direction with a slight increase near where the mining tributary enters Pearson Creek (Figure 25).

Using floodplain assemblages, floodplain conceptual diagrams were developed and the geomorphic history of lower Pearson Creek was determined (Table 10). During the pre-mining period (prior to 1885), Holocene and post-Holocene terraces were being built and vertical accretion was the dominant form of sedimentation. The mining period was characterized by large inputs of sediment, channel instability, and both vertical and lateral accretion. Since mining ceased, the channel has undergone some recovery (contraction of the channel margins) and has been dominated by vertical accretion with some limited lateral accretion in Zone II and significant amount of lateral accretion in Zone III.

The geomorphic form of lower Pearson Creek is influenced by three hydrologic controls: Pearson Creek dominated (Zone I); Transition zone (Zone II); James River dominated (Zone III). Increasing sediment thickness downstream indicates that bed aggradation and overbank sedimentation has occurred (Figure 35). Also, Pearson Creek changes from a relatively straight channel (sinuosity= 1.1) in Zone I to a more meandering channel (sinuosity=1.8) in Zone II and III (Figure 42). The change in sediment thickness and planform could be attributed a base level rise of the James River caused by in-channel aggradation. Flood waters would have been able to travel further up Pearson Creek and encourage deposition where the stream entered the backflooded areas and lost the ability to transport sediment.

Management Implications

Past mining operations along lower Pearson Creek have introduced an extensive amount of metals into the floodplains, yet management practices have not been implemented. Geochemical data show the magnitude of Zn and geomorphic processes describe the distribution of Zn and its potential to be eroded. Suggested guidelines for determining harmful levels of pollutants in sediment are scattered throughout the literature. The Screening Quick Reference Tables (SQuiRTs) were developed from reviews of the literature in an attempt to set some consistent guidelines (Table 12). Target values are safe levels that mitigation should attempt to reach while Intervention values are levels at which mitigation should begin. MacDonald et al. (2000) is one source in the literature that provides similar guidelines (Table 12). Threshold Effect

Table 12. Guidelines for Zn concentration in freshwater sediment.

Source	Zinc (ppm)	Exceedance (%)	Pb (ppm)	Exceedance (%)
TEC*	121	57	35.8	58
PEC*	459	33	128	28
Target†	16	100	55	51
Intervention†	350	37	530	9

*TEC and PEC values from MacDonald et al. (2000)
†Target and Intervention values from SQuiRTs (2008)

Concentrations (TEC) are “values below which effects are unlikely to occur,” or “non-toxic,” while Probable Effect Concentrations (PEC) are “values above which harmful effects are likely to be observed,” or “toxic.” At Pearson Creek, the Target value for Zn is exceeded by 100% of the samples and for Pb by 51% of the samples. The Intervention value for Zn is exceeded by 37% of the samples and for Pb by 9% of the samples. The TEC value for Zn is exceeded by 57% of the samples and for Pb by 58% of the samples. The PEC is for Zn is exceeded by 33% of the samples and for Pb by 28% of the samples. Target values for Zn are unrealistic in this area since the background concentration of Zn is greater the Target value. However, since Zn and Pb exceed the PEC and Intervention values, some remediation might be required, the specifics of which are beyond the scope of this thesis.

Based on the data presented here, any remediation that does take place should focus on the Channel Fill assemblages in Zone I (Figure 44, Figure 45). These areas contain the highest concentrations of Zn and Pb and make up only 11% of the total area yet they currently store approximately one third of the total amount of Zn and Pb in the study area. However, Channel Fill assemblages in each zone have high concentrations of Zn and Pb. The map of the distribution of assemblages for the study area could be used to guide managers to locations containing large amounts of both Zn and Pb (Figure 44).

Future Work

This study focused on developing a timeline of the geomorphic evolution near the confluence of Pearson Creek and the James River using the stratigraphic distribution of mining pollutants along valley cross-sections. An important aspect not researched here is the mobility of the pollution. When studying pollutants in any natural system, identifying their source(s) is important to developing remediation plans. Due to the presence of elevated Zn levels near the channel margins, floodplain reworking (bank erosion) could reintroduce Zn into Pearson Creek where it could be transported downstream and into the James River.

Also, a similar study along the James River, downstream of Pearson Creek, could help in understanding how larger Ozarks streams store sediment and how they have responded to post-settlement land use changes. Similarly, research in more heavily mined basins, such as the Spring River near Joplin, the Big River within the Old Lead Belt, and other parts of the country, would further increase the understanding of how mining has affected the fluvial geomorphic history of streams.

The biological impact of Zn in the sediment along lower Pearson Creek is unknown. Zn is essential for the healthy development of many plant and animal species, however, at the levels observed in this study, it could be toxic if present in a form that makes it readily bioavailable. A survey of Zn in biota present within and around the channels could help determine to what extent the system is being affected.

Conclusions

Analysis of physical and geochemical data from floodplains along lower Pearson Creek yields the following final conclusions:

(1) Historical mining practices have resulted in extensive Zn pollution. Zn is present in concentrations from 18 ppm up to 12,395 ppm, has a mean value of 600 ppm, and exceeds background levels in 70% of the samples. Over 33% of the floodplain samples evaluated are greater than 459 ppm, the Probable Effects Concentration determined by MacDonald et al. (2000). Approximately 90.9 Mg

of Zn, 22.3 Mg of Pb, and 140,883 Mg of contaminated sediment is stored along lower Pearson. Channel Fill assemblages are the site of the most storage with approximately 50% of the total Zn (51.1 Mg) and 55% of the total Pb (12.2 Mg) present within them. Furthermore, approximately 33% of the Zn (29.8 Mg) and 26% of the Pb (5.9 Mg) stored in the entire study area is located within the Channel Fill assemblage in Zone I alone.

(2) Elevation and distance away from the channel and distance downstream are major controlling factors in the distribution of Zn in floodplains. An inverse relationship exists between Zn concentration and surface elevation above the thalweg. This indicates that flood frequency has limited the distribution of Zn.

(3) Past land use changes elevated sedimentation rates along Pearson Creek. Sedimentation rates were highest during the mining period (mean= 2.20 cm/yr) and decreased during the post-mining period (mean= 0.64 cm/yr). Soil loss from agricultural fields magnified the mining signal by mixing with mining-related sediment, thereby creating the illusion that high sedimentation rates during the mining period were solely due to mining practices. Furthermore, the decreased sedimentation rates following the mining period are likely the combined result of land use change from row crop farming to pasture farming and the implementation of better soil management practices.

Pollutants introduced into streams are affected by hydrologic and geomorphologic processes that disperse contaminated sediment along channels and on floodplains. The impact of land use changes has been shown to increase upland erosion, sediment yields, and downstream channel and floodplain sedimentation. Pearson Creek has undergone extensive sedimentation and channel changes since the mining period began and has incorporated mining-related metals into its floodplain deposits. The dynamic nature of fluvial systems warrants exploration into how these pollutants might be remobilized in the future. Further research is needed to better understand the source of the contamination and assess the potential threat to residents in the area.

LITERATURE CITED

Axtmann, E.V., Luoma, S.N., 1991. Large-scale distribution of metal contamination in the fine-grained sediments of the Clark Fork River, Montana, U.S.A. Applied Geochemistry 6, 75-88.

Beach, T., 1994. The fate of eroded soil: Sediment sinks and sediment budgets of agrarian landscapes in Southern Minnesota. Annals of the Association of American Geographers 84, 5-28.

Biron, P.M., Roy, A.G., Best, J.L., Boyer, C.J., 1993. Bed morphology and sedimentology at the confluence of unequal depth channels. Geomorphology 8, 115-129.

Brakenridge, G.R., 1981. Late Quaternary floodplain sedimentation along the Pomme de Terre River, Southern Missouri. Quaternary Research 15, 62-76.

Brakenridge, G.R., 1988. River flood regime and floodplain stratigraphy. In: Baker, V.R., Kochel, R.C., Patton, P.C. (Eds.), Flood Geomorphology. Wiley, Chichester, UK, 139-157.

Bradley, S.B., 1989. Incorporation of metalliferous sediments from historic mining into river floodplains. GeoJournal 19, 5-14.

Bradley, S.B., Cox, J.J., 1986. Heavy metals in the Hamps and Manifold valleys, North Straffordshire, U.K.: Distribution in floodplain soils. The Science of the Total Environment 50, 103-128.

Brewer, P.A., Taylor, M.P., 1997. The spatial distribution of heavy metal contaminated sediment across terraced floodplains. Catena 30, 229-249.

Brosius, L., and Sawin R.S., 2001. Lead and zinc mining in Kansas. Kansas Geological Survey Public Information Circular 17. Retrieved 31 January 2009 from http://www.kgs.ku.edu/Publications/pic17/pic17_1.html.

Bullard, L., Thomson, K.C., Vandike, J.E., 2001. The springs of Greene County, Missouri. Water Resources Report No. 68, 120 pp.

Carlson, J., 1999. Zinc mining contamination and sedimentation rates of historical overbank deposits, Homey Creek watershed, Southwest Missouri. Master's Thesis, Missouri State University, 164 pp.

Ciszewski, D., Malik, I., 2004. The use of heavy metal concentrations and dendrochronology in the reconstruction of sediment accumulation, Mala Panew River Valley, southern Poland. Geomorphology 58, 161-174.

De Serres, B., Roy, A.G., Biron, P.M., Best, J.L., 1999. Three-dimensional structure of flow at a confluence of river channels with discordant beds. Geomorphology 26, 313-335.

Division of Geology and Land Survey (DGLS), 2008. Inventory of Mines, Occurrences, and Prospects in Missouri (shapefile). Missouri Department of Natural Resources.

Fairbanks, J., Tuck, C.E., 1915. Past and Present of Greene County: Early and Recent History and Genealogical Records of Many of the Representative Citizens. Bowen, Indianapolis, IN, 1, 1933 pp.

Faulkner, D.J., 1998. Spatially variable historical alluviation and channel incision in west-central Wisconsin. Annals of the Association of American Geographers 88, 666-685.

Frederick, B.S., 2001. Spatial distribution of phosphorous in fluvial sediments from the James River Basin, SW Missouri. Master's Thesis, Missouri State University, 99 pp.

Graf, W.L., 1996. Transport and deposition of plutonium-contaminated sediments by fluvial processes, Los Alamos Canyon, New Mexico. GSA Bulletin 108, 1342-1355.

Horowitz, A.J., 1991. A primer on sediment-trace element chemistry (2nd edition). Lewis Publishers, Chelsea, MI, 136 pp.

Horton, J.M., 2003. Channel geomorphology and restoration guidelines for Springfield Plateau streams, South Dry Sac Watershed, southwest Missouri. Master's Thesis, Missouri State University, 150 pp.

Hughes, H.E., 1982. Soil Survey of Greene and Lawrence Counties, Missouri. United States Department of Agriculture, Soil Conservation Service and Missouri Agricultural Experiment Station, 160 pp.

Hudson-Edwards, K.A., 2003. Sources, mineralogy, chemistry and fate of heavy metal-bearing particles in mining-affected river systems. Mineralogical Magazine 67, 205-217.

Hudson-Edwards, K.A., Macklin, M.G., Curtis, C.D., Vaughan, D.J., 1998. Chemical remobilization of contaminant metals within floodplain sediments in an incising system: Implications for dating and chemostratigraphy. Earth Surface Processes and Landforms 23, 671-684.

Jacobson, R.B., Primm, A.T., 1994. Historical land-use changes and potential effects on stream disturbance in the Ozark Plateaus, Missouri. U.S. Geological Survey Open-File Report 94-333, 95 pp.

Kabata-Pendias, A., H. Pendias, 2000. Trace elements in soils and plants (3rd edition). CRC Press, Boca Raton, FL, 331 pp.

Kiekens, L., 1995. Zinc. In: Alloway, B.J. (Ed.) Heavy Metals in Soils (2nd edition). Blackie Academic and Professional, Glasgow, UK, 284-305.

Knighton, D., 1998. Fluvial forms and processes: A new perspective. Oxford University Press, New York, NY, 383 pp.

Knox, J.C., 1977. Human impacts on Wisconsin stream channels. Annals of the Association of American Geographers 67, 323-342.

Knox, J.C., 1987. Historical valley floor sedimentation in the Upper Mississippi Valley. Annals of the Association of American Geographers 77, 224-244.

Knox, J.C., 1989. Valley floor sedimentation in the Upper Mississippi Valley: Reply. Annals of the Association of American Geographers 79, 601-608.

Leenaers, H., 1989. Downstream changes of total and partitioned metal concentrations in the flood deposits of the River Geul (The Netherlands). GeoJournal 19, 37-43.

Lecce, S.A., 1997. Spatial patterns of historical overbank sedimentation on floodplain evolution, Blue River, Wisconsin. Geomorphology 18, 265-277.

Lecce, S.A., Pavlowsky, R.T., 1997. Storage of mining-related zinc in floodplain sediments, Blue River, Wisconsin. Physical Geography 18, 424-439.

Lecce, S.A., Pavlowsky, R.T., 2001. Use of mining-contaminated sediment tracers to investigate the timing and rates of historical flood plain sedimentation. Geomorphology 38, 85-108.

Lecce, S., Pavlowsky, R., Schlomer, G., 2008. Mercury contamination of active channel sediment and floodplain deposits from historic gold mining at Gold Hill, North Carolina, USA. Environmental Geology 55, 113-121.

Legleiter, K.J., 1999. GIS analysis of channel changes due to a small dam on the James River, SW Missouri. Master's Thesis, Missouri State University, 178 pp.

Lewin, J., Davies, B.E., Wolfenden, P.J., 1977. Interactions between channel change and historic mining sediments. In: Gregory, K.J. (Ed.), River Channel Changes. Wiley, Chichester, UK, 353-367.

Lewin, J., Wolfenden, P.J., 1978. The assessment of sediment sources: A field experiment. Earth Surface Processes 3, 171-178.

Macklin, M.G., 1985. Floodplain sedimentation in the upper Axe Valley, Mendip, England. Transactions of the Institute of British Geographers 10, 235-244.

MacDonald, D.D., Ingersoll, C.G., Berger, T.A., 2000. Development and evaluation of consensus-based sediment quality guidelines for freshwater ecosystems. Archives of Environmental Contamination and Toxicology 39, 20-31.

Magilligan, F.J., 1985. Historical floodplain sedimentation in the Galena River basin, Wisconsin and Illinois. Annals of the Association of American Geographers 75, 583-594.

Marron, D.C., 1992. Floodplain storage of mine tailings in the Belle Fourche River system: A sediment budget approach. Earth Surface Processes and Landforms 17, 675-685.

Merrington, G., Alloway, B.J., 1994. The flux of Cd, Cu, Pb, and Zn in mining polluted soils. Water, Air, and Soil Pollution 73, 333-344.

Midwestern Regional Climate Center, 2009. Historical climate summaries online data. Retrieved 4, August 2009 from <http://mcc.sws.uiuc.edu/climate_midwest/mwclimate_data_summaries.htm#>.

Missouri Department of Natural Resources (MoDNR), 2008. A Brownsfield Targeted Assessment of the Greene County Mines Site. 32 pp.

Natural Resources Conservation Service (NRCS), 2008. Official Soil Series Descriptions. USDA-NRCS, Lincoln, NE. Retrieved 22 August 2008 from http://soils.usda.gov/technical/classification/osd/index.html.

Owen, M.R., Pavlowsky, R.T, 2000. Historical mining pollution and overbank sedimentation along the James River, SW Missouri. Illustrated Paper. 96th Annual Meeting of the Association of American Geographers, Pittsburgh, PA.

Ozarks Environmental and Water Resources Institute (OEWRI), 2007a. Standard Operating Procedure: Vario EL III CHNOS Elemental Analyzer Operation. Missouri State University.

Ozarks Environmental and Water Resources Institute (OEWRI), 2007b. Standard Operating Procedure: X-MET3000TXS+ Handheld XRF Analyzer. Missouri State University.

Ozarks Environmental and Water Resources Institute (OEWRI), 2007c. Standard Operating Procedure for: Organic Matter in Sediment, Loss on Ignition Method. Missouri State University.

Ozarks Environmental and Water Resources Institute (OEWRI), 2008. Standard Operating Procedure: LS 13 320 Laser Diffraction Particle Size Analyzer Operation. Missouri State University.

Pavlowsky, R.T., 1995. Fluvial transport and long-term mobility of mining related zinc. In: Tailings and mine waste ’95, Balekema, Rotterdam, 395-404.

Rafferty, M.D., 1996. Rude Pursuits and Rugged Peaks: Schoolcraft's Ozark Journal, 1818-1819. University of Arkansas Press, Fayetteville, AR, 170 pp.

Rafferty, M.D., 1980. The Ozarks Land and Life. University of Oklahoma Press, Norman, OK, 282 pp.

Rhoads, B.L., Kentworthy, S.T., 1994. Flow structure at an asymmetrical stream confluence. Geomorphology 11, 273-293.

Rhoads, B.L., Riley, J.D., Mayer, D.R., 2009. Response of bed morphology and bed material texture to hydrological conditions at an asymmetrical stream confluence. Geomorphology 109, 161-173.

Roy, A.G., Woldenberg, M.J., 1986. A model for changes in channel form at a river confluence. Journal of Geology 94, 402-411.

Sauer, C.O., 1920. The geography of the Ozark Highland of Missouri. University of Chicago, 245 pp. Reprint: Greenwood Press, New York, NY, 1968.

Shepard, L., Gutiérrez, M., 1999. Metal retention in a thin karstic soil, Christian County, Missouri. Environmental Geology 37, 107-111.

Smith, J.D., Lambing, J.H., Nimick, D.A., Parrett, C., Ramey, M., Schafer, W., 1998. Geomorphology, flood-plain tailings, and metal transport in the Upper Clark Fork Valley, Montana. United States Geological Survey Water-Resources Investigations Report 98-4170, 56 pp.

Soil Survey Division Staff, 1993. Soil Survey Manual. Soil Conservation Service, U.S. Department of Agriculture Handbook 18.

Springfield-Greene County Library (SGCL), 2007. Historical population data for Springfield and Greene County, Missouri. Retrieved 27 February 2009 from <http://thelibrary.org/faq/files/mohistoricalpopulation.cfm>.

Taggart, A.F., 1945. Handbook of mineral dressing: Ores and industrial minerals. Wiley, New York, NY, 1679 pp.

Tannehill, T.D., 2002. Spatial trends of non-point pollutants in bottom sediment of Lake Springfield, southwest Missouri. Master's Thesis, Missouri State University, 89 pp.

Thomson, K.C., 1986. Geology of Greene County, Missouri. Watershed Management Coordinating Committee, Springfield, MO, 86 pp.

Trimble, J.C., 2001. Spatial patterns and floodplain contributions of mining-related contaminants in Chat Creek, Southwest Missouri. Master's Thesis, Missouri State University, 171 pp.

Trimble, S.W. and Lund, S.W., 1982. Soil conservation and the reduction of erosion and sedimentation in the Cook Creek Basin, Wisconsin. U.S. Geological Survey Professional Paper 1234, 35 pp.

Unde, M.G., Dhakal, S., 2009. Sediment characteristics at river confluences: a case study of the Mula-Kas confluence, Maharashtra, India. Progress in Physical Geography 33, 208-223.

U.S. Army Corps of Engineers (USACE), 1970. Floodplain formation: James River and Tributaries: Springfield Missouri Part II. United States Army, Little Rock, AR, 34 pp.

U.S. Census Bureau, 2008a. Missouri - Place and County Subdivision: Table GCT-T1-R Population Estimates (geographies ranked by estimate). 2007 Population Estimates Program. Retrieved 21 August 2008 from <http://factfinder.census.gov/servlet/GCTTable?_bm=y&-geo_id=04000US29&-_box_head_nbr=GCT-T1-R&-ds_name=PEP_2007_EST&-_lang=en&-redoLog=false&-format=ST-9S&-mt_name=PEP_2007_EST_GCTT1R_ST9S&-_sse=on>.

U.S. Census Bureau, 2008b. March 27, 2008 Press Release: Table 2. Population Change in the 100 Fastest-Growing Metropolitan Statistical Areas: July 1, 2006 to July 1, 2007. Retrieved 21 August 2008 from <http://www.census.gov/Press-Release/www/releases/archives/cb08-49table2.xls>.

U.S. Geological Survey (USGS), 2008. Water Resources of the United States Annual Data Report. Department of the Interior. Retrieved 9 September 2008 from <http://wdr.water.usgs.gov/wy2008/pdfs/07050690.2008.pdf>.

Walling, D.E., 1999. Linking land use, erosion, and sediment yields in river basins. Hydrobiologia 410, 223-240.

Wyllie, R.G., 2002. Relationship of dam construction and riparian buffer vegetation to historical channel changes, Little Sac River, southwest Missouri. Master's Thesis, Missouri State University, 154 pp.

APPENDICES

Appendix A. Sample Attributes

Appendix A-1. Latitude and Longitude of locations.

Site	Tape (m)	Latitude DD	Longitude DD
1A	39.6	37.17145	-93.19666
1A	51.0	37.17149	-93.19684
1A	60.3	37.17149	-93.19696
1A	82.0	37.17151	-93.19719
1A	102.0	37.17152	-93.19742
1A	107.5	37.17152	-93.19744
1B	38.3	37.17077	-93.19676
1B	68.0	37.17079	-93.19710
1B	107.0	37.17081	-93.19753
2	66.0	37.16937	-93.19612
2	91.0	37.16928	-93.19644
2	102.9	37.16924	-93.19654
3A	36.4	37.16852	-93.19555
3A	58.0	37.16838	-93.19573
3A	91.5	37.16815	-93.19598
3A	108.5	37.16804	-93.19611
3B	11.0	37.16793	-93.19507
3B	30.2	37.16789	-93.19528
3B	48.0	37.16786	-93.19549
3B	77.0	37.16781	-93.19580
4A	7.0	37.16734	-93.19558
4A	25.5	37.16750	-93.19550
4A	36.0	37.16756	-93.19539
4A	49.0	37.16768	-93.19535
4B	29.5	37.16758	-93.19591
4C	13.0	37.16735	-93.19603
4D	0.0	37.16643	-93.19584
4D	33.0	37.16643	-93.19621
4D	47.0	37.16644	-93.19636
5	0.0	37.16582	-93.19555
5	50.0	37.16584	-93.19612
5	103.0	37.16575	-93.19671
6	28.0	37.16517	-93.19620

Appendix A-1 Continued. Latitude and Longitude of locations.

Site	Tape (m)	Latitude DD	Longitude DD
6	61.0	37.16509	-93.19657
6	76.1	37.16502	-93.19672
BG1	2.3	37.23332	-93.15394
BG2	3	37.22263	-93.17068
BG3	-	37.20719	-93.19823
Cutbank DS 1B	-	37.16996	-93.19711
Drape DS 1B	-	37.17060	-93.19764
~5m US of 4B	-	37.16755	-93.19586
Tailings Trib.	-	37.16822	-93.19173
Tailings Pile	-	37.16825	-93.19157

Appendix A-2. Sample properties.

Sample	Site	Tape (m)	Depth (cm)		Munsell Color
			Min	Max	
PC 1	4C	-	0	0	-
PC 2*	4C	13	0	12	-
PC 3*	4C	13	12	30	-
PC 4*	4C	13	30	45	-
PC 5*	4C	13	45	65	-
PC 6*	4C	13	65	80	-
PC 7*	4C	13	80	100	-
PC 8*	4C	13	100	120	-
PC 9	~5m US of 4B	-	0	0	-
PC 10	Tailings Trib.	-	0	0	-
PC 11	Tailings Trib.	-	0	0	-
PC 12	Tailings Pile	-	0	0	-
PC 13	Tailings Pile	-	0	0	-
PC 14	1B	107	0	8	10 YR 3/2
PC 15	1B	107	8	18	7.5 YR 3/3
PC 16	1B	107	18	30	7.5 YR 3/3
PC 17	1B	107	30	40	7.5 YR 3/3
PC 18	1B	107	40	55	10 YR 3/2
PC 19	1B	107	55	70	10 YR 3/2
PC 20	1B	107	70	83	7.5 YR 3/3
PC 21	1B	107	83	96	7.5 YR 3/3
PC 22	1B	107	96	116	7.5 YR 3/3
PC 23	1B	107	116	136	7.5 YR 3/3
PC 24	1B	107	136	157	7.5 YR 3/3
PC 25	1B	107	157	183	Gleyed
PC 26	1B	107	183	203	Gleyed
PC 27	1B	38.3	0	10	10 YR 3/3
PC 28	1B	38.3	10	20	10 YR 3/3
PC 29	1B	38.3	20	30	10 YR 3/3
PC 30	1B	38.3	30	45	7.5 YR 3/3
PC 31	1B	38.3	45	60	7.5 YR 3.3
PC 32	1B	38.3	60	70	10 YR 4/3
PC 33	1B	38.3	70	85	10 YR 3/3
PC 34	1B	38.3	85	100	10 YR 3/3
PC 35	1B	38.3	100	120	10 YR 3/3
PC 36	1B	38.3	120	140	10 YR 3/3
PC 37	1B	38.3	140	160	10 YR 3/3
PC 38	1B	38.3	160	183	10 YR 3/3
PC 39	2	66	0	10	10 YR 3/3

* Not used in study

Appendix A-2 Continued. Sample properties.

Sample	Site	Tape (m)	Depth (cm)		Munsell Color
			Min	Max	
PC 40	2	66	10	20	10 YR 3/3
PC 41	2	66	20	30	10 YR 3/3
PC 42	2	66	30	50	7.5 YR 4/3
PC 43	2	66	50	70	7.5 YR 4/4
PC 44	2	66	70	90	7.5 YR 4/4
PC 45	2	66	90	102	7.5 YR 4/4
PC 46	2	102.9	0	7	
PC 47	2	102.9	7	20	
PC 48	2	102.9	20	35	
PC 49	2	102.9	35	50	
PC 50	2	102.9	50	62	
PC 51	2	102.9	62	74	
PC 52	2	102.9	74	86	
PC 53	2	102.9	86	98	
PC 54	2	102.9	98	110	
PC 55	2	102.9	110	135	
PC 56	2	102.9	135	160	
PC 57	2	102.9	160	193	
PC 58	2	102.9	193	226	
PC 59	2	102.9	226	256	
PC 60	5	0	0	15	10 YR 4/3
PC 61	5	0	15	28	10 YR 4/3
PC 62	5	0	28	50	10 YR 4/4
PC 63	5	0	50	70	10 YR 4/4
PC 64	5	0	70	85	10 YR 4/4
PC 65	5	0	85	110	10 YR 4/4
PC 66	5	0	110	132	10 YR 4/4
PC 67	5	0	132	150	Gravel
PC 68	5	50	0	12	10 YR 3/2
PC 69	5	50	12	22	10 YR 3/2
PC 70	5	50	22	34	10 YR 3/3
PC 71	5	50	34	45	10 YR 3/3
PC 72	5	50	45	60	10 YR 3/3
PC 73	5	50	60	80	10 YR 3/3
PC 74	5	50	80	100	10 YR 3/3
PC 75	5	50	100	115	10 YR 3/3
PC 76	5	50	115	130	10 YR 3/3
PC 77	5	50	130	150	10 YR 3/2
PC 78	5	50	150	170	10 YR 3/2
PC 79	5	50	170	190	7.5 YR 3/2

Appendix A-2 Continued. Sample properties.

Sample	Site	Tape (m)	Depth (cm)		Munsell Color
			Min	Max	
PC 80	5	50	190	220	7.5 YR 3/2
PC 81	5	50	220	250	Gleyed
PC 82	5	50	250	270	Gleyed
PC 83	5	50	270	293	Gleyed
PC 84	5	103	0	10	
PC 85	5	103	10	20	
PC 86	5	103	20	39	
PC 87	5	103	39	63	
PC 88	5	103	63	76	
PC 89	5	103	76	90	
PC 90	5	103	90	105	
PC 91	5	103	105	120	
PC 92	5	103	120	130	
PC 93	5	103	130	150	
PC 94	5	103	150	170	
PC 95	5	103	170	190	
PC 96	5	103	190	210	
PC 97	5	103	210	225	
PC 98	1A	39.6	0	15	
PC 99	1A	39.6	15	30	
PC 100	1A	39.6	30	46	
PC 101	1A	107.5	0	15	
PC 102	1A	107.5	15	30	
PC 103	1A	107.5	30	45	
PC 104	1A	107.5	45	60	
PC 105	1A	107.5	60	75	
PC 106	1A	107.5	75	90	
PC 107	1A	107.5	90	105	
PC 108	1A	107.5	105	130	
PC 109	1A	107.5	130	150	
PC 110	1A	107.5	150	170	
PC 111	1A	107.5	170	190	
PC 112	1A	107.5	190	210	
PC 113	1A	107.5	210	235	
PC 114	3A	36.4	0	10	
PC 115	3A	36.4	10	25	
PC 116	3A	36.4	25	40	
PC 117	3A	36.4	40	55	
PC 118	3A	36.4	55	75	
PC 119	3A	36.4	75	90	

Appendix A-2 Continued. Sample properties.

Sample	Site	Tape (m)	Depth (cm) Min	Depth (cm) Max	Munsell Color
PC 120	3A	58	0	10	
PC 121	3A	58	10	25	
PC 122	3A	58	25	40	
PC 123	3A	58	40	55	
PC 124	3A	58	55	70	
PC 125	3A	58	70	85	
PC 126	3A	58	85	100	
PC 127	3A	58	100	125	
PC 128	3A	58	125	140	
PC 129	3A	58	140	160	Gleyed
PC 130	3A	58	160	180	Gleyed
PC 131	3A	58	180	200	Gleyed
PC 132	3A	58	200	220	Gleyed
PC 133	3A	58	220	232	Gleyed
PC 134	3B	30.2	0	15	
PC 135	3B	30.2	15	30	
PC 136	3B	30.2	30	45	
PC 137	3B	30.2	45	66	
PC 138	3B	30.2	66	90	
PC 139	3B	30.2	90	110	
PC 140	3B	30.2	110	130	
PC 141	3B	30.2	130	152	
PC 142	3B	30.2	152	170	
PC 143	3B	30.2	170	185	
PC 144	3B	30.2	185	200	
PC 145	3B	30.2	200	217	
PC 146	3B	30.2	217	235	
PC 147	3B	30.2	235	255	
PC 148	3B	30.2	255	270	
PC 149	3B	30.2	270	285	
PC 150	3B	77	0	12	
PC 151	3B	77	12	35	
PC 152	3B	77	35	55	
PC 153	3B	77	55	75	
PC 154	3B	77	75	95	
PC 155	3B	77	95	115	
PC 156	3B	77	115	128	
PC 157	3B	77	128	140	
PC 158	3B	77	140	155	
PC 159	3B	77	155	175	

Appendix A-2 Continued. Sample properties.

Sample	Site	Tape (m)	Depth (cm)		Munsell Color
			Min	Max	
PC 160	3B	77	175	201	
PC 161	4A	7	0	14	10YR 4/3
PC 162	4A	7	14	30	10YR 4/3
PC 163	4A	7	30	50	10YR 4/3
PC 164	4A	7	50	70	10YR 4/3
PC 165	4A	7	70	90	10YR 4/3
PC 166	4A	7	90	110	10YR 4/3
PC 167	4A	7	110	130	10YR 4/3
PC 168	4A	7	130	158	10YR 4/3
PC 169	4A	7	158	180	10YR 4/4
PC 170	4A	7	180	205	10YR 4/4
PC 171	4A	7	205	225	10YR 3/6
PC 172	4A	7	225	248	10YR 3/6
PC 173	4A	25.5	0	15	10YR 4/3
PC 174	4A	25.5	15	25	10YR 4/4
PC 175	4A	25.5	25	35	10YR 4/4
PC 176	4A	25.5	35	45	10YR 4/4
PC 177	4A	25.5	45	55	10YR 4/4
PC 178	4A	25.5	55	74	10YR 4/4
PC 179	4A	25.5	74	90	10YR 4/3
PC 180	4A	25.5	90	110	10YR 4/3
PC 181	4A	25.5	110	127	10YR 4/3
PC 182	4A	25.5	127	145	10YR 3/3
PC 183	4A	25.5	145	165	10YR 3/3
PC 184	4A	25.5	165	185	10YR 3/3
PC 185	4A	25.5	185	197	10YR 3/3
PC 186	4A	25.5	197	225	10YR 3/1
PC 187	4A	25.5	225	250	10YR 3/1
PC 188	4A	25.5	250	275	10YR 3/1
PC 189	4A	25.5	275	306	10YR 3/1
PC 190	4B	29.5	0	14	10YR 3/3
PC 191	4B	29.5	14	30	7.5YR 3/3
PC 192	4B	29.5	30	45	7.5YR 3/3
PC 193	4B	29.5	45	61	7.5YR 3/3
PC 194	4B	29.5	61	80	7.5YR 3/3
PC 195	4B	29.5	80	92	7.5YR 3/3
PC 196	4B	29.5	92	107	7.5YR 3/3
PC 197	4B	29.5	107	125	7.5YR 3/3
PC 198	4B	29.5	125	140	7.5YR 3/3
PC 199	4B	29.5	140	155	7.5YR 3/3

Appendix A-2 Continued. Sample properties.

Sample	Site	Tape (m)	Depth (cm)		Munsell Color
			Min	Max	
PC 200	4B	29.5	155	170	7.5YR 3/3
PC 201	4B	29.5	170	190	7.5YR 3/3
PC 202	4B	29.5	190	210	7.5YR 4/3
PC 203	4B	29.5	210	230	7.5YR 4/3
PC 204	4B	29.5	230	275	7.5YR 4/3
PC 205	4C	13	0	16	10YR 3/3
PC 206	4C	13	16	26	7.5YR 3/3
PC 207	4C	13	26	37	7.5YR 3/3
PC 208	4C	13	37	49	7.5YR 4/2
PC 209	4C	13	49	61	7.5YR 4/3
PC 210	4C	13	61	74	7.5YR 4/3
PC 211	4C	13	74	91	7.5YR 4/2
PC 212	4C	13	91	105	7.5YR 3/3
PC 213	4C	13	105	122	7.5YR 3/3
PC 214	4C	13	122	140	10YR 3/2
PC 215	4C	13	140	163	10YR 3/2
PC 216	4C	13	163	180	7.5YR 3/2
PC 217	4C	13	180	200	7.5YR 3/2
PC 218	4C	13	200	234	7.5YR 3/2
PC 219	4C	13	234	265	Gleyed
PC 220	4C	13	265	292	Gleyed
PC 221	6	28	0	13	10YR 3/2
PC 222	6	28	13	30	10YR 3/3
PC 223	6	28	30	45	10YR 3/3
PC 224	6	28	45	60	10YR 3/3
PC 225	6	28	60	80	10YR 3/3
PC 226	6	28	80	100	10YR 3/3
PC 227	6	28	100	120	10YR 3/3
PC 228	6	28	120	137	10YR 3/3
PC 229	6	28	137	162	7.5YR 3/3
PC 230	6	61	0	16	10YR 3/3
PC 231	6	61	16	30	10YR 3/3
PC 232	6	61	30	45	10YR 3/3
PC 233	6	61	45	60	10YR 3/3
PC 234	6	61	60	75	10YR 3/3
PC 235	6	61	75	90	10YR 3/3
PC 236	6	61	90	110	10YR 3/3
PC 237	6	61	110	120	10YR 4/2|10YR 3/3
PC 238	6	61	120	130	10YR 4/2|10YR 3/3
PC 239	6	61	130	142	10YR 4/2|10YR 3/3

Appendix A-2 Continued. Sample properties.

Sample	Site	Tape (m)	Depth (cm)		Munsell Color
			Min	Max	
PC 240	6	61	142	155	10YR 3/3 | 4/6 | 2/2
PC 241	6	61	155	170	10YR 3/3 | 4/6 | 2/2
PC 242	6	61	170	190	10YR 3/3 | 4/6 | 2/2
PC 243	6	61	190	210	10YR 3/3 | 4/6 | 2/2
PC 244	6	61	210	230	10YR 3/3 | 4/6 | 2/2
PC 245	6	61	230	250	10YR 3/3 | 4/6 | 2/2
PC 246	6	61	250	262	Gleyed
PC 247	6	61	262	282	Gleyed
PC 248	6	61	282	302	Gleyed
PC 249	6	61	302	321	Gleyed
PC 250	6	76.1	0	10	10YR 3/2
PC 251	6	76.1	10	25	10YR 3/3
PC 252	6	76.1	25	40	10YR 3/3
PC 253	6	76.1	40	55	10YR 3/3
PC 254	6	76.1	55	67	10YR 3/3
PC 255	6	76.1	67	90	10YR 3/3
PC 256	6	76.1	90	110	10YR 3/3
PC 257	6	76.1	110	125	10YR 3/3
PC 258	6	76.1	125	140	10YR 3/3
PC 259	4C	-	-	-	-
PC 260	1A	39.6	0	36	10YR 3/3
PC 261	1A	39.6	36	88	10YR 3/3
PC 262	1A	51	0	23	10YR 3/2
PC 263	1A	51	23	43	10YR 3/2
PC 264	1A	60.3	0	30	10YR 3/2
PC 265	1A	60.3	30	48	10YR 3/2
PC 266	1A	82	0	34	10YR 3/2
PC 267	1A	82	34	66	10YR 3/2
PC 268	1A	82	66	85	10YR 3/3
PC 269	1A	102	0	24	10YR 3/3
PC 270	1A	102	24	57	10YR 3/2
PC 271	1B	68	0	15	10YR 3/2
PC 272	1B	68	15	34	10YR 3/2
PC 273	1B	68	34	50	10YR 3/3
PC 274	1B	68	50	66	10YR 3/3
PC 275	2	91	0	16	10YR 3/2
PC 276	2	91	16	30	10YR 3/2
PC 277	2	91	30	45	10YR 3/2
PC 278	2	91	45	58	10YR 3/2
PC 279	2	91	58	75	10YR 4/3

Appendix A-2 Continued. Sample properties.

Sample	Site	Tape (m)	Depth (cm)		Munsell Color
			Min	Max	
PC 280	2	91	75	90	10YR 4/3
PC 281	2	91	90	105	10YR 4/3
PC 282	2	91	105	120	10YR 4/3
PC 283	2	91	120	137	10YR 4/3
PC 284	2	91	137	165	Gleyed
PC 285	2	91	165	190	Gleyed
PC 286	3A	91.5	0	15	10YR 3/2
PC 287	3A	91.5	15	30	10YR 3/3
PC 288	3A	91.5	30	50	10YR 3/3
PC 289	3A	91.5	50	70	10YR 3/2
PC 290	3A	91.5	70	90	10YR 3/2
PC 291	3A	91.5	90	110	10YR 3/2
PC 292	3A	91.5	110	130	10YR 3/2
PC 293	3A	91.5	130	160	10YR 3/2
PC 294	3A	91.5	160	185	10YR 3/2
PC 295	3A	91.5	185	215	10YR 3/2
PC 296	3A	91.5	215	235	10YR 3/2
PC 297	3A	91.5	235	255	Gleyed
PC 298	3A	91.5	255	275	Gleyed
PC 299	3A	91.5	275	299	Gleyed
PC 300	3A	108.5	0	15	10YR 3/2
PC 301	3A	108.5	15	37	7.5YR 3/2
PC 302	3A	108.5	37	63	7.5YR 3/2
PC 303	3A	108.5	63	98	10YR 3/2
PC 304	3A	108.5	98	130	10YR 3/2
PC 305	3A	108.5	130	160	10YR 3/2
PC 306	3A	108.5	160	191	10YR 3/2
PC 307	3B	11	0	15	10YR 3/2
PC 308	3B	11	15	33	10YR 3/2
PC 309	3B	11	33	48	10YR 3/3
PC 310	3B	11	48	66	7.5YR 4/3
PC 311	3B	11	66	78	7.5YR 4/3
PC 312	3B	11	78	90	7.5YR 4/3
PC 313	3B	49	0	15	10YR 3/2
PC 314	3B	49	15	30	10YR 3/2
PC 315	3B	49	30	45	10YR 3/2
PC 316	3B	49	45	60	10YR 3/2
PC 317	3B	49	60	75	10YR 3/2
PC 318	3B	49	75	90	10YR 3/2
PC 319	3B	49	90	105	10YR 3/2

Appendix A-2 Continued. Sample properties.

Sample	Site	Tape	Depth (cm)		Munsell Color
		(m)	Min	Max	
PC 320	3B	49	105	120	10YR 3/2
PC 321	3B	49	120	133	10YR 3/2
PC 322	3B	49	133	158	10YR 3/2
PC 323	3B	49	158	175	10YR 3/2
PC 324	3B	49	175	191	Gleyed
PC 325	Cutbank DS 1B	-	0	30	-
PC 326	Cutbank DS 1B	-	30	45	-
PC 327	Cutbank DS 1B	-	45	55	-
PC 328	Cutbank DS 1B	-	55	70	-
PC 329	Cutbank DS 1B	-	70	85	-
PC 330	Cutbank DS 1B	-	85	100	-
PC 331	Cutbank DS 1B	-	100	115	-
PC 332	Drape DS 1B	-	0	10	10YR 3/2
PC 333	Drape DS 1B	-	10	25	7.5YR 3/2
PC 334	Drape DS 1B	-	25	40	7.5YR 3/2
PC 335	Drape DS 1B	-	40	60	7.5YR 3/2
PC 336	Drape DS 1B	-	60	85	10YR 3/2
PC 337	Drape DS 1B	-	85	110	10YR 3/2
PC 338	Drape DS 1B	-	110	130	Gleyed
PC 339	Drape DS 1B	-	130	160	Gleyed
PC 340	Drape DS 1B	-	160	192	Gleyed
PC 341	4A	36	0	25	7.5YR 3/2
PC 342	4A	36	25	50	7.5YR 3/2
PC 343	4A	36	50	75	10YR 4/1
PC 344	4A	36	75	100	10YR 4/1
PC 345	4A	49	0	25	7.5YR 3/2
PC 346	4A	49	25	50	10YR 3/2
PC 347	4A	49	50	75	10YR 3/2
PC 348	4A	49	75	100	10YR 3/2
PC 349	4D	0	0	15	10YR 3/2
PC 350	4D	0	15	30	7.5/10YR 3/2
PC 351	4D	0	30	45	7.5/10YR 3/2
PC 352	4D	0	45	60	7.5/10YR 3/2
PC 353	4D	0	60	75	7.5/10YR 3/2
PC 354	4D	0	75	90	7.5/10YR 3/2
PC 355	4D	0	90	105	7.5/10YR 3/2
PC 356	4D	0	105	120	7.5/10YR 3/2
PC 357	4D	0	120	135	7.5/10YR 3/2
PC 358	4D	0	135	160	7.5/10YR 3/2
PC 359	4D	0	160	185	7.5/10YR 3/2

Appendix A-2 Continued. Sample properties.

Sample	Site	Tape (m)	Depth (cm)		Munsell Color
			Min	Max	
PC 360	4D	0	185	210	7.5/10YR 3/2
PC 361	4D	0	210	235	7.5/10YR 3/2
PC 362	4D	0	235	260	7.5/10YR 3/2
PC 363	4D	0	260	285	7.5/10YR 3/2
PC 364	4D	0	285	316	7.5/10YR 3/2
PC 365	4D	0	316	340	Gleyed
PC 366	4D	26.6	0	30	-
PC 367	4D	33	0	25	7.5YR 3/2
PC 368	4D	33	25	40	7.5YR 3/2
PC 369	4D	33	40	55	7.5YR 3/2
PC 370	4D	33	55	70	7.5YR 3/2
PC 371	4D	33	70	85	7.5YR 3/2
PC 372	4D	33	85	100	7.5YR 3/2
PC 373	4D	33	100	122	7.5YR 3/2
PC 374	4D	33	122	130	10YR 3/2
PC 375	4D	33	130	150	10YR 3/2
PC 376	4D	33	150	170	10YR 3/2
PC 377	4D	33	170	190	10YR 3/2
PC 378	4D	33	190	220	10YR 2/2
PC 379	4D	33	220	250	10YR 2/2
PC 380	4D	33	250	285	10YR 2/2
PC 381	4D	33	285	305	10YR 3/1
PC 382	4D	33	305	335	10YR 3/1
PC 383	4D	33	335	365	Gleyed
PC 384	4D	33	365	405	Gleyed
PC 385	4D	47	0	35	10YR 4/3
PC 386	4D	47	35	50	10YR 4/3
PC 387	4D	47	50	65	10YR 3/3
PC 388	4D	47	65	80	10YR 3/2
PC 389	4D	47	80	98	7.5YR 3/2
PC 390	BG1	2.3	0	20	10YR 4/3
PC 391	BG1	2.3	20	35	10YR 4/3
PC 392	BG1	2.3	35	50	10YR 4/3
PC 393	BG2	3	0	15	10YR 3/2
PC 394	BG2	3	15	30	10YR 3/2
PC 395	BG2	3	30	45	10YR 3/2
PC 396	BG3	-	0	10	10YR 4/3
PC 397	BG3	-	10	25	10YR 4/3
PC 398	BG3	-	25	40	10YR 3/2

Appendix B. Textural Data

Appendix B. Textural data used in this study.

Sample	Percent Sand (2000-62.5μm)	Percent Silt (62.5-3.9μm)	Percent Clay (<3.9μm)	Mean (μm)	d_{10} (μm)	d_{50} (μm)	d_{90} (μm)
PC 1	19.30	63.22	17.47	61.9	2.1	20.4	199.6
PC 2*	2.97	75.92	21.11	19.38	1.72	14.79	43.37
PC 3*	3.51	75.39	21.10	19.90	1.72	15.14	44.73
PC 4*	5.37	75.30	19.33	22.23	1.89	16.61	50.64
PC 5*	5.32	77.03	17.65	23.05	2.02	18.56	49.73
PC 6*	24.90	59.78	15.31	73.20	2.44	26.91	225.08
PC 7*	5.84	74.13	20.03	22.53	1.82	16.56	50.98
PC 8*	4.80	73.86	21.33	21.12	1.69	15.46	46.48
PC 9	16.13	73.68	10.19	38.70	3.77	34.85	74.24
PC 10	53.21	36.68	10.11	428.66	3.82	90.96	1,128.92
PC 11	64.50	27.84	7.65	533.64	5.55	518.14	1,249.27
PC 12	28.19	63.53	8.28	65.37	5.03	42.29	119.62
PC 13	37.34	53.41	9.26	112.67	4.27	46.64	307.65
PC 14	9.90	70.28	19.82	29.85	1.90	15.69	62.91
PC 15	4.39	73.97	21.65	20.66	1.73	13.75	43.26
PC 16	2.07	74.88	23.05	17.58	1.63	13.11	39.73
PC 17	5.89	71.71	22.40	23.71	1.62	14.17	47.62
PC 18	1.88	75.01	23.11	17.67	1.56	13.00	41.14
PC 19	7.31	71.48	21.21	24.01	1.72	14.34	50.57
PC 20	6.75	70.43	22.82	23.14	1.59	12.96	49.84
PC 21	4.83	72.14	23.03	20.35	1.59	12.16	42.96
PC 22	6.53	72.24	21.23	23.55	1.69	13.12	50.02
PC 23	7.42	71.93	20.64	26.18	1.68	13.01	52.94
PC 24	7.75	71.20	21.05	24.37	1.62	12.86	50.44
PC 25	8.34	71.40	20.26	24.75	1.71	13.70	53.85
PC 26	3.17	72.73	24.10	18.27	1.50	13.18	41.13
PC 27	14.73	63.68	21.59	45.96	1.76	15.96	104.87
PC 28	13.92	63.80	22.28	44.71	1.67	15.65	99.49
PC 29	17.69	60.80	21.51	66.98	1.72	16.96	211.28
PC 30	16.59	62.25	21.16	55.23	1.73	17.74	139.65
PC 31	17.09	63.95	18.96	51.77	1.93	19.58	126.49
PC 32	17.08	65.46	17.46	38.35	2.12	21.73	94.26
PC 33	9.36	73.17	17.46	26.21	2.07	19.17	61.48
PC 34	4.85	75.81	19.35	21.13	1.86	15.95	45.44
PC 35	10.61	69.98	19.40	29.50	1.89	17.50	66.52
PC 36	6.25	71.44	22.30	24.23	1.63	14.09	47.87

* Not used in study

Appendix B Continued. Textural data used in this study.

Sample	Percent Sand (2000-62.5μm)	Percent Silt (62.5-3.9μm)	Percent Clay (<3.9μm)	Mean (μm)	d_{10} (μm)	d_{50} (μm)	d_{90} (μm)
PC 37	6.28	69.28	24.43	23.54	1.53	12.32	48.38
PC 38	10.03	70.42	19.55	31.09	1.81	15.34	63.62
PC 39	5.77	73.91	20.33	20.90	1.87	14.40	46.62
PC 40	5.24	74.44	20.33	20.46	1.81	14.15	44.40
PC 41	3.87	75.56	20.58	19.23	1.75	12.97	41.03
PC 42	3.51	76.62	19.87	18.41	1.73	12.50	38.85
PC 43	1.53	76.65	21.81	17.10	1.60	13.66	36.76
PC 44	1.89	76.40	21.71	17.29	1.62	13.46	36.55
PC 45	1.50	75.69	22.80	16.92	1.55	12.56	35.03
PC 46	11.24	70.98	17.78	31.70	2.12	18.27	69.76
PC 47	3.93	74.34	21.73	20.07	1.70	14.83	45.46
PC 48	3.64	75.36	21.00	20.53	1.70	16.06	45.38
PC 49	4.98	74.58	20.43	21.22	1.76	15.82	47.44
PC 50	11.25	70.96	17.79	32.39	2.10	18.41	69.57
PC 51	7.72	73.50	18.78	24.25	1.95	17.61	56.74
PC 52	8.54	73.56	17.90	25.81	2.05	19.59	59.49
PC 53	6.93	74.53	18.54	23.69	1.97	17.48	54.08
PC 54	5.31	75.26	19.43	21.39	1.86	15.83	48.55
PC 55	11.85	70.09	18.06	30.16	2.05	20.05	69.42
PC 56	10.29	69.19	20.52	27.24	1.76	17.10	64.58
PC 57	9.41	68.66	21.93	27.54	1.66	16.02	60.89
PC 58	4.76	70.85	24.39	19.71	1.55	13.16	45.24
PC 59	12.41	65.69	21.90	46.36	1.73	16.05	84.59
PC 60	3.59	79.98	16.43	22.43	2.18	19.24	45.10
PC 61	2.81	80.68	16.51	21.69	2.17	18.84	43.85
PC 62	3.61	80.88	15.51	23.66	2.26	21.13	46.90
PC 63	6.88	78.25	14.87	29.67	2.38	22.30	52.62
PC 64	13.48	72.74	13.78	42.74	2.60	24.39	97.57
PC 65	24.68	62.68	12.64	68.66	2.87	28.29	218.59
PC 66	36.65	51.81	11.54	103.77	3.21	35.10	296.36
PC 67	43.19	45.87	10.94	141.16	3.44	40.97	404.49
PC 68	7.38	71.50	21.13	25.72	1.83	14.41	51.63
PC 69	3.67	74.39	21.94	19.74	1.70	14.04	42.15
PC 70	5.03	74.82	20.15	22.60	1.81	16.12	46.52
PC 71	6.74	73.21	20.04	24.98	1.85	16.06	50.40
PC 72	5.30	75.30	19.39	23.23	1.86	16.39	46.76
PC 73	4.66	75.42	19.92	20.92	1.82	15.12	45.78
PC 74	3.57	76.05	20.38	19.80	1.77	14.33	44.25

Appendix B Continued. Textural data used in this study.

Sample	Percent Sand (2000-62.5μm)	Percent Silt (62.5-3.9μm)	Percent Clay (<3.9μm)	Mean (μm)	d_{10} (μm)	d_{50} (μm)	d_{90} (μm)
PC 75	3.71	75.72	20.57	19.89	1.74	14.28	45.20
PC 76	3.56	74.67	21.77	18.89	1.61	13.10	42.11
PC 77	3.63	75.22	21.14	19.50	1.65	12.74	43.43
PC 78	15.19	66.55	18.26	41.56	1.95	17.78	168.35
PC 79	6.85	72.64	20.51	21.77	1.71	14.46	47.30
PC 80	10.55	70.34	19.11	30.39	1.82	15.52	84.29
PC 81	14.64	66.74	18.62	33.48	1.90	17.63	95.05
PC 82	4.61	74.18	21.21	23.02	1.73	16.69	46.35
PC 83	3.00	74.58	22.42	19.77	1.63	15.50	43.57
PC 84	3.88	74.00	22.12	19.49	1.72	13.92	44.46
PC 85	1.98	74.13	23.89	17.55	1.57	12.98	39.94
PC 86	4.77	72.62	22.61	22.16	1.60	14.56	45.43
PC 87	7.52	73.76	18.71	26.25	1.95	18.23	56.03
PC 88	9.84	71.49	18.66	28.09	1.96	19.22	62.99
PC 89	15.84	68.74	15.43	34.83	2.37	25.80	78.75
PC 90	9.71	70.49	19.81	26.72	1.87	18.59	62.69
PC 91	7.77	70.52	21.70	24.08	1.72	15.87	56.49
PC 92	7.25	71.03	21.73	23.87	1.70	15.85	54.39
PC 93	5.57	71.76	22.67	22.44	1.63	15.19	48.32
PC 94	3.28	72.69	24.03	18.71	1.53	12.86	40.67
PC 95	3.98	71.91	24.11	20.01	1.53	13.13	42.66
PC 96	3.69	69.28	27.03	18.61	1.40	10.37	39.38
PC 97	7.24	70.64	22.11	25.76	1.75	14.67	50.69
PC 98	5.00	74.15	20.84	21.11	1.76	15.43	46.91
PC 99	6.22	72.64	21.14	23.54	1.74	15.62	49.90
PC 100	23.42	60.16	16.42	101.89	2.26	22.96	440.02
PC 101	4.07	75.76	20.17	20.38	1.81	15.43	44.03
PC 102	3.80	75.32	20.88	19.78	1.75	14.71	43.03
PC 103	3.95	75.13	20.92	20.04	1.76	14.75	43.22
PC 104	3.23	74.55	22.22	18.89	1.67	13.76	41.14
PC 105	3.59	73.91	22.49	19.41	1.64	13.49	41.51
PC 106	3.04	74.39	22.57	18.60	1.63	13.37	40.63
PC 107	3.55	74.36	22.09	19.48	1.67	13.63	41.47
PC 108	3.17	74.61	22.21	18.86	1.65	13.48	40.26
PC 109	2.95	75.10	21.95	18.67	1.67	13.61	39.48
PC 110	2.87	75.24	21.90	18.53	1.68	13.52	38.97
PC 111	2.75	74.81	22.44	18.11	1.64	13.06	38.05
PC 112	2.62	74.89	22.50	17.84	1.64	12.91	37.48

Appendix B Continued. Textural data used in this study.

Sample	Percent Sand (2000-62.5μm)	Percent Silt (62.5-3.9μm)	Percent Clay (<3.9μm)	Mean (μm)	d_{10} (μm)	d_{50} (μm)	d_{90} (μm)
PC 113	2.78	74.66	22.56	18.21	1.62	13.13	38.26
PC 114	5.48	75.71	18.82	22.80	1.95	15.69	45.55
PC 115	2.89	77.15	19.96	19.23	1.81	14.69	39.32
PC 116	2.82	77.04	20.14	19.04	1.80	14.47	38.90
PC 117	2.23	76.14	21.63	17.83	1.69	13.44	36.94
PC 118	1.94	76.23	21.83	17.37	1.68	13.14	36.00
PC 119	1.91	75.93	22.16	17.12	1.66	12.92	35.76
PC 120	4.55	74.95	20.50	21.38	1.79	14.42	43.06
PC 121	4.92	73.69	21.40	21.37	1.72	14.51	44.92
PC 122	4.65	76.03	19.33	22.28	1.86	16.07	45.33
PC 123	3.61	76.74	19.65	19.83	1.85	15.10	43.74
PC 124	3.60	76.79	19.61	20.35	1.84	15.18	43.10
PC 125	1.38	78.56	20.07	17.29	1.79	14.32	36.38
PC 126	3.02	75.10	21.88	18.57	1.69	13.88	41.21
PC 127	2.99	76.17	20.84	19.15	1.75	14.95	41.28
PC 128	3.72	74.33	21.95	19.68	1.68	14.69	43.21
PC 129	3.31	73.02	23.67	18.30	1.56	13.05	40.74
PC 130	3.76	76.98	19.26	20.59	1.88	16.03	43.76
PC 131	3.77	76.15	20.07	20.36	1.81	15.58	43.64
PC 132	4.14	76.59	19.27	21.14	1.89	16.27	45.00
PC 133	4.71	76.42	18.87	21.94	1.92	16.80	46.69
PC 134	6.93	73.28	19.78	24.64	1.85	16.14	51.39
PC 135	4.12	75.67	20.21	20.75	1.78	15.09	43.40
PC 136	4.08	75.39	20.53	20.91	1.77	15.56	44.01
PC 137	4.68	75.52	19.80	21.89	1.83	16.45	46.64
PC 138	4.04	76.54	19.41	21.00	1.85	15.76	44.64
PC 139	2.99	78.00	19.01	20.01	1.88	15.73	42.39
PC 140	3.87	77.73	18.39	21.16	1.93	16.49	43.85
PC 141	5.47	76.25	18.28	23.33	1.96	17.95	49.33
PC 142	12.34	76.53	11.13	35.00	3.37	31.77	67.78
PC 143	13.01	75.41	11.59	34.80	3.21	28.42	70.80
PC 144	14.72	73.15	12.13	35.97	3.06	29.54	74.23
PC 145	8.85	73.06	18.09	26.58	2.05	18.84	60.65
PC 146	8.61	73.07	18.32	26.49	2.02	18.58	59.77
PC 147	6.57	73.81	19.62	23.94	1.86	16.33	51.79
PC 148	2.15	75.89	21.96	18.23	1.68	13.83	41.59
PC 149	2.39	74.88	22.73	18.28	1.64	13.56	42.12
PC 150	3.41	76.76	19.83	20.20	1.84	15.87	44.63

Appendix B Continued. Textural data used in this study.

Sample	Percent Sand (2000-62.5μm)	Percent Silt (62.5-3.9μm)	Percent Clay (<3.9μm)	Mean (μm)	d_{10} (μm)	d_{50} (μm)	d_{90} (μm)
PC 151	2.57	76.55	20.88	19.07	1.74	15.03	42.04
PC 152	2.22	76.58	21.20	18.24	1.73	14.24	40.19
PC 153	0.73	77.86	21.41	17.17	1.73	13.86	37.87
PC 154	1.53	78.66	19.81	18.61	1.82	15.45	39.88
PC 155	1.45	78.77	19.78	18.54	1.82	15.41	39.70
PC 156	2.08	76.14	21.79	18.06	1.67	14.16	39.46
PC 157	2.48	76.77	20.75	18.77	1.74	14.84	40.30
PC 158	3.06	76.19	20.75	19.32	1.76	14.86	41.40
PC 159	3.78	75.67	20.56	20.09	1.77	14.93	42.89
PC 160	8.09	71.85	20.06	28.39	1.84	15.81	53.54
PC 161	3.41	79.50	17.09	21.46	2.08	17.72	43.24
PC 162	3.02	80.65	16.33	21.64	2.15	18.53	43.13
PC 163	4.39	79.88	15.74	24.52	2.24	19.66	45.96
PC 164	4.24	80.63	15.12	24.11	2.33	20.54	46.84
PC 165	4.96	79.56	15.48	26.14	2.29	20.28	47.57
PC 166	4.40	79.47	16.13	24.72	2.19	19.31	45.97
PC 167	5.32	77.40	17.28	26.65	2.06	17.80	46.01
PC 168	6.88	74.71	18.42	29.40	1.95	16.29	47.68
PC 169	15.86	66.15	17.98	62.77	2.03	17.01	241.17
PC 170	24.44	59.25	16.31	90.83	2.25	19.92	332.16
PC 171	48.73	40.32	10.95	201.67	3.47	51.43	544.77
PC 172	72.03	22.01	5.96	321.48	9.16	265.90	756.73
PC 173	5.53	75.46	19.01	22.81	1.91	16.05	46.57
PC 174	2.91	77.54	19.55	19.32	1.82	15.29	39.88
PC 175	3.26	77.43	19.31	20.26	1.86	16.14	42.77
PC 176	3.18	77.39	19.43	20.00	1.84	15.82	41.92
PC 177	3.45	78.11	18.44	20.83	1.93	16.64	43.37
PC 178	6.43	77.73	15.84	25.23	2.27	19.81	54.02
PC 179	5.81	77.14	17.06	24.11	2.11	18.00	50.70
PC 180	2.37	79.02	18.61	19.93	1.91	16.09	40.71
PC 181	1.64	78.94	19.42	19.00	1.85	16.04	40.18
PC 182	3.95	75.37	20.67	21.12	1.77	15.76	45.66
PC 183	5.53	73.99	20.48	22.97	1.79	16.43	47.36
PC 184	4.66	74.99	20.35	22.15	1.78	16.24	46.49
PC 185	4.41	73.20	22.39	20.99	1.66	14.43	44.19
PC 186	4.28	74.16	21.56	20.96	1.71	14.67	44.08
PC 187	5.21	74.12	20.66	23.20	1.78	14.98	45.88
PC 188	96.79	1.95	1.26	26.12	1.98	17.54	52.04

Appendix B Continued. Textural data used in this study.

Sample	Percent Sand (2000-62.5μm)	Percent Silt (62.5-3.9μm)	Percent Clay (<3.9μm)	Mean (μm)	d_{10} (μm)	d_{50} (μm)	d_{90} (μm)
PC 189	100.00	0.00	0.00	56.15	2.13	18.98	161.20
PC 190	4.13	75.75	20.13	20.52	1.81	15.52	44.79
PC 191	3.85	74.81	21.34	19.90	1.72	14.75	43.51
PC 192	3.87	76.13	20.00	20.16	1.82	15.15	43.66
PC 193	2.34	76.58	21.08	19.07	1.72	15.08	42.31
PC 194	4.38	78.13	17.49	21.91	2.05	17.41	46.80
PC 195	3.78	77.44	18.78	20.24	1.90	15.61	43.63
PC 196	3.25	80.07	16.68	21.51	2.11	18.40	42.79
PC 197	7.89	74.17	17.94	25.38	2.04	18.18	57.43
PC 198	3.82	73.91	22.27	19.52	1.67	13.54	42.13
PC 199	4.37	74.75	20.88	20.75	1.76	15.29	44.62
PC 200	3.82	74.96	21.22	20.78	1.73	15.17	43.96
PC 201	5.60	73.18	21.22	23.22	1.73	15.37	47.44
PC 202	3.85	74.77	21.38	20.17	1.72	14.65	43.01
PC 203	2.72	74.79	22.48	17.98	1.65	12.69	38.11
PC 204	9.66	72.69	17.65	33.68	2.07	18.18	61.65
PC 205	6.48	73.50	20.02	24.68	1.82	15.88	50.09
PC 206	7.51	72.86	19.63	27.33	1.86	16.74	53.94
PC 207	6.72	74.74	18.53	24.86	1.97	17.69	53.73
PC 208	8.76	75.43	15.81	28.78	2.30	21.10	60.26
PC 209	5.91	76.26	17.83	24.08	2.01	18.13	51.11
PC 210	11.61	70.06	18.33	35.45	1.99	18.80	72.17
PC 211	14.73	68.50	16.77	48.81	2.20	20.84	96.63
PC 212	6.38	74.87	18.76	24.50	1.95	17.37	52.07
PC 213	6.66	73.91	19.43	24.82	1.88	16.93	51.07
PC 214	3.31	75.81	20.88	20.00	1.76	15.00	42.65
PC 215	5.43	77.09	17.48	24.54	2.07	18.34	47.91
PC 216	6.08	78.01	15.91	27.16	2.25	20.33	50.40
PC 217	6.56	76.98	16.47	28.09	2.18	19.89	51.20
PC 218	9.04	74.14	16.82	34.26	2.14	19.79	58.44
PC 219	9.42	72.08	18.51	35.27	1.98	17.19	59.83
PC 220	7.50	73.11	19.39	28.48	1.91	15.78	50.80
PC 221	2.02	79.09	18.89	18.98	1.91	15.53	40.18
PC 222	2.41	80.88	16.70	21.22	2.14	17.82	42.32
PC 223	2.05	81.08	16.87	20.85	2.11	17.69	41.81
PC 224	1.52	81.37	17.12	20.16	2.07	17.27	40.41
PC 225	2.11	80.46	17.43	19.89	2.03	16.85	40.31
PC 226	0.59	81.60	17.81	18.54	2.00	16.30	38.39

Appendix B Continued. Textural data used in this study.

Sample	Percent Sand (2000-62.5µm)	Percent Silt (62.5-3.9µm)	Percent Clay (<3.9µm)	Mean (µm)	d_{10} (µm)	d_{50} (µm)	d_{90} (µm)
PC 227	0.44	80.64	18.92	17.60	1.88	15.11	37.02
PC 228	0.41	79.69	19.90	16.80	1.81	14.05	35.85
PC 229	0.44	78.92	20.64	16.29	1.75	13.33	35.19
PC 230	2.45	77.09	20.46	18.42	1.77	14.41	38.97
PC 231	2.89	78.61	18.50	21.20	1.93	17.20	42.97
PC 232	2.55	78.54	18.91	20.21	1.90	16.89	42.73
PC 233	2.97	77.39	19.64	20.41	1.85	15.54	41.94
PC 234	2.12	77.72	20.16	18.74	1.80	14.41	39.43
PC 235	2.38	76.16	21.45	18.34	1.73	13.46	40.30
PC 236	3.69	77.82	18.50	21.49	1.97	17.35	46.52
PC 237	5.31	76.46	18.23	23.00	2.01	16.99	50.73
PC 238	3.91	79.28	16.82	23.23	2.16	19.55	50.42
PC 239	2.66	76.59	20.75	19.69	1.78	14.77	46.32
PC 240	1.20	75.88	22.92	16.91	1.64	12.84	37.51
PC 241	2.84	75.20	21.95	18.53	1.69	13.72	40.45
PC 242	1.85	75.85	22.30	17.36	1.66	13.20	38.93
PC 243	0.64	75.33	24.03	15.86	1.53	12.06	36.03
PC 244	0.29	75.13	24.59	15.22	1.53	11.44	35.10
PC 245	0.19	75.24	24.57	14.62	1.52	11.05	33.29
PC 246	0.81	77.01	22.19	16.60	1.67	13.09	36.82
PC 247	1.81	74.54	23.65	16.49	1.59	11.72	35.90
PC 248	2.09	76.81	21.09	18.34	1.75	14.22	40.79
PC 249	7.69	73.94	18.37	26.25	2.02	17.63	54.51
PC 250	3.17	77.14	19.69	19.71	1.85	15.43	43.13
PC 251	4.27	75.07	20.66	20.40	1.76	14.89	43.89
PC 252	2.58	76.14	21.28	18.71	1.72	14.39	41.60
PC 253	3.82	75.59	20.58	20.06	1.75	15.32	42.90
PC 254	5.02	73.31	21.67	20.69	1.70	14.66	46.15
PC 255	3.93	73.86	22.21	19.34	1.67	13.83	43.23
PC 256	3.30	72.50	24.21	17.90	1.56	12.31	41.09
PC 257	5.43	72.04	22.52	23.92	1.65	13.54	45.43
PC 258	6.15	72.19	21.65	24.74	1.71	14.65	47.94
PC 259	2.23	71.48	26.29	15.51	1.39	10.43	35.77
PC 260	11.06	69.71	19.23	34.88	1.89	17.73	69.45
PC 261	12.55	69.70	17.74	60.66	2.06	19.22	75.62
PC 262	9.93	70.49	19.59	34.25	1.85	16.84	63.06
PC 263	12.45	68.21	19.35	55.87	1.88	17.32	87.98
PC 264	4.08	75.39	20.53	20.56	1.77	15.69	46.04

Appendix B Continued. Textural data used in this study.

Sample	Percent Sand (2000-62.5μm)	Percent Silt (62.5-3.9μm)	Percent Clay (<3.9μm)	Mean (μm)	d_{10} (μm)	d_{50} (μm)	d_{90} (μm)
PC 265	4.11	75.56	20.33	20.58	1.78	15.70	46.45
PC 266	4.40	73.55	22.05	21.44	1.68	14.24	45.51
PC 267	7.24	70.24	22.53	27.38	1.64	14.42	52.04
PC 268	10.49	68.28	21.23	36.27	1.74	15.95	66.72
PC 269	2.40	75.96	21.64	18.69	1.70	14.40	41.83
PC 270	8.16	69.53	22.31	26.73	1.67	14.38	54.06
PC 271	13.52	68.36	18.12	36.40	2.07	18.39	90.56
PC 272	3.75	74.85	21.40	20.16	1.71	15.25	45.84
PC 273	2.08	73.52	24.40	17.25	1.53	12.42	39.81
PC 274	3.69	71.90	24.41	19.98	1.54	12.58	42.73
PC 275	3.32	76.53	20.16	20.11	1.82	15.60	45.14
PC 276	3.71	75.92	20.37	20.47	1.80	15.72	46.25
PC 277	1.74	74.61	23.65	17.44	1.59	12.90	40.00
PC 278	1.53	74.49	23.98	17.09	1.57	12.64	39.21
PC 279	1.70	76.26	22.03	17.91	1.68	13.94	39.93
PC 280	2.86	75.68	21.46	19.22	1.72	14.63	43.49
PC 281	2.17	76.96	20.87	18.83	1.76	14.79	41.96
PC 282	2.90	75.57	21.52	19.80	1.69	15.33	45.30
PC 283	6.93	71.11	21.97	26.53	1.68	15.18	51.53
PC 284	6.12	72.95	20.93	23.56	1.77	15.57	49.61
PC 285	4.59	71.46	23.94	20.31	1.53	12.86	43.35
PC 286	8.19	72.07	19.74	28.54	1.84	16.54	55.61
PC 287	5.81	73.27	20.92	24.39	1.73	15.37	48.30
PC 288	6.37	73.04	20.59	25.25	1.75	16.03	50.71
PC 289	2.06	77.50	20.45	18.64	1.74	14.67	41.75
PC 290	1.80	76.11	22.09	18.29	1.64	14.40	41.04
PC 291	1.20	76.75	22.05	17.70	1.71	14.16	39.17
PC 292	0.99	78.29	20.72	18.10	1.71	15.01	39.30
PC 293	0.67	77.99	21.34	17.35	1.67	14.30	37.91
PC 294	0.47	77.90	21.63	17.03	1.66	13.95	37.40
PC 295	0.93	76.68	22.40	17.14	1.69	13.65	38.07
PC 296	1.28	77.38	21.33	17.83	1.69	14.33	39.21
PC 297	1.22	77.30	21.48	17.65	1.71	14.09	38.97
PC 298	0.89	77.47	21.63	17.12	1.72	13.64	37.89
PC 299	0.79	76.86	22.35	16.59	1.67	13.02	36.94
PC 300	12.07	69.95	17.98	33.79	2.06	19.15	74.07
PC 301	9.60	70.52	19.87	32.25	1.83	17.32	61.69
PC 302	2.97	74.57	22.46	19.28	1.64	14.58	43.75

Appendix B Continued. Textural data used in this study.

Sample	Percent Sand (2000-62.5μm)	Percent Silt (62.5-3.9μm)	Percent Clay (<3.9μm)	Mean (μm)	d_{10} (μm)	d_{50} (μm)	d_{90} (μm)
PC 303	0.94	75.87	23.18	16.88	1.61	13.28	37.78
PC 304	0.91	77.27	21.82	17.42	1.70	14.12	38.40
PC 305	0.74	76.77	22.49	16.84	1.66	13.46	37.40
PC 306	0.58	76.43	22.99	16.52	1.62	13.02	36.97
PC 307	3.83	75.63	20.54	19.48	1.81	13.75	39.54
PC 308	2.68	75.87	21.45	17.88	1.73	13.22	37.54
PC 309	2.08	76.22	21.70	16.97	1.71	12.93	35.81
PC 310	1.29	74.61	24.10	15.13	1.57	11.25	33.24
PC 311	0.16	74.82	25.03	13.78	1.56	10.35	31.24
PC 312	0.02	74.93	25.05	13.52	1.55	10.29	30.73
PC 313	2.16	76.75	21.10	18.30	1.73	14.23	40.80
PC 314	0.56	78.57	20.87	17.40	1.73	14.37	38.04
PC 315	0.43	77.06	22.51	16.52	1.64	13.26	36.64
PC 316	1.07	79.34	19.58	18.76	1.82	15.98	39.98
PC 317	1.32	79.19	19.48	19.06	1.83	16.23	40.62
PC 318	2.89	77.95	19.16	21.24	1.86	16.62	42.61
PC 319	3.62	76.97	19.41	21.25	1.84	16.36	43.25
PC 320	3.68	76.16	20.16	21.04	1.79	15.80	43.12
PC 321	3.99	74.42	21.59	20.93	1.67	15.11	43.47
PC 322	3.80	73.97	22.23	19.88	1.63	14.63	42.95
PC 323	4.05	74.61	21.34	20.20	1.71	14.90	43.44
PC 324	4.11	75.25	20.63	20.36	1.77	15.17	43.67
PC 325	20.66	61.11	18.22	75.23	2.04	21.01	246.41
PC 326	23.21	62.76	14.04	45.39	2.66	29.73	103.21
PC 327	27.58	58.15	14.28	90.95	2.60	27.83	262.68
PC 328	11.92	69.45	18.63	41.29	1.97	18.66	72.21
PC 329	9.83	72.40	17.77	28.91	2.06	21.59	63.04
PC 330	16.54	66.50	16.96	37.00	2.16	23.76	84.29
PC 331	3.38	75.57	21.05	20.31	1.76	15.90	44.99
PC 332	2.27	76.30	21.43	17.99	1.72	13.72	39.77
PC 333	1.83	74.75	23.42	17.25	1.60	12.80	39.25
PC 334	2.74	73.53	23.74	18.01	1.55	12.95	41.27
PC 335	2.59	76.07	21.34	18.72	1.70	14.41	41.56
PC 336	2.27	75.56	22.16	17.72	1.65	13.38	39.20
PC 337	1.29	76.86	21.85	17.20	1.69	13.49	38.13
PC 338	1.50	76.56	21.94	17.23	1.69	13.27	38.36
PC 339	1.74	75.83	22.42	17.34	1.65	13.15	38.83
PC 340	1.95	75.16	22.89	17.43	1.62	12.98	39.45

Appendix B Continued. Textural data used in this study.

Sample	Percent Sand (2000-62.5µm)	Percent Silt (62.5-3.9µm)	Percent Clay (<3.9µm)	Mean (µm)	d_{10} (µm)	d_{50} (µm)	d_{90} (µm)
PC 341	4.75	73.15	22.10	20.89	1.67	13.29	42.43
PC 342	3.53	76.39	20.08	20.43	1.79	15.43	41.83
PC 343	3.93	75.89	20.18	20.81	1.78	15.78	42.96
PC 344	3.95	72.67	23.39	19.12	1.58	12.96	40.68
PC 345	5.26	73.94	20.80	22.74	1.75	14.49	44.36
PC 346	3.81	76.48	19.71	21.14	1.83	16.06	43.25
PC 347	4.06	77.78	18.16	22.22	1.96	17.78	45.46
PC 348	4.37	77.29	18.34	22.54	1.96	17.73	45.90
PC 349	0.99	79.37	19.64	17.70	1.84	14.64	37.96
PC 350	3.03	78.68	18.30	20.62	1.96	16.83	43.49
PC 351	2.92	79.93	17.15	21.62	2.07	18.62	44.56
PC 352	1.74	78.02	20.24	18.47	1.79	14.88	40.13
PC 353	3.90	76.79	19.31	21.26	1.87	16.83	46.30
PC 354	1.76	77.14	21.10	17.92	1.73	14.09	39.09
PC 355	1.54	77.07	21.38	17.58	1.70	13.86	38.46
PC 356	0.57	75.09	24.33	16.01	1.55	12.10	36.56
PC 357	1.34	76.93	21.73	17.76	1.68	14.32	38.92
PC 358	1.66	76.41	21.93	17.94	1.66	14.27	39.30
PC 359	2.13	77.42	20.45	19.00	1.77	15.38	40.98
PC 360	2.29	79.16	18.54	20.58	1.94	17.54	43.13
PC 361	1.96	78.71	19.33	19.65	1.87	16.45	41.84
PC 362	2.34	78.47	19.19	20.00	1.88	16.68	42.46
PC 363	3.29	78.10	18.61	21.23	1.92	17.64	44.64
PC 364	3.77	78.32	17.90	22.04	1.99	18.41	46.01
PC 365	6.43	75.97	17.60	27.10	2.05	18.73	50.99
PC 366	9.21	70.94	19.85	28.97	1.85	17.17	60.18
PC 367	3.51	76.50	19.99	20.19	1.82	15.77	44.16
PC 368	3.17	75.42	21.41	19.44	1.72	14.81	43.21
PC 369	4.39	76.53	19.08	21.66	1.91	16.96	47.91
PC 370	3.77	77.67	18.56	21.12	1.94	16.80	46.43
PC 371	6.92	75.03	18.05	24.34	2.01	18.73	55.40
PC 372	5.08	75.41	19.51	22.07	1.88	16.82	49.92
PC 373	3.60	75.77	20.62	20.9	1.8	15.1	42.7
PC 374	5.09	74.99	19.92	22.69	1.81	16.20	46.12
PC 375	4.22	75.96	19.82	21.68	1.82	16.20	44.62
PC 376	3.64	76.35	20.01	20.74	1.81	15.55	42.90
PC 377	3.07	76.35	20.58	19.82	1.77	14.95	41.35
PC 378	2.77	76.19	21.04	19.06	1.72	14.33	39.99

Appendix B Continued. Textural data used in this study.

Sample	Percent Sand (2000-62.5μm)	Percent Silt (62.5-3.9μm)	Percent Clay (<3.9μm)	Mean (μm)	d_{10} (μm)	d_{50} (μm)	d_{90} (μm)
PC 379	2.49	75.72	21.79	18.12	1.67	13.44	38.25
PC 380	2.25	75.76	21.99	17.64	1.65	13.05	36.95
PC 381	2.43	76.12	21.45	18.06	1.67	13.63	37.76
PC 382	2.35	76.03	21.62	17.72	1.67	13.41	37.24
PC 383	3.12	77.33	19.56	19.43	1.87	14.77	40.20
PC 384	3.47	77.59	18.95	20.21	1.93	15.44	41.90
PC 385	5.42	74.72	19.87	22.81	1.84	15.88	46.92
PC 386	4.33	76.39	19.29	21.50	1.89	15.66	44.00
PC 387	3.33	76.02	20.65	19.90	1.80	15.28	42.60
PC 388	4.36	76.57	19.07	21.68	1.92	16.82	46.28
PC 389	2.96	74.77	22.27	18.63	1.69	13.92	40.38
PC 390	0.00	78.79	21.21	13.47	1.78	11.99	27.63
PC 391	3.14	73.67	23.19	17.84	1.62	12.58	38.84
PC 392	4.69	73.91	21.40	20.16	1.73	13.86	42.62
PC 393	81.26	13.77	4.97	587.16	13.12	572.87	1170.89
PC 394	43.97	42.53	13.50	226.16	2.80	39.49	703.49
PC 395	74.61	18.57	6.82	659.28	7.11	603.07	1454.39
PC 396	16.51	65.27	18.21	54.92	2.03	19.75	126.79
PC 397	16.57	62.57	20.86	75.04	1.79	16.71	300.44
PC 398	15.44	62.13	22.43	69.29	1.66	15.47	218.70

Appendix C. Geochemical Data

Appendix C-1. Pb, Zn, Fe, Mn, and Ca geochemical data used in this study.

Sample	Pb ppm	Zn ppm	Fe ppm	Mn ppm	Ca ppm
PC 1	159	1,097	20,313	1,209	46,961
PC 2*	96	427	18,617	1,232	16,050
PC 3*	254	1,538	18,892	1,235	19,024
PC 4*	572	2,019	19,208	1,241	43,412
PC 5*	408	1,964	18,111	1,255	27,502
PC 6*	1,702	4,517	21,440	1,204	85,626
PC 7*	366	2,714	20,960	1,464	38,427
PC 8*	119	957	16,758	1,218	13,861
PC 9	1,263	1,793	24,392	1,143	134,569
PC 10	722	3,624	20,559	1,250	135,587
PC 11	890	3,120	19,200	1,435	123,281
PC 12	4,768	4,608	21,442	927	181,893
PC 13	1,594	7,596	20,996	915	178,657
PC 14	51	195	17,348	1,173	11,007
PC 15	61	170	18,171	1,262	4,874
PC 16	61	267	17,426	1,291	3,399
PC 17	73	440	17,716	1,370	4,468
PC 18	142	675	16,914	1,379	5,699
PC 19	285	829	17,245	1,305	9,761
PC 20	192	829	19,240	1,424	7,230
PC 21	32	145	17,996	1,189	3,229
PC 22	35	127	18,724	1,123	4,397
PC 23	29	95	19,559	1,236	3,590
PC 24	30	90	19,982	971	2,995
PC 25	22	69	19,305	279	2,619
PC 26	25	99	21,568	537	3,758
PC 27	129	697	19,887	1,403	17,035
PC 28	131	818	19,830	1,409	14,604
PC 29	127	912	20,185	1,545	16,712
PC 30	220	1,639	19,650	1,601	13,449
PC 31	533	3,999	20,216	1,481	30,174
PC 32	1,142	6,386	19,779	1,252	57,868
PC 33	553	2,254	17,750	1,380	41,914
PC 34	279	1,714	14,782	1,110	14,306
PC 35	398	2,247	17,844	1,365	24,541
PC 36	30	216	19,466	1,256	9,410

ND Below detection
* Not used in study

Appendix C-1 Continued. Pb, Zn, Fe, Mn, and Ca geochemical data used in this study.

Sample	Pb ppm	Zn ppm	Fe ppm	Mn ppm	Ca ppm
PC 37	51	343	22,911	2,475	8,724
PC 38	39	241	19,466	465	5,659
PC 39	37	148	14,327	1,104	6,181
PC 40	33	133	13,991	1,286	2,739
PC 41	22	61	14,454	1,217	2,178
PC 42	18	44	15,155	1,011	1,413
PC 43	ND	61	16,330	642	2,049
PC 44	25	55	19,647	597	1,773
PC 45	25	52	20,004	411	1,604
PC 46	81	341	17,432	1,061	24,932
PC 47	97	324	18,747	1,187	13,901
PC 48	115	535	16,348	1,302	9,503
PC 49	233	1,180	16,753	1,225	16,810
PC 50	148	668	16,647	1,133	33,148
PC 51	1,015	2,606	18,835	1,195	56,875
PC 52	576	2,919	19,227	1,353	61,404
PC 53	437	1,878	17,690	1,208	34,620
PC 54	337	1,620	15,978	1,328	20,132
PC 55	888	2,001	19,792	1,391	47,669
PC 56	451	1,524	20,345	2,584	46,997
PC 57	138	473	19,734	1,926	18,913
PC 58	72	274	18,812	874	29,551
PC 59	57	182	22,102	770	33,385
PC 60	24	47	13,424	862	1,661
PC 61	ND	49	12,683	970	1,319
PC 62	23	25	15,532	532	1,722
PC 63	ND	28	15,181	343	1,206
PC 64	ND	19	14,936	222	1,496
PC 65	21	25	14,786	232	1,359
PC 66	ND	18	15,737	506	1,107
PC 67	19	18	15,089	520	1,231
PC 68	64	233	17,853	1,198	11,776
PC 69	63	227	15,832	1,064	6,119
PC 70	90	485	16,228	1,108	6,666
PC 71	97	536	15,416	993	7,775
PC 72	109	525	17,586	1,189	7,647
PC 73	161	772	16,803	1,094	11,585
PC 74	204	719	18,065	1,204	15,445

ND Below detection

Appendix C-1 Continued. Pb, Zn, Fe, Mn, and Ca geochemical data used in this study.

Sample	Pb ppm	Zn ppm	Fe ppm	Mn ppm	Ca ppm
PC 75	137	379	16,365	1,172	12,791
PC 76	32	86	17,570	1,266	11,666
PC 77	29	68	17,181	1,066	9,051
PC 78	26	50	16,639	1,041	26,120
PC 79	ND	83	18,399	1,080	13,234
PC 80	ND	79	19,269	1,320	13,867
PC 81	25	68	20,090	705	4,646
PC 82	25	66	20,463	277	3,671
PC 83	29	84	20,660	249	3,982
PC 84	72	352	17,570	1,132	19,128
PC 85	74	290	17,877	1,138	12,129
PC 86	103	497	17,553	1,173	7,017
PC 87	606	1,830	18,273	1,127	39,879
PC 88	734	2,328	20,197	1,302	61,779
PC 89	1,185	1,584	20,089	1,232	83,805
PC 90	596	1,989	20,041	1,370	53,244
PC 91	220	1,639	19,391	1,411	43,918
PC 92	292	880	18,150	1,291	34,999
PC 93	31	99	16,548	1,378	10,190
PC 94	38	71	18,419	1,382	11,295
PC 95	23	47	18,607	1,184	9,243
PC 96	29	67	18,520	673	6,990
PC 97	30	88	16,786	455	11,728
PC 98	106	545	18,580	1,320	8,299
PC 99	95	535	18,778	1,519	9,986
PC 100	246	2,298	20,326	1,312	45,350
PC 101	69	295	15,623	1,079	3,940
PC 102	154	574	17,177	1,411	3,406
PC 103	81	350	14,640	1,190	3,705
PC 104	27	74	15,240	1,181	1,704
PC 105	38	91	17,390	1,091	2,495
PC 106	41	126	17,898	908	2,585
PC 107	26	58	18,284	791	1,942
PC 108	26	61	19,133	858	2,035
PC 109	ND	59	19,389	819	1,809
PC 110	23	48	19,756	757	1,517
PC 111	23	55	20,062	929	1,642
PC 112	ND	50	20,761	911	1,879

ND Below detection

Appendix C-1 Continued. Pb, Zn, Fe, Mn, and Ca geochemical data used in this study.

Sample	Pb ppm	Zn ppm	Fe ppm	Mn ppm	Ca ppm
PC 113	ND	57	20,783	1,275	2,112
PC 114	34	112	14,264	1,055	4,653
PC 115	36	111	15,089	1,125	2,225
PC 116	29	113	13,636	1,030	2,268
PC 117	28	84	14,660	990	2,568
PC 118	23	41	17,453	816	2,025
PC 119	23	47	19,376	643	2,243
PC 120	59	169	16,821	1,114	9,398
PC 121	60	240	17,797	1,310	4,954
PC 122	105	367	15,135	1,105	6,187
PC 123	335	1,106	17,012	1,238	21,322
PC 124	252	1,049	17,160	1,257	20,199
PC 125	151	476	16,016	1,303	9,683
PC 126	108	241	16,245	1,488	13,870
PC 127	ND	58	16,082	1,558	8,317
PC 128	32	70	19,764	5,870	10,823
PC 129	28	67	24,455	3,731	17,028
PC 130	23	68	18,298	204	10,015
PC 131	22	73	19,706	314	14,453
PC 132	ND	73	17,919	250	11,236
PC 133	22	69	17,817	194	13,543
PC 134	70	345	17,666	1,240	14,963
PC 135	51	179	17,643	1,239	5,607
PC 136	61	204	16,048	1,255	6,361
PC 137	130	401	16,865	1,342	12,030
PC 138	289	934	17,161	1,187	19,937
PC 139	276	733	16,844	1,116	28,482
PC 140	240	743	15,802	1,118	18,394
PC 141	350	1,642	17,429	1,443	28,915
PC 142	1,085	1,518	25,560	1,620	137,172
PC 143	1,496	2,573	19,226	1,085	105,030
PC 144	2,270	3,151	19,628	1,168	117,698
PC 145	489	1,237	18,503	1,121	71,355
PC 146	632	1,083	18,924	912	67,354
PC 147	266	334	17,075	843	28,721
PC 148	157	387	16,768	808	18,435
PC 149	125	320	18,421	600	20,907
PC 150	71	270	18,763	1,228	31,139

ND Below detection

Appendix C-1 Continued. Pb, Zn, Fe, Mn, and Ca geochemical data used in this study.

Sample	Pb ppm	Zn ppm	Fe ppm	Mn ppm	Ca ppm
PC 151	80	227	18,229	1,260	19,301
PC 152	53	164	17,360	1,182	15,038
PC 153	ND	59	18,420	993	4,862
PC 154	30	65	19,305	989	4,828
PC 155	21	70	20,151	937	3,773
PC 156	36	78	20,319	3,863	4,095
PC 157	25	58	22,074	1,017	3,562
PC 158	ND	79	23,037	3,426	4,648
PC 159	25	83	18,607	681	3,338
PC 160	27	81	18,495	564	2,813
PC 161	64	205	15,169	1,011	4,542
PC 162	86	246	14,655	1,000	3,682
PC 163	ND	131	13,933	917	2,742
PC 164	26	57	13,853	843	2,493
PC 165	ND	51	14,640	829	1,549
PC 166	16	55	15,478	797	1,739
PC 167	ND	47	16,219	778	1,705
PC 168	ND	61	17,452	942	1,880
PC 169	19	65	18,236	996	1,527
PC 170	19	69	19,240	836	2,408
PC 171	19	49	16,844	763	2,303
PC 172	11	30	13,615	443	1,431
PC 173	61	189	17,788	1,141	13,374
PC 174	55	139	16,953	1,106	3,871
PC 175	43	115	15,086	1,110	3,169
PC 176	81	218	16,465	1,266	5,990
PC 177	156	397	15,470	1,207	11,752
PC 178	524	1,256	17,641	1,100	45,576
PC 179	396	1,230	17,416	1,134	32,864
PC 180	157	392	15,774	1,133	12,462
PC 181	158	213	16,214	1,104	10,954
PC 182	114	233	17,968	1,174	21,363
PC 183	27	70	15,381	1,347	9,006
PC 184	ND	43	16,363	1,571	9,714
PC 185	ND	40	20,815	3,554	8,062
PC 186	24	54	15,797	256	12,555
PC 187	21	70	16,821	223	25,297
PC 188	23	71	16,242	231	19,832

ND Below detection

Appendix C-1 Continued. Pb, Zn, Fe, Mn, and Ca geochemical data used in this study.

Sample	Pb ppm	Zn ppm	Fe ppm	Mn ppm	Ca ppm
PC 189	19	75	16,139	277	38,750
PC 190	57	224	17,263	1,221	13,045
PC 191	76	303	18,403	1,314	4,849
PC 192	110	697	18,028	1,351	7,236
PC 193	231	992	16,475	1,293	14,528
PC 194	355	830	15,915	1,013	23,563
PC 195	228	555	16,756	1,157	23,332
PC 196	219	1,101	15,670	1,212	11,379
PC 197	1,097	1,274	19,081	1,272	52,161
PC 198	64	800	16,303	1,321	7,279
PC 199	52	141	16,914	1,371	11,789
PC 200	47	123	17,526	1,381	13,831
PC 201	23	48	18,551	867	17,018
PC 202	23	54	17,201	442	19,107
PC 203	26	72	18,451	219	28,344
PC 204	18	63	18,435	220	27,104
PC 205	89	848	17,813	1,160	16,782
PC 206	272	1,360	18,962	1,312	20,576
PC 207	520	1,547	19,564	1,235	33,162
PC 208	737	1,793	18,237	1,003	54,704
PC 209	474	1,864	17,687	1,218	31,566
PC 210	511	2,051	17,344	1,136	30,144
PC 211	1,015	3,539	19,903	1,325	52,738
PC 212	171	2,105	17,419	1,145	22,975
PC 213	75	481	15,578	1,070	9,336
PC 214	22	61	16,429	717	16,681
PC 215	46	123	17,722	300	11,686
PC 216	ND	58	17,799	261	2,643
PC 217	22	69	16,872	975	2,453
PC 218	34	127	19,270	411	3,247
PC 219	20	81	20,785	ND	3,881
PC 220	26	80	15,907	34	3,732
PC 221	44	142	15,310	948	4,098
PC 222	49	189	14,749	946	2,655
PC 223	55	200	14,847	910	2,816
PC 224	39	113	15,388	860	2,304
PC 225	31	75	16,581	921	1,883
PC 226	28	58	17,141	875	2,071

ND Below detection

Appendix C-1 Continued. Pb, Zn, Fe, Mn, and Ca geochemical data used in this study.

Sample	Pb ppm	Zn ppm	Fe ppm	Mn ppm	Ca ppm
PC 227	ND	59	17,723	933	1,858
PC 228	30	66	18,064	941	2,213
PC 229	24	64	19,157	1,004	2,239
PC 230	52	137	19,388	1,108	5,092
PC 231	49	143	16,466	1,079	2,736
PC 232	69	228	15,998	1,055	4,792
PC 233	144	431	16,326	1,170	8,323
PC 234	190	440	16,415	1,051	11,641
PC 235	272	749	17,190	1,206	14,036
PC 236	254	863	16,639	1,152	23,396
PC 237	765	755	18,526	1,180	51,630
PC 238	550	877	18,823	1,292	65,689
PC 239	238	677	19,717	1,383	46,128
PC 240	88	268	18,946	1,600	22,716
PC 241	69	116	16,361	1,434	9,939
PC 242	ND	77	21,024	1,374	9,633
PC 243	39	71	22,130	1,171	9,039
PC 244	30	42	18,966	693	7,840
PC 245	30	68	23,665	928	11,133
PC 246	23	53	16,596	627	13,570
PC 247	24	50	18,868	813	15,236
PC 248	22	55	16,796	511	17,956
PC 249	ND	53	14,555	347	13,096
PC 250	69	270	18,197	1,065	22,028
PC 251	65	298	18,206	1,166	16,716
PC 252	82	298	19,542	1,222	13,258
PC 253	78	259	18,118	1,192	12,076
PC 254	100	535	18,680	1,189	13,447
PC 255	99	434	18,438	1,217	14,725
PC 256	88	467	18,977	1,149	10,920
PC 257	92	628	19,145	1,215	13,064
PC 258	105	732	19,100	1,170	18,306
PC 259	76	365	19,356	383	31,485
PC 260	101	563	18,336	1,435	15,148
PC 261	759	2,894	18,607	1,226	47,435
PC 262	176	466	19,516	1,185	19,367
PC 263	222	2,067	19,772	1,329	23,606
PC 264	115	440	18,666	1,224	22,392

ND Below detection

Appendix C-1 Continued. Pb, Zn, Fe, Mn, and Ca geochemical data used in this study.

Sample	Pb ppm	Zn ppm	Fe ppm	Mn ppm	Ca ppm
PC 265	325	1,053	19,183	1,189	29,297
PC 266	109	695	17,910	1,274	14,661
PC 267	110	614	18,713	1,580	11,496
PC 268	126	836	19,269	1,577	15,239
PC 269	98	396	16,824	1,324	12,090
PC 270	127	569	19,060	1,956	9,309
PC 271	86	350	18,057	1,294	33,335
PC 272	130	475	18,419	1,157	24,747
PC 273	84	708	19,285	1,283	9,901
PC 274	99	808	19,264	1,582	8,916
PC 275	204	855	16,674	1,146	24,306
PC 276	301	1,232	17,927	1,303	24,842
PC 277	62	266	18,046	1,240	9,433
PC 278	80	291	18,349	1,194	6,934
PC 279	159	550	17,501	1,221	9,355
PC 280	598	988	17,656	1,358	26,965
PC 281	315	865	17,126	1,347	21,514
PC 282	272	501	20,194	1,105	25,163
PC 283	101	249	20,631	1,015	12,613
PC 284	33	76	16,918	529	10,395
PC 285	26	78	17,667	379	15,470
PC 286	91	460	17,186	1,150	15,336
PC 287	118	564	17,883	1,305	10,338
PC 288	159	800	17,407	1,293	10,122
PC 289	335	790	17,516	1,222	19,064
PC 290	66	196	17,001	1,131	9,125
PC 291	24	91	19,286	1,024	4,699
PC 292	ND	71	19,812	883	3,123
PC 293	20	67	20,052	962	3,091
PC 294	30	74	20,218	1,154	4,185
PC 295	30	83	23,161	1,549	3,673
PC 296	23	87	20,888	197	2,806
PC 297	28	77	20,213	158	2,467
PC 298	24	80	19,347	448	2,647
PC 299	19	83	20,520	117	2,836
PC 300	88	677	19,156	1,189	38,953
PC 301	86	875	19,138	1,142	21,625
PC 302	82	366	18,378	1,235	13,435

ND Below detection

Appendix C-1 Continued. Pb, Zn, Fe, Mn, and Ca geochemical data used in this study.

Sample	Pb ppm	Zn ppm	Fe ppm	Mn ppm	Ca ppm
PC 303	ND	85	19,451	1,228	7,081
PC 304	23	139	19,391	1,244	4,064
PC 305	ND	68	21,444	1,445	4,074
PC 306	ND	71	21,105	1,972	2,843
PC 307	47	121	14,735	1,359	3,735
PC 308	41	106	15,794	1,404	1,724
PC 309	28	60	15,303	1,310	1,715
PC 310	27	55	18,949	824	2,064
PC 311	35	60	23,992	393	1,636
PC 312	31	60	23,814	546	1,676
PC 313	58	202	18,371	1,166	15,517
PC 314	45	113	17,892	1,219	5,463
PC 315	29	64	19,340	1,076	6,719
PC 316	28	71	19,896	1,094	3,924
PC 317	23	67	19,457	1,012	3,373
PC 318	ND	75	19,860	1,089	3,003
PC 319	ND	73	20,080	1,069	3,258
PC 320	26	66	19,722	1,186	2,577
PC 321	28	68	21,312	4,172	3,080
PC 322	25	74	21,288	4,958	3,281
PC 323	28	79	21,607	2,007	3,725
PC 324	26	85	19,226	462	2,889
PC 325	188	1,485	20,526	1,433	24,857
PC 326	3,236	12,395	23,918	1,219	106,690
PC 327	824	5,822	20,555	1,280	54,481
PC 328	716	5,803	18,476	1,271	34,746
PC 329	1,071	5,010	22,170	1,489	65,412
PC 330	1,004	5,487	21,662	1,351	57,465
PC 331	33	322	17,117	1,174	15,210
PC 332	50	207	16,130	1,124	6,954
PC 333	94	517	19,285	1,505	4,737
PC 334	137	1,027	23,655	1,670	9,929
PC 335	219	609	16,316	1,214	8,971
PC 336	64	190	18,481	1,221	5,245
PC 337	26	77	18,756	1,150	3,099
PC 338	28	75	19,448	1,017	2,113
PC 339	21	84	20,281	826	2,774
PC 340	28	80	21,137	724	2,400

ND Below detection

Appendix C-1 Continued. Pb, Zn, Fe, Mn, and Ca geochemical data used in this study.

Sample	Pb ppm	Zn ppm	Fe ppm	Mn ppm	Ca ppm
PC 341	76	203	18,702	1,298	13,784
PC 342	56	120	16,714	1,225	5,162
PC 343	24	40	16,855	1,364	7,141
PC 344	31	64	20,655	1,081	9,905
PC 345	78	235	18,115	1,244	11,516
PC 346	36	105	17,781	1,075	3,983
PC 347	22	72	18,977	892	2,853
PC 348	23	67	19,028	1,141	2,799
PC 349	46	119	16,803	1,023	6,552
PC 350	47	173	14,883	937	1,506
PC 351	71	230	14,424	967	2,666
PC 352	157	410	16,361	1,105	9,262
PC 353	184	542	16,985	1,206	12,678
PC 354	88	241	16,147	1,097	4,576
PC 355	88	138	15,207	1,189	4,406
PC 356	73	136	17,144	1,262	6,488
PC 357	39	81	16,347	1,288	5,518
PC 358	ND	53	17,151	1,355	6,430
PC 359	25	56	16,893	1,195	7,715
PC 360	21	52	16,049	1,129	4,558
PC 361	21	62	18,075	906	3,992
PC 362	28	72	20,736	1,328	3,560
PC 363	24	68	20,702	813	3,100
PC 364	31	70	19,816	344	3,567
PC 365	21	75	14,957	ND	4,572
PC 366	106	661	19,205	1,346	36,861
PC 367	74	323	18,484	1,274	17,365
PC 368	115	737	19,447	1,543	11,724
PC 369	358	1,522	18,110	1,355	29,874
PC 370	379	1,567	17,329	1,265	26,887
PC 371	627	1,905	18,679	1,288	45,826
PC 372	239	1,439	18,126	1,231	30,960
PC 373	ND	134	18,070	1,124	7,227
PC 374	ND	193	19,125	944	4,528
PC 375	23	89	19,560	973	3,692
PC 376	33	112	19,474	997	3,499
PC 377	30	78	20,070	975	4,292
PC 378	ND	80	20,494	1,027	3,541

ND Below detection

Appendix C-1 Continued. Pb, Zn, Fe, Mn, and Ca geochemical data used in this study.

Sample	Pb ppm	Zn ppm	Fe ppm	Mn ppm	Ca ppm
PC 379	25	84	21,099	922	3,493
PC 380	25	111	20,973	1,081	2,913
PC 381	28	73	22,849	487	2,717
PC 382	23	78	24,092	268	3,574
PC 383	18	69	13,778	ND	3,273
PC 384	22	78	13,975	ND	3,427
PC 385	128	481	17,186	1,316	8,563
PC 386	217	1,003	16,306	1,283	12,741
PC 387	143	301	16,831	1,203	10,533
PC 388	192	488	17,296	1,296	14,949
PC 389	ND	64	17,449	1,368	4,242
PC 390	23	43	15,250	1,276	1,885
PC 391	ND	36	15,342	1,493	1,907
PC 392	18	32	14,312	1,365	1,202
PC 393	ND	62	17,716	977	12,806
PC 394	ND	78	19,783	1,669	19,624
PC 395	19	60	17,590	702	11,054
PC 396	31	64	19,360	1,235	12,888
PC 397	28	54	22,201	1,284	3,809
PC 398	21	54	20,828	956	3,748

ND Below detection

Appendix C-2. Ti, Cr, Sr, Zr, and Mo geochemical data not used in this study.

Sample	Ti ppm	Cr ppm	Sr ppm	Zr ppm	Mo ppm
PC 1	4,962	ND	58	514	23
PC 2*	4,541	24	65	609	29
PC 3*	5,029	65	66	616	34
PC 4*	4,221	24	63	509	29
PC 5*	4,123	ND	61	603	34
PC 6*	3,367	11	62	327	33
PC 7*	4,667	ND	73	545	30
PC 8*	5,150	ND	65	687	33
PC 9	1,567	8	60	191	28
PC 10	2,851	139	85	217	30
PC 11	3,022	33	123	227	23
PC 12	536	161	90	116	23
PC 13	490	81	94	122	21
PC 14	4,330	43	64	537	28
PC 15	5,151	37	67	587	33
PC 16	5,379	13	59	620	29
PC 17	5,314	66	63	667	25
PC 18	5,266	0	59	607	33
PC 19	4,632	62	62	594	24
PC 20	5,563	ND	66	597	25
PC 21	5,144	27	61	583	31
PC 22	5,423	24	66	612	33
PC 23	5,891	104	66	593	28
PC 24	5,497	30	58	596	24
PC 25	5,162	16	64	612	28
PC 26	5,749	71	64	597	30
PC 27	4,501	30	60	564	34
PC 28	4,172	ND	55	588	31
PC 29	4,762	ND	63	545	32
PC 30	4,643	11	62	607	28
PC 31	4,230	40	72	562	28
PC 32	3,547	17	72	486	28
PC 33	3,463	11	65	520	32
PC 34	4,387	26	63	548	37
PC 35	4,213	ND	59	537	27
PC 36	5,636	48	70	665	28
PC 37	4,744	32	63	590	28
PC 38	4,676	1	58	608	35

ND Below detection
* Not used in study

Appendix C-2 Continued. Ti, Cr, Sr, Zr, and Mo geochemical data not used in this study.

Sample	Ti ppm	Cr ppm	Sr ppm	Zr ppm	Mo ppm
PC 39	4,989	11	61	639	28
PC 40	5,234	46	68	664	34
PC 41	5,326	20	67	624	26
PC 42	5,718	ND	73	640	26
PC 43	5,303	8	72	607	26
PC 44	5,954	7	70	613	25
PC 45	5,813	91	71	562	26
PC 46	3,779	17	62	577	30
PC 47	4,645	7	58	612	27
PC 48	4,694	69	66	687	29
PC 49	4,312	ND	59	581	29
PC 50	3,441	14	66	617	24
PC 51	3,258	24	67	455	26
PC 52	3,489	18	68	531	29
PC 53	3,982	35	65	494	33
PC 54	4,119	11	65	561	28
PC 55	3,140	ND	62	424	28
PC 56	3,618	2	62	470	28
PC 57	4,446	ND	55	573	23
PC 58	4,475	ND	57	539	23
PC 59	4,378	44	54	570	26
PC 60	4,847	14	54	692	29
PC 61	4,844	36	56	684	33
PC 62	4,801	88	53	723	29
PC 63	4,365	43	51	695	30
PC 64	4,892	ND	50	709	31
PC 65	4,404	68	47	604	36
PC 66	4,049	37	42	514	30
PC 67	3,807	7	44	457	21
PC 68	4,465	ND	62	552	34
PC 69	4,324	1	52	567	31
PC 70	4,762	39	55	662	31
PC 71	3,928	67	58	621	28
PC 72	5,302	50	65	681	26
PC 73	4,446	25	57	614	36
PC 74	4,661	ND	55	607	28
PC 75	4,729	48	60	620	38
PC 76	4,820	ND	63	658	32
PC 77	4,614	10	60	593	32

ND Below detection

Appendix C-2 Continued. Ti, Cr, Sr, Zr, and Mo geochemical data not used in this study.

Sample	Ti ppm	Cr ppm	Sr ppm	Zr ppm	Mo ppm
PC 78	3,999	31	53	558	27
PC 79	4,529	12	58	576	34
PC 80	4,488	7	55	592	30
PC 81	5,196	38	52	625	34
PC 82	5,177	53	61	664	30
PC 83	5,018	ND	58	649	27
PC 84	4,089	ND	61	552	34
PC 85	4,679	ND	55	586	26
PC 86	4,650	ND	59	635	37
PC 87	3,582	ND	60	505	34
PC 88	3,309	2	54	443	32
PC 89	2,381	8	65	339	29
PC 90	3,576	60	61	450	34
PC 91	3,944	ND	67	491	29
PC 92	4,276	ND	57	555	32
PC 93	4,524	ND	61	692	33
PC 94	5,198	41	73	635	33
PC 95	4,833	ND	62	595	23
PC 96	4,967	16	65	577	32
PC 97	4,525	31	64	595	27
PC 98	4,482	11	58	594	26
PC 99	4,916	7	61	621	28
PC 100	4,568	ND	81	467	24
PC 101	4,798	13	61	641	28
PC 102	5,503	44	61	666	31
PC 103	5,518	70	68	650	25
PC 104	5,898	48	68	674	28
PC 105	5,378	3	67	662	31
PC 106	5,639	17	69	645	25
PC 107	5,639	84	73	651	23
PC 108	5,473	ND	66	623	29
PC 109	5,132	ND	65	582	30
PC 110	5,049	47	72	591	32
PC 111	5,398	48	67	575	32
PC 112	5,229	51	72	572	26
PC 113	4,937	45	79	558	30
PC 114	5,163	15	62	631	33
PC 115	6,216	41	67	702	30
PC 116	5,700	71	69	649	32

ND Below detection

Appendix C-2 Continued. Ti, Cr, Sr, Zr, and Mo geochemical data not used in this study.

Sample	Ti ppm	Cr ppm	Sr ppm	Zr ppm	Mo ppm
PC 117	5,466	ND	71	606	32
PC 118	5,324	49	66	585	31
PC 119	5,480	59	68	574	36
PC 120	4,153	ND	60	553	28
PC 121	5,176	54	60	648	33
PC 122	4,771	79	57	637	31
PC 123	4,532	7	64	525	25
PC 124	4,366	2	60	522	26
PC 125	4,942	30	64	548	40
PC 126	4,466	ND	69	560	35
PC 127	4,681	70	58	628	33
PC 128	5,099	ND	67	615	32
PC 129	4,687	ND	70	575	24
PC 130	4,811	ND	57	589	25
PC 131	4,704	102	65	596	30
PC 132	4,274	ND	60	589	32
PC 133	4,005	25	59	593	26
PC 134	4,370	3	61	601	28
PC 135	4,975	39	66	659	30
PC 136	5,119	ND	63	641	30
PC 137	4,957	24	65	643	36
PC 138	4,212	ND	65	563	26
PC 139	3,940	22	62	489	33
PC 140	4,568	23	67	579	25
PC 141	3,843	12	59	542	24
PC 142	1,744	54	64	198	22
PC 143	2,201	42	62	316	25
PC 144	1,460	43	60	234	23
PC 145	3,089	43	63	406	29
PC 146	3,156	23	61	431	25
PC 147	4,203	ND	63	556	32
PC 148	4,523	52	62	542	29
PC 149	4,752	71	65	523	31
PC 150	4,079	55	65	556	25
PC 151	4,289	11	64	576	34
PC 152	4,430	ND	63	565	27
PC 153	4,939	ND	58	563	27
PC 154	5,077	ND	66	587	25
PC 155	4,941	28	63	603	33

ND Below detection

Appendix C-2 Continued. Ti, Cr, Sr, Zr, and Mo geochemical data not used in this study.

Sample	Ti ppm	Cr ppm	Sr ppm	Zr ppm	Mo ppm
PC 156	5,049	30	64	580	28
PC 157	5,142	24	59	579	31
PC 158	5,183	44	62	611	26
PC 159	4,926	22	60	585	35
PC 160	4,989	4	62	595	32
PC 161	4,840	11	57	651	29
PC 162	4,987	39	51	696	34
PC 163	4,857	32	53	693	34
PC 164	4,730	80	56	683	31
PC 165	5,270	56	53	681	35
PC 166	4,616	65	51	631	30
PC 167	4,948	87	53	605	29
PC 168	5,112	ND	49	550	29
PC 169	5,095	71	58	526	24
PC 170	4,916	52	61	479	23
PC 171	4,647	4	52	394	26
PC 172	3,104	75	31	254	33
PC 173	5,043	ND	62	531	23
PC 174	4,872	64	62	615	29
PC 175	4,915	24	59	635	23
PC 176	4,877	17	58	657	33
PC 177	4,557	35	65	623	35
PC 178	3,568	ND	58	456	30
PC 179	4,134	11	60	529	33
PC 180	4,964	21	61	598	27
PC 181	4,729	29	56	599	36
PC 182	4,640	31	61	590	27
PC 183	4,784	ND	65	680	31
PC 184	4,470	11	56	648	27
PC 185	4,742	59	69	630	29
PC 186	4,629	18	64	607	31
PC 187	4,339	4	65	529	27
PC 188	4,064	6	59	577	29
PC 189	3,798	4	54	504	29
PC 190	4,334	ND	60	574	36
PC 191	5,297	4	62	664	29
PC 192	5,021	35	66	653	29
PC 193	4,502	ND	60	573	26
PC 194	3,907	ND	54	503	34

ND Below detection

Appendix C-2 Continued. Ti, Cr, Sr, Zr, and Mo geochemical data not used in this study.

Sample	Ti ppm	Cr ppm	Sr ppm	Zr ppm	Mo ppm
PC 195	4,310	3	69	537	37
PC 196	4,961	15	59	643	32
PC 197	3,342	6	61	460	34
PC 198	5,272	ND	63	617	32
PC 199	5,200	34	57	617	29
PC 200	4,877	19	66	643	30
PC 201	4,383	ND	67	638	24
PC 202	4,337	9	65	600	30
PC 203	4,413	28	73	505	24
PC 204	4,291	56	60	551	29
PC 205	4,318	30	57	580	29
PC 206	4,267	ND	60	587	36
PC 207	4,215	ND	61	564	21
PC 208	3,129	27	60	434	22
PC 209	3,829	14	59	500	33
PC 210	3,852	25	62	501	26
PC 211	3,686	29	71	460	25
PC 212	4,135	19	62	596	35
PC 213	4,693	46	60	666	35
PC 214	4,228	36	59	609	30
PC 215	5,035	42	55	657	28
PC 216	4,800	94	59	670	30
PC 217	4,914	67	54	661	38
PC 218	4,839	63	59	636	21
PC 219	5,246	64	59	603	29
PC 220	5,467	54	62	575	26
PC 221	4,663	12	55	594	34
PC 222	4,959	7	61	667	34
PC 223	5,229	67	55	701	35
PC 224	5,133	74	52	661	33
PC 225	5,043	103	58	630	25
PC 226	5,489	61	61	640	28
PC 227	5,355	41	59	603	30
PC 228	5,076	30	62	593	26
PC 229	5,524	49	62	554	35
PC 230	5,541	54	64	613	26
PC 231	5,093	82	55	683	29
PC 232	4,992	ND	59	652	26
PC 233	5,259	ND	57	633	32

ND Below detection

Appendix C-2 Continued. Ti, Cr, Sr, Zr, and Mo geochemical data not used in this study.

Sample	Ti ppm	Cr ppm	Sr ppm	Zr ppm	Mo ppm
PC 234	4,908	39	63	547	26
PC 235	4,610	ND	59	534	30
PC 236	3,899	29	55	586	28
PC 237	2,878	31	59	419	30
PC 238	2,917	ND	53	406	27
PC 239	3,812	ND	69	469	28
PC 240	4,171	ND	66	528	27
PC 241	4,803	26	64	571	26
PC 242	5,641	46	69	593	23
PC 243	4,964	34	71	553	30
PC 244	5,361	ND	66	580	34
PC 245	5,565	33	74	555	29
PC 246	4,733	82	67	557	25
PC 247	4,925	59	65	511	34
PC 248	3,977	18	63	576	29
PC 249	4,178	11	60	583	29
PC 250	4,034	55	60	534	32
PC 251	3,677	ND	62	549	27
PC 252	4,686	46	64	548	21
PC 253	4,290	1	60	579	33
PC 254	4,673	60	62	568	29
PC 255	4,574	55	62	573	32
PC 256	4,848	6	70	540	29
PC 257	4,208	36	57	521	28
PC 258	4,514	ND	64	513	28
PC 259	4,118	38	59	354	24
PC 260	4,292	37	63	575	26
PC 261	3,463	50	66	434	20
PC 262	4,242	ND	60	561	27
PC 263	4,844	ND	70	542	29
PC 264	4,110	ND	66	563	22
PC 265	3,655	ND	59	527	23
PC 266	4,290	ND	60	572	29
PC 267	4,376	40	55	573	30
PC 268	4,692	ND	59	565	33
PC 269	4,325	11	61	591	33
PC 270	5,553	ND	74	626	32
PC 271	3,759	16	62	504	28
PC 272	3,942	ND	60	547	32

ND Below detection

Appendix C-2 Continued. Ti, Cr, Sr, Zr, and Mo geochemical data not used in this study.

Sample	Ti ppm	Cr ppm	Sr ppm	Zr ppm	Mo ppm
PC 273	4,572	31	62	576	28
PC 274	4,932	22	61	574	30
PC 275	3,672	ND	60	549	32
PC 276	3,871	6	60	560	26
PC 277	4,590	33	64	569	28
PC 278	5,059	79	68	606	29
PC 279	4,840	8	65	612	31
PC 280	4,070	ND	60	524	32
PC 281	4,199	ND	66	593	33
PC 282	3,655	ND	55	551	33
PC 283	5,179	36	63	640	27
PC 284	4,993	26	63	659	29
PC 285	4,949	ND	74	577	31
PC 286	4,084	0	55	556	29
PC 287	4,376	3	51	590	33
PC 288	4,486	14	60	626	26
PC 289	4,149	41	60	562	33
PC 290	4,770	88	65	620	35
PC 291	4,721	37	61	588	27
PC 292	4,728	92	57	584	28
PC 293	5,091	50	62	582	26
PC 294	4,792	56	67	602	30
PC 295	4,968	71	64	611	24
PC 296	5,340	60	66	619	26
PC 297	5,005	49	59	573	32
PC 298	5,209	40	67	582	33
PC 299	5,249	54	64	557	34
PC 300	3,855	23	66	519	20
PC 301	4,369	21	58	560	28
PC 302	4,361	26	61	598	38
PC 303	4,733	ND	57	567	28
PC 304	4,679	32	61	585	33
PC 305	4,920	32	60	603	33
PC 306	5,136	8	67	577	31
PC 307	5,326	13	68	567	32
PC 308	5,929	77	71	603	26
PC 309	5,447	24	75	585	30
PC 310	5,680	29	72	542	31
PC 311	5,809	23	68	490	28

ND Below detection

Appendix C-2 Continued. Ti, Cr, Sr, Zr, and Mo geochemical data not used in this study.

Sample	Ti ppm	Cr ppm	Sr ppm	Zr ppm	Mo ppm
PC 312	5,812	16	69	475	32
PC 313	4,674	ND	65	523	24
PC 314	5,360	19	63	614	33
PC 315	5,352	30	64	577	27
PC 316	5,146	10	65	618	28
PC 317	5,226	6	62	594	30
PC 318	5,171	48	58	596	27
PC 319	4,962	57	61	579	33
PC 320	5,018	39	66	626	33
PC 321	5,139	35	65	629	34
PC 322	5,028	72	65	600	30
PC 323	5,524	31	60	612	29
PC 324	5,198	50	63	603	28
PC 325	4,604	17	63	543	30
PC 326	2,421	23	81	277	22
PC 327	3,849	ND	69	463	29
PC 328	3,872	ND	64	479	25
PC 329	3,660	ND	66	413	29
PC 330	3,755	ND	64	435	27
PC 331	4,706	ND	61	664	29
PC 332	4,397	ND	60	523	38
PC 333	5,360	43	65	595	30
PC 334	5,419	29	61	562	33
PC 335	4,791	19	55	583	22
PC 336	5,776	83	65	616	31
PC 337	5,233	6	62	595	23
PC 338	5,437	13	66	586	35
PC 339	5,909	19	66	581	28
PC 340	5,425	24	63	573	21
PC 341	4,748	51	62	516	24
PC 342	5,239	16	61	641	29
PC 343	5,175	ND	60	648	41
PC 344	5,127	ND	70	577	23
PC 345	4,856	ND	61	538	25
PC 346	5,127	33	62	617	25
PC 347	5,217	18	61	628	28
PC 348	5,267	15	58	609	29
PC 349	4,826	29	57	560	31
PC 350	4,793	4	52	630	31

ND Below detection

Appendix C-2 Continued. Ti, Cr, Sr, Zr, and Mo geochemical data not used in this study.

Sample	Ti ppm	Cr ppm	Sr ppm	Zr ppm	Mo ppm
PC 351	5,194	2	55	716	33
PC 352	4,957	ND	61	586	27
PC 353	4,510	21	60	637	28
PC 354	5,184	43	61	615	27
PC 355	5,098	20	60	603	27
PC 356	5,211	60	61	569	27
PC 357	5,210	29	64	641	27
PC 358	5,104	3	61	591	25
PC 359	4,635	18	63	593	26
PC 360	5,010	ND	62	650	23
PC 361	5,020	15	58	595	26
PC 362	5,511	12	64	616	32
PC 363	4,689	67	55	606	27
PC 364	4,895	24	57	623	27
PC 365	4,868	16	59	611	27
PC 366	4,016	ND	63	530	35
PC 367	4,059	7	64	568	26
PC 368	5,094	48	64	630	28
PC 369	4,144	11	62	541	32
PC 370	4,154	5	60	517	25
PC 371	3,750	26	65	474	34
PC 372	4,343	ND	57	530	42
PC 373	5,596	52	61	634	26
PC 374	5,196	59	58	574	28
PC 375	5,578	52	61	626	27
PC 376	5,236	7	56	607	37
PC 377	5,209	ND	69	571	23
PC 378	5,257	ND	59	581	24
PC 379	5,835	40	69	538	32
PC 380	5,032	28	70	535	25
PC 381	5,299	50	64	533	31
PC 382	5,784	44	66	558	23
PC 383	4,998	61	62	589	28
PC 384	4,974	49	62	582	27
PC 385	5,057	ND	52	597	38
PC 386	4,968	1	69	592	23
PC 387	5,031	15	58	607	35
PC 388	4,288	ND	62	641	31
PC 389	5,598	17	63	619	28

ND Below detection

Appendix C-2 Continued. Ti, Cr, Sr, Zr, and Mo geochemical data not used in this study.

Sample	Ti ppm	Cr ppm	Sr ppm	Zr ppm	Mo ppm
PC 390	5,713	34	72	621	34
PC 391	5,864	ND	72	647	34
PC 392	5,403	ND	67	629	39
PC 393	2,665	39	28	212	29
PC 394	3,185	ND	49	389	33
PC 395	2,897	35	27	213	30
PC 396	4,584	ND	56	605	30
PC 397	4,989	47	50	471	22
PC 398	4,815	36	55	531	32

ND Below detection

Total Carbon, Nitrogen, and Sulfur Analysis. Carbon, Nitrogen, and Sulfur analysis was done with a Vario EL III CHNOS Elemental Analyzer per instructions from the standard operating procedures on 97 samples (OEWRI, 2007a). After sample preparation, approximately 20 mg of each sample were transferred into separate tin foil "boats," formed into pellets using a hand press, and then loaded into the carousel. Two LDs, two foil blanks, and one natural standard were analyzed with each carousel. The foil-wrapped pellet is then dropped into the instrument where it undergoes catalytic combustion at 1150 C. The C, N, and S gases released are injected into a reduction tube where the vapors are cooled to 850 C and reduced into a detectable form. Water is removed from the gases via drying tubes and then separated into C, N, and S. Helium is used to carry nitrogen and sulfur to separate thermal conductivity detectors where the concentrations of each element are determined.

Appendix C-3. Carbon, nitrogen, and sulfur data

Sample	Nitrogen (%)	Carbon (%)	Sulfur (%)	Nitrogen (mg)	Carbon (mg)	Sulfur (mg)
PC 1	0.20	3.74	0.14	0.04	0.79	0.03
PC 2*	0.26	3.09	(0.09)	0.06	0.65	0.02
PC 3*	0.15	2.41	(0.09)	0.03	0.51	0.02
PC 4*	0.10	3.17	(0.07)	0.02	0.67	0.01
PC 5*	0.11	2.68	(0.04)	0.02	0.56	0.01
PC 6*	0.08	5.31	0.26	0.02	1.12	0.06
PC 7*	0.11	3.02	(0.05)	0.02	0.64	0.01
PC 8*	0.11	1.49	(0.02)	0.02	0.31	0.00
PC 9	0.07	7.65	0.15	0.01	1.61	0.03
PC 10	0.04	6.13	0.12	0.01	1.31	0.03
PC 11	0.06	7.93	0.24	0.01	1.68	0.05
PC 12	0.06	9.33	0.55	0.01	1.97	0.12
PC 13	0.04	8.06	0.40	0.01	1.70	0.08
PC 14	0.36	4.33	(0.04)	0.08	0.91	0.01
PC 15	0.25	2.63	(0.03)	0.05	0.55	0.01
PC 16	0.14	1.35	(0.02)	0.03	0.28	0.00

( ) Values below detection
* Not used in study

Appendix C-3 Continued. Carbon, nitrogen, and sulfur data

Sample	Nitrogen (%)	Carbon (%)	Sulfur (%)	Nitrogen (mg)	Carbon (mg)	Sulfur (mg)
PC 17	0.12	1.41	(0.02)	0.03	0.30	0.01
PC 18	0.11	1.50	(0.02)	0.02	0.32	0.00
PC 19	0.14	2.06	(0.03)	0.03	0.43	0.01
PC 20	0.15	1.93	(0.02)	0.03	0.41	0.00
PC 21	0.16	1.55	(0.02)	0.03	0.33	0.00
PC 22	0.16	1.84	(0.03)	0.03	0.39	0.01
PC 23	0.13	1.24	(0.02)	0.03	0.26	0.00
PC 24	0.10	0.83	(0.02)	0.02	0.18	0.00
PC 25	0.09	0.74	(0.02)	0.02	0.16	0.00
PC 26	0.10	0.86	(0.01)	0.02	0.18	0.00
PC 27	0.24	3.02	(0.03)	0.05	0.64	0.01
PC 28	0.18	2.37	(0.04)	0.04	0.50	0.01
PC 29	0.14	2.11	(0.08)	0.03	0.44	0.02
PC 30	0.12	2.08	(0.03)	0.03	0.44	0.01
PC 31	0.10	3.00	0.26	0.02	0.63	0.05
PC 32	0.10	5.01	0.33	0.02	1.06	0.07
PC 33	0.09	3.32	0.09	0.02	0.70	0.02
PC 34	0.10	2.01	(0.04)	0.02	0.42	0.01
PC 35	0.11	2.86	0.09	0.02	0.60	0.02
PC 36	0.12	1.57	(0.01)	0.03	0.33	0.00
PC 37	0.16	1.76	(0.02)	0.04	0.37	0.00
PC 38	0.19	1.73	(0.03)	0.04	0.36	0.01
PC 39	0.27	2.57	(0.03)	0.06	0.54	0.01
PC 40	0.19	1.98	(0.02)	0.04	0.42	0.00
PC 41	0.12	1.06	(0.01)	0.03	0.22	0.00
PC 42	0.09	0.65	(0.01)	0.02	0.14	0.00
PC 43	0.06	0.38	(0.01)	0.01	0.08	0.00
PC 44	0.06	0.38	(0.)	0.01	0.08	0.00
PC 45	0.06	0.33	(0.)	0.01	0.07	0.00
PC 46	0.34	4.74	(0.04)	0.07	1.00	0.01
PC 47	0.18	2.15	(0.03)	0.04	0.45	0.01
PC 48	0.11	1.52	(0.03)	0.02	0.32	0.01
PC 49	0.12	2.20	(0.04)	0.03	0.46	0.01
PC 50	0.26	4.12	(0.04)	0.06	0.87	0.01
PC 51	0.10	3.85	0.07	0.02	0.81	0.01
PC 52	0.12	3.70	0.05	0.03	0.78	0.01
PC 53	0.12	3.23	(0.02)	0.03	0.68	0.00
PC 54	0.09	2.33	(0.02)	0.02	0.49	0.00
PC 55	0.09	4.22	0.06	0.02	0.89	0.01

( )   Values below detection

Appendix C-3 Continued. Carbon, nitrogen, and sulfur data

Sample	Nitrogen (%)	Carbon (%)	Sulfur (%)	Nitrogen (mg)	Carbon (mg)	Sulfur (mg)
PC 56	0.09	3.30	(0.04)	0.02	0.70	0.01
PC 57	0.11	1.92	(0.02)	0.02	0.40	0.00
PC 58	0.14	2.24	0.05	0.03	0.47	0.01
PC 59	0.17	2.47	0.11	0.04	0.52	0.02
PC 60	0.16	1.38	(0.03)	0.03	0.29	0.01
PC 61	0.16	1.16	(0.02)	0.03	0.24	0.00
PC 62	(0.05)	0.31	(0.01)	0.01	0.06	0.00
PC 63	(0.04)	0.26	(0.01)	0.01	0.05	0.00
PC 64	(0.03)	0.22	(0.01)	0.01	0.05	0.00
PC 65	(0.05)	0.25	(0.01)	0.01	0.05	0.00
PC 66	(0.03)	0.23	(0.)	0.01	0.05	0.00
PC 67	(0.03)	0.18	(0.01)	0.01	0.04	0.00
PC 68	0.35	3.76	(0.04)	0.07	0.79	0.01
PC 69	0.21	1.90	(0.02)	0.04	0.40	0.01
PC 70	0.12	1.40	(0.02)	0.03	0.30	0.01
PC 71	0.15	1.70	(0.02)	0.03	0.36	0.00
PC 72	0.12	1.35	(0.02)	0.03	0.28	0.00
PC 73	0.12	1.87	(0.02)	0.03	0.39	0.00
PC 74	0.10	1.85	(0.03)	0.02	0.39	0.01
PC 75	0.12	1.67	(0.03)	0.03	0.35	0.01
PC 76	0.12	1.52	(0.02)	0.03	0.32	0.00
PC 77	0.12	1.35	(0.02)	0.03	0.28	0.00
PC 78	0.11	2.30	(0.01)	0.02	0.48	0.00
PC 79	0.13	1.48	(0.01)	0.03	0.31	0.00
PC 80	0.14	1.31	(0.01)	0.03	0.28	0.00
PC 81	0.11	1.07	(0.01)	0.02	0.23	0.00
PC 82	0.12	1.11	(0.02)	0.03	0.23	0.00
PC 83	0.12	1.15	(0.02)	0.03	0.24	0.00
PC 84	0.32	3.89	(0.05)	0.07	0.82	0.01
PC 85	0.21	2.20	0.08	0.05	0.46	0.02
PC 86	0.14	1.48	(0.04)	0.03	0.31	0.01
PC 87	0.12	3.49	0.08	0.03	0.73	0.02
PC 88	0.12	4.13	0.08	0.03	0.87	0.02
PC 89	(0.1)	5.41	(0.06)	0.02	1.14	0.01
PC 90	(0.09)	4.01	(0.05)	0.02	0.84	0.01
PC 91	0.12	3.57	(0.04)	0.03	0.75	0.01
PC 92	(0.11)	2.84	(0.03)	0.02	0.60	0.01
PC 93	0.13	1.29	(0.02)	0.03	0.27	0.00
PC 94	(0.1)	1.25	(0.02)	0.02	0.26	0.00

( ) Values below detection

Appendix C-3 Continued. Carbon, nitrogen, and sulfur data

Sample	Nitrogen (%)	Carbon (%)	Sulfur (%)	Nitrogen (mg)	Carbon (mg)	Sulfur (mg)
PC 95	(0.11)	1.38	(0.02)	0.02	0.29	0.00
PC 96	0.15	1.66	(0.02)	0.03	0.35	0.00
PC 97	0.15	1.84	(0.02)	0.03	0.39	0.00

( ) Values below detection

Inorganic and Organic Carbon Analysis. Loss on ignition (LOI) was used in conjunction with the C-N-S analyzer to determine the concentration of organic carbon present per instructions in the standard operating procedures (OEWRI, 2007c). A five gram sample was measured, placed in a porcelain crucible, and put in a muffle furnace set to 400 C for 6 hours. The samples were removed, cooled, and a second CNS analysis was used to determine the remaining carbon in the sample. Organic carbon was calculated by subtracting post-LOI CNS analysis (inorganic carbon) data from pre-LOI CNS analysis (total carbon) data.

Twenty-five samples were analyzed for IC/OC to determine if Zn was bonded to organic matter or inorganic matter. Buried soil horizons contain high amounts of organic carbon in the form of organic matter while mining sediments contain high amounts of inorganic carbon in the form of limestone ($CaCO_3$). CNS analysis does not distinguish between inorganic and organic carbon, making it is impossible to tell simply from the CNS results if a sample high in carbon is a buried soil or mining sediment. However, finding a relationship between Zn concentration and carbon is one way to distinguish between buried soils and mining sediment. If Zn is primarily bound to organic matter, a strong correlation will exist between Zn and organic carbon whereas a strong correlation between Zn and inorganic carbon will exist if Zn is primarily bound to the mining sediment (limestone). Figure C-1 shows total, inorganic, and organic carbon in relation to Zn (Appendix C.4). Samples used in the analysis were diverse in their Zn content, carbon content, and position in the core (top and bottom of core). The goal was to get a representative sample between mining sediment and the current organic-rich A horizon at the surface. The results show that Zn has a moderate positive correlation with total carbon (R^2=0.54), a strong positive correlation with inorganic carbon (R^2=0.83), and nearly zero correlation with organic carbon (R^2=0.0019). Based on these results, both mining sediment and buried soils contain high total carbon, however, mining sediment is characterized by high Zn concentrations while buried soils are characterized by low Zn concentrations. Therefore, buried horizons can be distinguished by the absence of Zn and mining sediment can be distinguished by the presence of Zn. Loss on ignition analysis of future samples would therefore not be necessary.

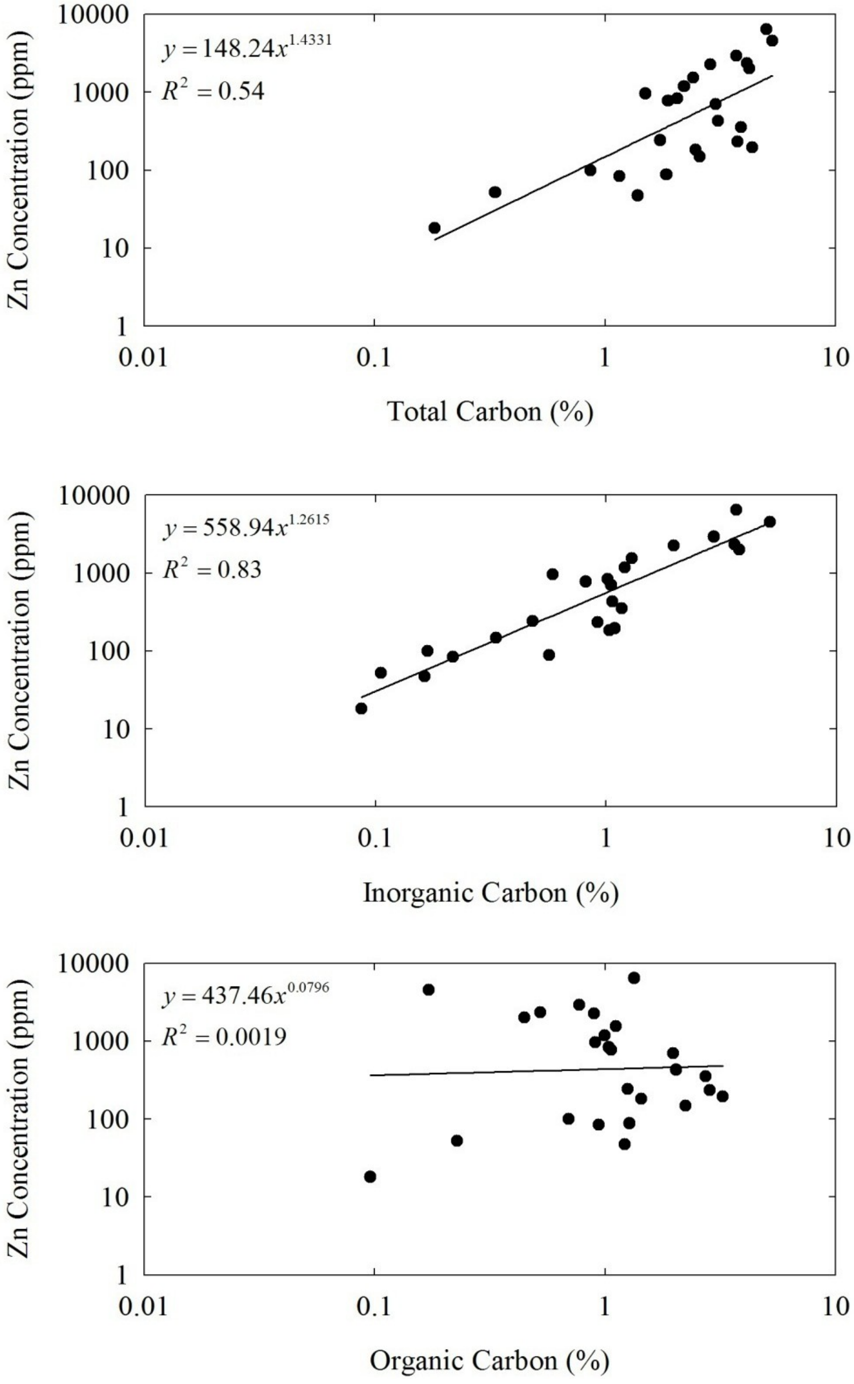

Figure C-1. Loss on ignition results for (A) total, (B) inorganic, and (C) organic carbon. The strong relationship between Zn and inorganic carbon indicates that Zn is primarily bonded to tailings sediment.

Appendix C-4. Total, inorganic, and organic carbon data from CNS and LOI analysis.

Sample	Total Carbon (%)	Inorganic Carbon (%)	Organic Carbon (%)
PC 14	4.33	1.09	3.24
PC 19	2.06	1.01	1.04
PC 2	3.09	1.06	2.03
PC 26	0.86	0.17	0.70
PC 27	3.02	1.05	1.97
PC 3	2.41	1.29	1.12
PC 32	5.01	3.67	1.34
PC 35	2.86	1.97	0.90
PC 38	1.73	0.48	1.25
PC 39	2.57	0.33	2.23
PC 45	0.33	0.11	0.23
PC 49	2.20	1.21	0.99
PC 52	3.70	2.93	0.77
PC 55	4.22	3.77	0.45
PC 59	2.47	1.03	1.43
PC 6	5.31	5.14	0.17
PC 60	1.38	0.16	1.22
PC 67	0.18	0.09	0.10
PC 68	3.76	0.92	2.84
PC 73	1.87	0.82	1.06
PC 8	1.49	0.59	0.91
PC 83	1.15	0.22	0.94
PC 84	3.89	1.17	2.73
PC 88	4.13	3.60	0.52
PC 97	1.84	0.57	1.28

Appendix D. Cross-section Data

All cross-section data start on river left (looking downstream) and proceed toward river right across the channel. References to banks (right or left) are also in relation to looking downstream. Elevation and depth to refusal are given as elevations relative to the thalweg elevation. Notes highlight key landforms, benchmarks, or other observations along the cross-section.

Appendix D-1. Cross-section data for Site 1A.

Tape (m)	Elevation Relative to TW (m)	Refusal Relative to TW (m)	Notes
0.0	2.65	0.30	Edge of field
5.0	2.72	0.20	
10.0	2.44	1.00	Rebar stake
11.0	2.42		
15.0	2.08		
18.0	2.07		
20.0	2.02		
21.9	2.04	1.85	Top of left bank
21.95	2.01		Bench mark stake (ground)
22.5	1.87		
23.0	1.00		
23.8	0.00		
24.9	0.00	0.05	Thalweg
27.6	0.07		Bed/bar
29.9	0.55		Bar crest
31.0	0.60		
33.7	0.90		
35.7	1.02	0.70	Base of fines
36.9	1.37		
38.5	1.70		
39.3	2.16		Top of right bank
39.6	2.17		
40.5	2.12		
42.4	1.05	0.45	Scour hole/old cut
43.4	1.11		Scour hole/old cut
45.3	1.40		
47.0	1.87		
51.5	2.78		Tree high water mark; off the tape
52.0			Bench mark stake
52.6	1.75	0.43	
54.4	1.45		
56.0		0.30	
58.4	1.47		
58.7	1.77		LT old tree (pedestal)
60.3	1.97	0.70	LT old tree base top
60.35	2.21		Bench mark tree notch; 1 m south of tape
60.8	1.95		Pedestal
61.7	1.62		
66.3	1.36	0.30	
70.9	1.42		
72.7	1.99		Pedestal- dead tree
74.2	1.98		Pedestal- dead tree
76.7	1.12	0.30	
77.15	1.18		

Appendix D-1 Continued. Cross-section data for Site 1A.

Tape (m)	Elevation Relative to TW (m)	Refusal Relative to TW (m)	Notes
78.5	1.72		
78.8	1.74		Pedestal 5m ds of tape, base
80.0	1.12		High point, 5m ds of tape
80.6	1.88		
82.0	2.19	1.00	5m ds of tape
82.7	0.93		
83.0	1.12		High pt 5m ds of tape
83.7	0.90	0.30	
85.0	1.34		Pedestal 5m ds of tape, base
88.3	1.25		
92.0		0.30	
97.8	1.34	1.44	
103.0	1.04	0.57	
105.0	1.52		
105.0	1.26		
106.0	2.15		
107.5	2.30		
110.2	1.67		
115.0	1.42		
119.0	1.24		
130.0	1.67		Right of way
133.0	1.98		Right of way
140.0	2.07		Right of way
146.0	2.37		
146.0	2.69		Tree notch at end of survey

Appendix D-2. Cross-section data for Site 1B.

Tape (m)	Elevation Relative to TW (m)	Refusal Relative to TW (m)	Notes
0.0	2.32	1.92	
7.0	2.66		
9.0	2.78	0.38	7.5YR at 65 cm
11.7	2.735		
13.4	2.98		
14.6	2.90		
16.0	2.86	0.56	Top of left bank; 7.5YR at 65 cm
17.6	2.81		Top of stake
19.5	2.02		
20.0		1.03	
21.3	1.60		
22.0	1.46	0.82	
23.0	1.34		
23.8	1.28	0.98	Edge of water
24.6	0.92		
26.0	0.60		
27.5	0.72	-0.28	
29.0	0.54		
30.4	0.15		
32.0	0.00	-0.10	
33.1	0.18		Edge of water
33.2	1.51		
34.1	2.12		Top of right bank
35.0	2.20		
37.0	2.24	0.48	
38.3	2.29		
40.0	2.12		
42.0	1.91		
43.0	1.78		
44.0	1.61	-0.21	
46.0	1.60		
47.5	1.60		
48.7	1.65		
50.0	1.68		
53.0	1.57	1.04	
56.0	1.54	0.44	
58.0	1.64		

Appendix D-2 Continued. Cross-section data for Site 1B.

Tape (m)	Elevation Relative to TW (m)	Refusal Relative to TW (m)	Notes
60.7	1.47		
62.0	1.37		
64.0	1.32		
65.0	1.34		
68.0	1.25		
72.0	1.12		
74.4	1.17		
77.0	1.28	0.32	
80.9	1.19		
83.0	1.14		
89.0	0.94	-0.41	Center of scoured channel
94.0	0.97	0.29	Toe of scoured channel
96.0	1.13	0.41	
97.4	1.56		
100.0	1.46	0.26	
102.0	1.55		
102.8	1.98		Top of bank of scoured channel
104.0	2.03		
107.0	2.01		Bench mark stake (ground)
110.0	1.99	-0.61	
112.0	1.98		
114.0	1.93		
118.0	1.90	0.68	
122.0	1.85		
123.7	1.66		
128.0	1.45	0.35	Flood chute?
133.5	1.74		
135.0	1.89		
138.0	1.97		
143.0	2.09		
148.0	2.23		
153.0	2.23	0.63	
156.5	2.28	2.12	
159.5	2.43	2.14	
162.0	2.38		
166.0	2.48		
169.0	2.53	2.37	

Appendix D-2 Continued. Cross-section data for Site 1B.

Tape (m)	Elevation Relative to TW (m)	Refusal Relative to TW (m)	Notes
172.0	2.70		
175.0	2.83		
178.0	2.93		Rebar stake (ground)
196.0	3.18		

Appendix D-3. Cross-section data for Site 2.

Tape (m)	Elevation Relative to TW (m)	Refusal Relative to TW (m)	Notes
0.0	3.23	2.73	
6.0		2.55	
13.0		2.35	
18.0	2.87	1.87	
23.0		1.72	
30.0		1.72	
43.0	2.57	0.77	
66.0	2.72	0.82	Edge of field
82.0	2.11	1.71	
86.0		1.81	
91.3	1.91	1.21	Center of flood chute
101.0		1.99	
102.9	2.20	-0.37	
105.0		1.73	
105.7	2.03		Edge of trail
106.7	1.78		Bench mark stake on left bank
107.0	1.47		Top of left bank
108.6	0.39	0.39	Toe, boulders in bank
110.2	0.24		
112.9	0.11		
114.3	0.00	-0.90	Thalweg
120.4	0.32		
120.8	0.58		Toe
120.9	1.54	0.54	Top of right bank
122.5	2.11		
124.0		1.39	
124.3	2.19		Top of colluvium?
127.0	2.80		Crest of colluvium?
129.1	3.25		Bench mark stake (ground), base of bluff

Appendix D-4. Cross-section data for Site 3A.

Tape (m)	Elevation Relative to TW (m)	Refusal Relative to TW (m)	Notes
0.0	2.74	1.84	
15.0	2.64	1.74	
30.1	2.71		
36.4	2.58	0.98	Fence near edge of field
38.7	2.55		
46.0	1.75	-0.90	
49.2	1.74		Center of flood chute
53.7	1.84		
58.0	2.12		
65.3	2.00	-0.67	Bench mark stake (ground)
68.0	2.04		
70.5	2.02		Top of left bank
71.4	0.46		Toe
75.3	0.58		
76.1	0.08		
76.9	0.00	-1.79	Thalweg
78.0	0.28		Edge of bar
80.2	0.30		
81.7	0.50		
84.4	0.70		Large debris jam on right bank
85.3	0.75		
85.9	0.84		
86.6	1.09		Toe
87.2	1.53		
88.5	1.81	-1.37	Top of right bank
89.5	1.61		Bench mark stake (ground), gravel splay
91.5	1.89		Toe of splay
95.0	1.37	-0.65	Scour area- large tree present
96.8	1.67		
99.0	1.57		
100.4	1.27	-1.33	
103.7	1.80		
108.5	1.72	-1.08	
109.5	1.55	-1.15	
119.5	1.59	-1.11	
129.5	1.19	1.09	
139.5	0.96	0.86	

Appendix D-4 Continued. Cross-section data for Site 3A.

Tape (m)	Elevation Relative to TW (m)	Refusal Relative to TW (m)	Notes
149.5	1.34	1.24	
154.5	2.34	2.34	

Appendix D-5. Cross-section data for Site 3B.

Tape (m)	Elevation Relative to TW (m)	Refusal Relative to TW (m)	Notes
0.0	2.79		
7.0	2.75		
9.3	2.56		
11.0	2.33	1.43	Bench mark stake (ground)
12.5		0.99	
14.0	2.26	0.91	
14.8	2.20	0.85	
15.5	1.82		Floodplain bench
16.6	0.85		Edge of water
16.7	0.68		Toe
18.2	0.09	-0.26	
20.8	0.00	-0.65	
22.5	0.22		
26.0	0.59		Toe
27.9	1.57		
30.2	2.13	-1.02	Edge of water
35.3	1.55	-0.55	
39.0	1.53		
44.0	1.66		
48.0	1.58	-1.07	
55.0	1.65		
67.0	1.52	-0.83	BM stake (ground)
72.0	1.54		
77.0	1.54		
83.0	1.49	-1.28	
89.0	1.40	-0.83	
94.0	1.46		
99.0	1.61		
104.0	1.45		
107.0	1.31		Toe of flood chute
111.0	0.98	-1.12	Thalweg of flood chute
117.0	1.06		
120.0	1.11		
123.0	1.00	0.98	
126.0	1.15		
129.0	1.33		
131.5	1.67		

Appendix D-5 Continued. Cross-section data for Site 3B.

Tape (m)	Elevation Relative to TW (m)	Refusal Relative to TW (m)	Notes
133.5	2.21		
135.5	2.91		

Appendix D-6. Cross-section data for Site 4A.

Tape (m)	Elevation Relative to TW (m)	Refusal Relative to TW (m)	Notes
0.0	3.07	0.52	Stake
3.0	2.84		
7.0	2.93	0.38	
10.7	2.69	0.49	
11.4	2.59		
12.0	2.58		Bankfull
12.7	0.93		
13.0	0.61		Toe
19.0	0.00	-1.25	Thalweg
21.8	0.04		
22.9	0.18		Toe
23.2	1.00		Bench
23.4	1.00		Bench (added pt)
24.2	1.90		
25.5	2.38	-0.68	Top of right bank
26.3	2.33	-0.77	
27.4	2.04		
28.6	1.72		Toe of berm
32.0	1.59		
36.0	1.53	-1.17	
42.0	1.62		
49.0	1.73		
55.0	1.78	-0.87	
62.0	1.84		
65.5	1.92		
68.3	2.40	0.00	
75.0	2.50	0.40	

Appendix D-7. Cross-section data for Site 4B.

Tape (m)	Elevation Relative to TW (m)	Refusal Relative to TW (m)	Notes
0.0	3.40	-0.03	
2.8	3.20		
6.5	2.90		
10.5	2.90	0.04	Bench mark stake (ground)
12.0	2.60		
14.1	2.10		
15.0	1.70		
16.4	1.40	-0.05	
18.2	1.30	-0.86	Edge of water
19.1	0.90		Toe
21.3	0.60		
23.0	0.20		
24.0	0.20		
25.3	0.00	-1.10	Thalweg
26.0	0.30		Toe
27.3	1.10		Edge of water
28.2	2.60		
29.5	2.60		
32.9	2.20	-0.15	
35.7	2.40		
40.3	2.60	-0.82	
44.0	2.50		
48.5	2.40		
51.7	2.40	0.90	Intersection of Site 3 at 90.3 m
56.1	2.50		
61.2	2.60	0.10	
65.0	2.50		
72.6	2.40	-0.21	
78.4	2.61		
84.0	2.64		
91.0	2.81		
94.0	3.04		
96.0	3.31	0.32	Bench mark

Appendix D-8. Cross-section data for Site 4C.

Tape (m)	Elevation Relative to TW (m)	Refusal Relative to TW (m)	Notes
0.0	2.55	-0.85	
6.0	2.46	-0.84	
7.6	2.18		
11.0	2.05		
13.0	1.98	-0.94	
15.0	2.03		
17.5	1.95	-0.75	Trail
19.8	1.83		Top of left bank
20.2	0.18	-1.82	Toe
21.0	0.02	-1.18	Thalweg 1
22.3	0.20		
23.7	0.36		
26.1	0.28	-0.82	
27.8	0.00	0.00	Thalweg 2
28.9	0.23		Toe
29.3	0.43		Edge of water
29.7	0.83		
30.0	0.93		
30.5	1.13	0.73	High Bf
31.7	0.95		
31.7	0.98		
32.6	1.23		
32.8	1.43		
33.2	1.73		
33.3	1.93	-1.07	
33.8	1.83		Top of right bank
35.4	2.13		
37.5	1.53		End of tape

Appendix D-9. Cross-section data for Site 4D.

Tape (m)	Elevation Relative to TW (m)	Refusal Relative to TW (m)	Notes
0.0	2.85	-0.65	Rebar stake
5.0	2.91	-1.34	Middle of trail
7.75	2.92		Top of left bank
9.0	0.43		Toe
10.2	0.10	-1.00	Thalweg
12.0	0.00		
13.6	0.72		
15.3	0.80	0.19	Low bar surface
17.5	0.92		
21.0	1.11		High bar surface
23.2	1.33		
26.6	1.23	0.93	Active floodplain; fines
30.0	1.84		
33.0	2.70	-1.35	Top of right bank
40.0	2.91		
50.0	2.92		
60.0	2.93	2.43	
70.0	3.02	2.82	
75.0	3.13	3.03	
80.0	3.51		Bluff

Appendix D-10. Cross-section data for Site 5.

Tape (m)	Elevation Relative to TW (m)	Refusal Relative to TW (m)	Notes
0.0	4.31	2.76	Field
10.0	5.03		
12.4	5.06	2.91	Bench mark 1 stake
12.75	5.00		Top of bank
17.5	0.66		Toe
18.6	0.45		Thalweg
21.8	0.77		Bar
24.5	1.22	0.62	Bar
26.6	1.33		Toe
27.6	1.65		
30.9	3.92	1.52	Top of bank
40.0	4.11		
50.5	3.74	0.81	
60.7	3.47	0.27	Bench mark 2 stake
63.8	3.40		Top of bank
66.55	0.73		Toe
70.5	0.48	0.48	Thalweg
71.1	0.69		
76.2	0.95		Low bar
78.0	1.07	1.07	Toe
78.7	1.45	1.25	Bankfull indicator
83.5	2.10		
85.0	2.14	1.92	
87.0	2.38		
89.0	2.80		
91.0	3.01		
93.0	3.29	1.01	
98.0	3.45		
103.0	3.43	0.92	
107.0	3.07		
108.5	2.80		
110.0	2.79		
113.3	2.91	1.24	Bench mark 3 stake; top of bank
115.9	0.24	-0.76	Toe
117.1	0.04	-0.76	
119.1	0.11	-0.29	
121.0	0.00		Thalweg

Appendix D-10 Continued. Cross-section data for Site 5.

Tape (m)	Elevation Relative to TW (m)	Refusal Relative to TW (m)	Notes
123.1	0.24		Toe
123.3	1.13		
127.3	3.59		
130.3	4.29		Top of bank
135.3	4.29		

Appendix D-11. Cross-section data for Site 6.

Tape (m)	Elevation Relative to TW (m)	Refusal Relative to TW (m)	Notes
0.0	3.52	0.82	Field
28.0	3.74		
30.5	3.74	0.33	Bench mark stake
42.0	3.24		
48.0	3.02	-0.13	
61.0	2.78	-0.43	
67.5	2.42	-0.57	Bench mark stake
70.7	1.75	-0.25	
76.1	1.68	-0.32	Top of left bank
77.6	1.05		
79.2	0.80		High bar
83.0	0.49		
86.6	0.13		
87.3	0.00	-0.95	Thalweg
87.9	0.30		
90.0	2.55	-0.23	Top of right bank
98.0	2.65		
108.0	2.12		
113.0	1.94	-1.26	
118.0	1.89		
128.0	1.75	-1.68	
135.5	1.98		
143.0	4.44		Peridge terrace (10 m NW and 4.5-5 m above last point)

Appendix D-12. Cross-section data for Site BG1.

Tape (m)	Elevation Relative to TW (m)	Refusal Relative to TW (m)	Notes
0.0	1.99	0.74	
2.2	1.95		Top of left bank
2.4	1.26		Edge of water
3.2	0.70		
3.5	0.38	0.18	Toe
4.8	0.00	-0.10	Thalweg
6.9	0.38		
8.4	0.61		
9.6	0.99	0.69	
10.2	1.24	0.64	Gravel Bar
11.2	1.47		
12.0	1.59	1.09	Gravel
14.0	1.61	1.21	Gravel

Appendix D-13. Cross-section data for Site BG2.

Tape (m)	Elevation Relative to TW (m)	Refusal Relative to TW (m)	Notes
0.0	1.37		
2.0	1.18	0.98	
4.1	0.76	0.56	
5.8	0.78		Top of left bank
6.2	0.39		
6.6	0.25		Edge of water
7.4	0.06	-0.14	
9.3	0.16		
12.0	0.00		
13.6	0.09	-0.11	
14.7	0.25		Edge of water
15.4	1.01		
16.1	1.37	1.07	Top of right bank
19.0	1.37		